From Fixed-Order Gain-Scheduling to Fixed-Structure LPV Controller Design

PAR

Zlatko EMEDI

EPFL

ÉCOLE POLYTECHNIQUE
FÉDÉRALE DE LAUSANNE

Suisse
2014

Art is never finished, only abandoned.
Leonardo da Vinci

To Nataša and Lenka

Acknowledgements

These last five years have been a big journey for me. Many people have crossed my ways over this period, and influenced my life and work in a positive manner, so I will use the opportunity to express my gratitude.

First and foremost, I would like to thank Alireza Karimi for the opportunity to perform my PhD thesis research with him in Laboratoire d'Automatique. Ali has been the source of endless support and encouragement, as well as the great teacher of both practical and theoretical aspects of control theory. The only thing I regret is that I have learned some things the hard way, as I was not listening carefully to his words. Thank you, Ali.

Next, I am grateful to committee members Olivier Sename, Sergio Savaresi and Dominique Bonvin for evaluating my PhD thesis, and Colin Jones for presiding over my thesis defense. Dominique has as well been a source of support and advices, especially on how to make a good presentation. I really appreciated Colin's course on MPC and learned a lot from it. I would like to thank Roland Longchamp on his great book on basic control theory, especially as it made me learn some control-related French. Philippe Müllhaupt provided many important inputs on control theory and mathematics, and I wish him all the best in his career. Optimal control and related topics were clarified to me by Timm Faulwasser and Gregory Francois, and I thank them on this.

My work with different laboratory setups would be impossible without Christophe and Francis and their expertise in hardware and data acquisition. Ruth, Francine, Sara and Eva were always there to help, and they deserve many thanks. I am thankful to Andrijana for introducing me to LA and providing many details on studying and life in general in Lausanne, and Milan Rapaić for his support over the times of finishing my master and PhD studies.

I thank all my officemates and labmates for a positive atmosphere in LA. I had a lot of fun time here, try to keep up the good spirit. Special thanks go to Sean, Gene, Sriniketh and Achille for both being good friends and working hard on improving my written English. With Mahdieh, Milan, Jean-Hubert, Andrea, Christoph K, Stefano, Simone, Gabriel, Willson, Ioannis, Basile and others I had many interesting discussions (both technical and less technical). Special thanks go to Predrag, my friend and gym guru, volleyball crew (especially Ludo and Sam), badminton boys (Milan, Martand, Tomasz, Predrag) and Uncontrollable musicians (Mirko, Sean, Maja, Simone).

My family has been a big support over these endless years of studying, and this is the time to thank them as I am finishing that journey. Special mention goes to Ana as the first grandchild of my parents, hence the source of fun and experience to all of us (Tamara and Arpi, you were

faster!). Except to all of my family, I would like to thank as well to my in-laws for being a real second family to me, and Biljana and Lazar for being like a family to us and for having fun and sharing important moments with us. Finally, my deepest gratitude goes to Nataša. Not only for her endless love, but as well for her support and belief in me in those moments when I did not believe in myself. Lenka, our pretty princess, thank you for staying in mama's tummy until the thesis was submitted, and even allowing me to have some sleep before my thesis defense!

Abstract

This thesis focuses on the development of some fixed-order controller design methods in the gain-scheduling/Linear Parameter Varying (LPV) framework. Gain-scheduled controllers designed using frequency-domain Single Input Single Output (SISO) models are considered first, followed by LPV controller design in the SISO transfer function setting and, finally, by Multiple Input Multiple Output (MIMO) LPV controller design in the state-space setting. In addition to the guarantee of closed-loop stability, each of the methods optimizes some classical performance measure, such as the $\mathscr{H}_\infty$ or $\mathscr{H}_2$ performance metrics. In the LPV state-space setting, the practical assumption of bounded scheduling parameter variations is taken into account in order to allow a higher performance level to be achieved.

The fixed-order gain-scheduled controller design method is based on frequency-domain models dependent on the scheduling parameters. Based on the linearly parameterized gain-scheduled controllers and desired open-loop transfer functions, the $\mathscr{H}_\infty$ performance of the weighted closed-loop transfer functions is presented in the Nyquist diagram as a set of convex constraints. No a posteriori interpolation is needed, so the stability and performance level are guaranteed for all values of scheduling parameters considered in the design. Controllers designed with this method are successfully applied to the international benchmark in adaptive regulation. These low-order controllers ensure good rejection of the multisinusoidal disturbance with time-varying frequencies on the active suspension testbed.

One issue related to the gain-scheduled controller design using the frequency response model is the computational burden due to the constraint sampling in the frequency domain. The other is a guarantee of stability and performance for all the values of scheduling parameters, not just those treated in design. To overcome these issues, a method for the design of fixed-order LPV controllers with the transfer function representation is proposed. The LPV controller parameterization considered in this approach leads to design variables in both the numerator and denominator of the controller. Stability and $\mathscr{H}_\infty$ performance conditions for all fixed values of scheduling parameters are presented in terms of Linear Matrix Inequalities (LMIs). With a problem of rejection of a multisinusoidal disturbance with time-varying frequencies in mind, LPV controller is designed for an LTI plant with a transfer function model.

The extension of these methods from SISO to MIMO systems is far from trivial. The state-space setting is used for this reason, as there the transition from SISO to MIMO systems is natural. A method for fixed-order output-feedback LPV controller design for continuous-time state-space LPV plants with affine dependence on scheduling parameters is proposed. Bounds on the scheduling parameters and their variation rates are exploited in design through the

Acknowledgements

use of affine Parameter Dependent Lyapunov Functions (PDLFs). The exponential decay rate, induced $\mathcal{L}_2$-norm and $\mathcal{H}_2$ performance constraints are expressed through a set of LMIs. The proposed method is applied to the 2DOF gyroscope experimental setup.

In practice control is performed using digital computers, so some effort needs to be put into the LPV controller discretization. If the discrete-time LPV model of the system is available, one may design the discrete-time controller directly. Hence, the MIMO LPV controller design method is proposed for the class of discrete-time LPV state-space plants affine in the scheduling parameters. A controller structure fixed by the user is preserved, since the controller parameters appear directly as decision variables in the convex optimization program. Limited scheduling parameter variations are treated through the use of PDLFs. Uncertainty in the scheduling parameter vector due to the sensor measurement error can be considered in the design. The iterative convex optimization procedure improves the upper bounds on the $\mathcal{H}_2$ or induced l_2-norm performance of the closed-loop system. The effectiveness of the method is illustrated via numerical comparison with a similar approach.

Key words: gain-scheduling; linear parameter varying; fixed-order controller design; parameter dependent Lyapunov functions; convex optimization; multisinusoidal disturbance rejection.

Résumé

Cette thèse concerne le développement de plusieurs méthodes pour la synthèse de régulateurs gain-scheduling/Linéaire à Paramètres Variants (LPV) d'ordre fixe. Dans un premier temps des régulateurs du type gain-scheduling conçus avec des modèles SISO fréquentiels sont considérés, suivi par la synthèse de régulateurs LPV dans le contexte de fonctions de transfert SISO. Finalement, la synthèse de régulateurs MIMO LPV avec des modèles d'état est abordée. En plus de la garantie de stabilité en boucle fermée, chaque méthode optimise une des mesures de performance classiques, telle que les jauges de performance $\mathscr{H}_\infty$ ou $\mathscr{H}_2$. Dans le contexte LPV avec modèle d'état, l'hypothèse réaliste que les variations du paramètre du scheduling sont bornées permet d'obtenir une meilleure performance.

La méthode de synthèse pour les régulateurs du type gain-scheduling d'ordre fixe est basé sur des modèles fréquentiels dépendant du scheduling parameters. En tenant compte des fonctions de transferts souhaitées en boucle fermée et des régulateurs du type gain-scheduling à paramètres linéaires, la performance $\mathscr{H}_\infty$ de la somme pondérée des fonctions de transfert en boucle fermée est formulée comme un ensemble de contraintes convexes dans le diagramme de Nyquist. Aucune interpolation postérieur est nécessaire, donc la stabilité et le niveau de performance sont assurés pour toute valeur du paramètre du scheduling prise en compte dans la synthèse. Des régulateurs conçus avec cette méthode sont appliquées avec succès au Benchmark international pour la régulation adaptive. Ces régulateurs de degré bas rejettent très bien la perturbation multi-sinusoïdale à fréquences variables sur le système de test pour suspension active.

La puissance computationnelle requise dû à l'échantillonnage de la contrainte dans le domaine fréquentielle est une des difficultés liées à la synthèse d'un régulateur du type gain-scheduling utilisant une réponse fréquentielle. L'autre désavantage est que la stabilité et la performance ne sont pas garanties pour les valeurs du paramètre de scheduling qui ne sont pas pris en compte dans la synthèse. Une méthode de synthèse de régulateur de degré fixe, basée sur la fonction de transfert, est proposée afin de résoudre ces deux difficultés. Dans cette approche, la parametrisation du régulateur LPV comporte des variables libres dans le numérateur et le dénominateur. Des conditions de stabilité, ainsi que de performance $\mathscr{H}_\infty$, pour toutes valeurs constantes des paramètre de scheduling sont présentées sous forme de LMIs. Motivé par le problème de rejection de perturbation multi-sinusoïdale, le régulateur LPV est adapté/appliqué à un système LTI avec un modèle en forme de fonction de transfert.

L'extension de ces méthodes au cas MIMO n'est pas évidente. Pour cette raison une représentation par modèle d'état est utilisé, car dans ce format la transition entre systèmes SISO et

MIMO devient naturel. Une méthode pour la synthèse de régulateurs LPV de degré fixe est proposée pour des systèmes représentés par un modèle d'état LPV, avec dépendance affine sur les scheduling parameters. Des bornes sur les valeurs et la vitesse de variation des scheduling parameters permettent l'utilisation de PDFLs pour la synthèse. Le taux de décroissance exponentielle, la norme $\mathscr{L}_2$, et l'indice de performance $\mathscr{H}_2$ sont exprimés à travers des LMIs. La méthode est appliquée à un gyroscope 2DOF expérimental.

Dans la pratique le régulateur est implémenté dans un ordinateur numérique, ce qui nécessite la discrétisation du régulateur LPV. Si un modèle discret du système LPV est disponible, la synthèse du régulateur discret se fait directement. Donc la méthode de synthèse de régulateur MIMO LPV est proposée pour l'ensemble de systèmes représentés par un modèle d'état discret à dépendance affine dans les paramètres de scheduling. La structure du régulateur spécifié par l'utilisateur est respectée, car les paramètres du régulateur apparaissent comme variables de décision dans le problème d'optimisation convexe. Des variations bornées du paramètre de scheduling sont traitées au travers des PDLFs. L'incertitude dans le paramètre de scheduling due à des erreurs de mesure peut être prise en compte dans la synthèse. La procédure d'optimisation itérative améliore la borne supérieure sur l'indice de performance $\mathscr{H}_2$ ou l_2 du système en boucle fermée. L'efficacité de cette approche est illustrée par une comparaison en simulation avec une méthode similaire.

Mots clefs : gain-scheduling ; linéaire à paramètres variants ; synthèse de régulateurs d'ordre fixe ; parameter dependent Lyapunov functions ; optimisation convexe ; rejection de perturbation multi-sinusoïdale.

List of Abbreviations

2DOF - 2-Degrees-Of-Freedom
BMI - Bilinear Matrix Inequality
CCOP - Convex-Concave Optimization Program
GUI - Graphical User Interface
I/O - Input/Output
KYP - Kalman-Yakubovich-Popov
LFT - Linear Fractional Transformation
LMI - Linear Matrix Inequality
LPV - Linear Parameter Varying
LTI - Linear Time-Invariant
MIMO - Multiple Input Multiple Output
PDLF - Parameter Dependent Lyapunov Function
PI - Proportional-Integral
PID - Proportional-Integral-Derivative
SDP - Semidefinite Programming
SISO - Single Input Single Output
SPR - Strictly Positive Real

Contents

Contents

List of Figures

List of Tables

1 Introduction

1.1 Motivation

The field of automatic control has come a long way since the application of the centrifugal governor in the 18th century to the problem of regulation of steam engine speed (James Watt, among others), and James Clark Maxwell's analysis of dynamics of governors [1]. With the seminal publications of Lyapunov [2], Nyquist [3] and Bode [4], a strong basis for the analysis of the stability of dynamical systems has been laid out. From the developed stability analysis methods, many different frameworks for the control of dynamical systems have gradually arisen in the past 50 years. This has led to advanced control mechanisms such as adaptive, robust or model predictive control, or nonlinear control principles such as feedback linearization, sliding mode control or backstepping. These advances have allowed the expansion of the applicability of automatic control theory from electromechanical systems (ranging from temperature control of a refrigerator to wind turbines and robotic arms), over aerospace engineering and the process industry, to different emerging applications such as the control of insulin injection or stock trading. More details on the history and development of the field of automatic control and classical and emerging applications can be found in a very informative and recent review paper [5].

However, the majority of practical applications of control theory still lies in the field of control of electromechanical systems. Control theory is widely applied in modern embedded systems, appearing as cheap, massively produced consumer electronics, in household appliances, in the automotive industry and in medical applications. The common characteristic of many of these applications is the scarcity of available resources in terms of memory and available processing power or time. Dynamical models used for the control law design are often of a high order, as simplification of the model could lead to an unreliable control law. If the controller design method cannot decouple the choice of the controller order from the model order, a controller with high implementation complexity is usually obtained. This clearly motivates the demand for the fixed-order controller design methods, as this class of control laws is very low-cost for real-time implementation in terms of both memory and processing power. Another advantage

of simpler control laws is that it is easier to ensure their numerical reliability and perform verification. The other important motivation for fixed-order controller design comes from the still ruling dominance of the Proportional-Integral/Proportional-Integral-Derivative (PI/PID) controller structure in industry. Many currently operating industrial processes are controlled by this simple, yet powerful and easily comprehensible, controller structure. Replacing them by the much more complex control strategy is often hard to enforce, as it would demand reallocation of resources and a lot of testing to verify all the safety aspects. These operations are time-consuming and expensive, and hence almost unacceptable by industrial practice standards in many such applications. It is important to mention here that the choice of controller order is not a trivial task in general. If the order is chosen too low, the obtained performance may be deemed unsatisfactory. In this case, a controller order has to be increased by the user until a satisfactory performance is obtained.

Another important issue related to the control solutions applied in industry is the controller structure. Restrictions on the controller structure may come from different sources. One simple restriction is a need for the presence of certain dynamics in the controller. Such a need comes from the well-known Internal Model Principle [6], which states that the dynamics of the persistently exciting reference or disturbance have to be replicated in the controller in order to achieve asymptotic tracking or disturbance rejection. The other, more complex, demands are related to a need for the decentralized or distributed structure of the controller. Namely, in the presence of a large number of sensors and actuators that are spatially distributed, communication may become very complicated or even impossible between some parts of the system. This leads to the desire for a control configuration in which the stability and good level of performance of the overall control system is guaranteed, in spite of a limited set of communication links. A method that can directly design low-order controllers with structural constraints respected can hence be very useful in practice.

In reality, many systems operate in such work regimes that a single Linear Time-Invariant (LTI) model cannot describe the behavior of the system sufficiently well. This is true for any system with nonlinear dynamics and a sufficiently large continuous space of operating points. However, this type of systems can often be described sufficiently well through a set of local LTI models for different operating points. In this case the gain-scheduling control paradigm can be applied successfully. The idea behind gain-scheduling is that a family of local linear controllers designed for these operating points performs well when the operating point varies slowly. Intuitively, it is expected that under this condition the local linear models capture the underlying nonlinear dynamics well enough. One merit of the gain-scheduling paradigm is its simplicity, thereby making it easy for engineers to understand and use. The other important feature is that the high level of performance achievable by the use of an LTI controller can be preserved by a gain-scheduled controller if the assumption of slow variation of the scheduling parameter is satisfied.

In the case that the operating point varies more abruptly the control system performance can, however, degrade drastically, and even the stability of the overall control system may

be jeopardized. The other issue that may appear is the inappropriate interpolation of the designed LTI controllers, as it can lead to the loss of performance, or even stability, even for the operating points included in the design set. This motivates the use of a more representative class of models. LPV models are characterized by dynamics similar to that of linear systems, but with model parameters depending on the time-varying scheduling parameters. These may just be a function of an operating point, or could depend on some external signal. The main merit of the LPV modeling and control paradigm is that it enables the use of linear systems theory tools for a wide class of nonlinear systems.

Different types of plant models are used for controller design in the gain-scheduling/LPV framework. Frequency-domain models are often considered in practice, for the reason that they can be obtained in a simple manner, without making any structural assumptions. In the case that scheduling parameters do not vary "too quickly", frequency-domain models dependent on scheduling parameters may be very useful as many practical performance specifications are stated in the frequency domain. If this assumption is not satisfied, the LPV paradigm provides a safer solution. Since some systems may be too complex to be modeled in acceptable time using underlying physical principles, input-output identification routines are usually employed when this is the case. Some available LPV model identification methods lead to input-output models in the polynomial setting. On the other hand, for some systems first principles modeling may be feasible, leading to LPV models with a state-space structure. The advantage of state-space LPV models is that the transition from SISO to MIMO systems is simpler than in the polynomial setting.

1.2 State of the Art

A review of gain-scheduling and LPV fixed-order controller design methods is now presented, with particular focus placed on multi-sinusoidal disturbance rejection as this presents an important contribution of this thesis.

1.2.1 Multi-sinusoidal disturbance rejection

The problem of periodic disturbance rejection appears in many engineering applications. These periodic disturbances often possess few dominant harmonics, and so they can be expressed as a combination of a few sinusoidal signals. Some of the practical applications in which periodic disturbances appear are hard disk [7] and optical disk drives [8], active noise control systems [9] and helicopter rotor blades [10].

In the case that the disturbance frequency is known, certain approaches, such as internal model control and repetitive control techniques, can be applied. If an unknown frequency can be measured directly or indirectly, which happens, for example, in some active noise control applications, adaptive feedforward control can be used to reject the disturbance. In [11], it is shown that the standard adaptive feedforward control algorithm is equivalent to

the internal model control law. A survey of different methods for the both the known and unknown disturbance frequency cases can be found in [12].

In practice it is not always possible to measure the disturbance frequency with a sensor, either because it is physically impossible to place the sensor at an appropriate place for measuring disturbance, or because the additional cost is too high. This motivates the use of parameter estimation methods to estimate the parameters of the disturbance model. Therefore, almost all unknown-frequency disturbance rejection algorithms generally lead to a *direct* or *indirect* adaptive implementation, which can be referred to as "adaptive regulation" since the controller parameters are *adapted* with respect to variations of parameters of the disturbance model. In [13], two such approaches are compared for an active suspension system. The first approach is a direct adaptive control scheme with the Youla-Kučera parameterization of the controller, so the disturbance is rejected by adjusting the parameters of the Youla-Kučera polynomial. The second approach is an indirect adaptive control scheme because the disturbance model is estimated first and then, based on the internal model principle, a new controller is calculated to reject the disturbance.

A benchmark on adaptive regulation, performed on the problem of multi-sinusoidal disturbance rejection for an active suspension setup, is presented in [14]. The main performance criteria are defined with regard to the closed-loop transfer operator between the output disturbance and measured output, as a good attenuation level in the frequency region of the disturbance and low amplification outside of this region. Different solutions are proposed, with all but one [15] using the Youla-Kučera parameterization as the basis for controller design [15, 16, 17, 18, 19, 20, 21]. Although these all lead to good performance, they come at the cost of having high controller order equal to that of the augmented plant. Additionally, even though the majority of the performance specifications is defined in the frequency domain, these methods need a reliable parametric model for the controller design.

In the case that the internal model principle solution is applied, the dynamics of the controller are scheduled by parameters which change as a function of the disturbance frequencies. This motivates the LPV controller design method for the rejection of sinusoidal disturbances described in [22]. In this approach, an LPV controller is designed with a guaranteed level of $\mathscr{H}_\infty$ performance based on the method proposed in [23, 24]. A single quadratic Lyapunov function is used for all values of the measured frequency. Hence, stability and performance are guaranteed even in the presence of infinitely fast disturbance frequency variations.

Discrete-time state-space state-feedback and full-order output-feedback LPV controller design methods for multi-sinusoidal disturbance rejection are proposed in [25, 26]. The state-feedback method [25] is based on the use of a single Lyapunov matrix, which, in the discrete-time case, is not necessary even for unlimited variations of the disturbance frequencies. The full-order output-feedback method [26] is implemented in two ways: using the Linear Fractional Transformation (LFT) framework for representing the influence of scheduling parameters on the plant and controller dynamics, and using the polytopic LPV description and

a Lyapunov function independent of the scheduling parameters. The order of the obtained LPV controller in both cases is equal to that of the augmented plant. All of these methods provide good performance in presented active noise cancellation and active vibration control experiments.

1.2.2 From the gain-scheduling to the LPV paradigm

The original gain-scheduled controller design methods are based on the use of local LTI models for a set of operating points of the underlying nonlinear plant. Namely, for each of these local models an LTI controller providing good performance is designed. In the second step, an interpolated gain-scheduled controller is obtained based on these local controllers, such that it covers the whole continuum of operating points defined by those used for design. As summarized in [27], the main requirements that have to be satisfied by the gain-scheduled controller are: (a) stability and performance for all operating points, and not just for those used for design, and (b) the parameters of the interpolated controller being smooth and continuous functions of the operating point to avoid discontinuous controller states and output signals. Many different approaches for the interpolation of local controllers to a gain-scheduled controller are discussed in the literature. Some of the strategies are direct interpolation between transfer functions or interpolations of zeros, poles and gains of controllers. Stability of some such schemes and propositions for more advanced interpolation techniques can also be found in the literature [28, 27, 29, 30, 31].

The main issue with interpolation of LTI controllers to a gain-scheduled controller is that the obtained gain-scheduled controller often does not guarantee stability and performance even for the operating points considered in design. To avoid the issue of interpolation and to prevent degradation of control system when the operating point changes considerably during operation, the transition from the gain-scheduling to LPV framework is proposed in [32, 33]. LPV systems can be thought of as a weighted combination of linear models, each valid at a specific operating point. The weightings for most of the systems may be considered smooth and continuous functions of the scheduling parameters that in turn depend on the operating point. These parameters can either be exogenous or endogenous signals, with the system states or outputs being an example of the latter. As a result, the dynamics become a function of time according to the trajectories of these signals.

The class of LPV controllers can be defined in a similar manner, with the modeling and control of LPV systems having become an important area of research in the past two decades [34], [35]. The motivation for this development is the use of linear systems theory tools for stability analysis and controller synthesis for a wide class of nonlinear systems [33]. Over the years, the theory of LPV systems has been successfully applied to modeling and control in different practical applications, such as for wind turbine control [36, 37], turbofan engines [38, 39], wafer stage [40], missile autopilot design [41, 42, 43, 44], semi-active suspension design [45] and active braking control [46]. More on applications of LPV framework can be found in recent

books [47, 48].

There are different methods for obtaining an LPV model of a system. One approach is the use of a nonlinear model derived from first principles and its LPV approximation in the operating range of interest. For some systems first-principles modeling may be too complex, or even impossible, which motivates the use of identification routines. As the LPV models produced by identification procedures are usually in discrete time [49, 50, 51, 52], both continuous- and discrete-time LPV controller design methods may be required.

Some methods for fixed-order LPV controller design in the transfer function setting are presented in [38, 53]. The method in [38] presents an extension of a robust controller design method [54], with a set of LMI constraints for $\mathscr{H}_\infty$ performance being obtained by the use of a central polynomial. In [53] a direct data-driven LPV controller design is proposed to avoid possible errors that may appear during modeling. According to [52], the use of transfer function models is very well aligned with industrial practice and the modeling paradigm in the SISO case. However, the extension to the MIMO case can be significantly more complex than in the state-space setting.

1.2.3   LPV MIMO controller design in the state-space setting

Some important results for stability analysis of uncertain and LPV polytopic continuous-time and discrete-time systems are presented in [55, 56, 57, 58]. It is important to emphasize here that even though uncertain and LPV systems share some common characteristics, the essential difference is the time-invariant nature of uncertain systems that is opposed to time-varying behavior of LPV systems. Hence, even though many analysis and synthesis tools for uncertain and LPV systems are based on similar premises, the important difference in their characters has to be kept in mind. One of the characteristics of listed LPV analysis methods is a polytopic or affine dependence of plant matrices on the scheduling parameters. The other important feature is a shift from the use of Lyapunov matrices independent of the scheduling parameters to the use of PDLFs. In practice scheduling parameters rarely vary infinitely fast, hence this shift improves the analysis of LPV systems with bounded scheduling parameter variations. The addition of slack matrix variables to the analysis conditions for stability and performance of LPV systems has a beneficial influence as well.

Ideas related to the LPV system analysis lead to further development of LPV controller synthesis methods. Some continuous-time LPV controller design strategies for LPV systems with a state-space description are presented in [59, 60, 61, 62]. A few recent publications cover the case of controller synthesis for discrete-time LPV systems affected by scheduling parameters with limited variations [63, 64, 65]. An observer-based controller design for LPV systems with uncertainty in the measurement of the scheduling parameter is considered in [66].

An important aspect of any LPV control approach is the manner in which the scheduling parameters are handled in the design process. In some of the approaches [67, 68], the LFT

framework is used to isolate the scheduling parameters. This allows the small-gain theorem to be used for the analysis of system stability, but with some conservatism introduced for the manner in which the LPV model is represented through the nominal LTI model and scheduling parameter matrix. Additionally, a single Lyapunov function is used for ensuring the closed-loop stability, which guarantees that the system remain stable even for infinitely fast variations of scheduling parameters, but which is often unnecessary and superfluous in practice. Considering a bound on the variation rate of scheduling parameters relaxes the controller synthesis problem by increasing the stabilizing controller space and possible performance gain. It should be emphasized that stability of some systems cannot even be analyzed using a single quadratic Lyapunov function [59], and that the bounds on the variation rate are often known.

PDLFs are applied to the problem of controller synthesis for uncertain and LPV systems in [59, 60, 69]. In [59] both state-feedback and full-order output feedback LPV controller design methods are treated, and in [60] a different full-order output-feedback controller design approach is proposed. Both of these lead to controller matrices that depend on derivatives of scheduling parameters, which are not measurable in the general case. In [60], this can be avoided by fixing a part of the structured Lyapunov matrix and using a scaling matrix to reduce the conservatism of the approach. The approach in [61] extends the method presented in [60] via the addition of a scalar optimization variable that guarantees at least the same performance as obtained by the original method. However, this possible performance improvement comes at the cost of increased computation time, as a line search over the added variable has to be performed and for each examined value of the added variable a Semidefinite Programming (SDP) problem has to be solved.

All of the aforementioned methods result in a controller in either state-feedback or full-order output-feedback form. For online reconstruction of the full-order controller, time-consuming linear algebraic operations need to be carried out. Moreover, the order of the controller may be too high since it depends on the augmented plant model order. Some methods for LPV controller reduction are available [70], but there is no guarantee of preserving stability or performance of the original LPV system with the reduced-order controller. On the other hand, a state-feedback LPV controller demands state estimation, which is a non-trivial task for LPV systems. Often, the users may have a preference for a certain controller structure. Decentralized [71] or distributed [72] controller structures may be essential in order to achieve low complexity of the overall control system. However, for both state-feedback and full-order output-feedback controller design methods the controller is recovered by applying a nonlinear transformation to the solution of the optimization problem. This means that the user-requested controller structure cannot be preserved. Finally, the resources available for control are highly limited in most practical applications, even if this is improving in newer applications. As well, lower complexity leads to easier verification of numerical reliability of the applied control law. All of these motivate the need for development of methods for the direct design of low-order fixed-structure output-feedback LPV controllers, which are easier and cheaper to implement, have lower execution times and are simpler for verification.

In [73], the authors develop a fixed-structure state-space discrete-time LPV controller design method with guaranteed induced l_2-norm performance. Performance analysis conditions from [74] are convexified around the slack variable matrix, and its value is updated based on its relation with the Lyapunov matrix. An appropriate two-step iterative optimization scheme is used to improve induced l_2-norm performance. Direct optimization over the controller variables in one of the steps allows the user to tune the controller order and structure. As this method is founded on a premise similar to that of some of the other methods proposed in this thesis, it is reasonable to use it as a basis for comparison.

1.3   Contributions and Organization of the Thesis

This thesis describes the development of some fixed-order gain-scheduled and LPV controller design methods. The contributions are summarized as follows:

- A fixed-order gain-scheduled controller design method based on frequency-domain models dependent on the scheduling parameters is proposed. The shaping of the weighted closed-loop transfer functions is performed in the Nyquist diagram through the use of convex optimization tools, and through the use of linearly parameterized gain-scheduled controllers and desired open-loop transfer function. A benefit of the method is that no a posteriori interpolation over the scheduling parameter space is needed, as the gain-scheduled controller is a direct output of the optimization procedure. The method is applied to the international benchmark problem of multi-sinusoidal disturbance rejection. Even though it is the only low-order solution to the benchmark problem, a comparable level of performance for the rejection of multi-sinusoidal disturbance with time-varying frequencies on the active suspension testbed is achieved.

- A method for the fixed-order LPV controller design in the polynomial setting is proposed to overcome the issues of sampling constraints in the frequency domain and scheduling parameter space, and to guarantee stability and performance level for all the values of scheduling parameters. Additionally, the considered LPV controller parameterization allows treating both the numerator and denominator of the controller as design variables. Stability and $\mathscr{H}_\infty$ performance conditions are exploited to cast the design problem as a convex SDP problem. As the motivating application is the rejection of multi-sinusoidal disturbance with time-varying frequencies, the design of an LPV controller for an LTI plant is considered.

- To enable a natural transition from SISO to MIMO systems, a method for fixed-order output-feedback LPV controller design for continuous-time state-space LPV plants with affine dependence on scheduling parameters is proposed. PDLFs are used in order to exploit bounds on the scheduling parameters and their variation rates in the design. Three different algorithms based on iterative convex optimization schemes are proposed for the design. Different performance measures — namely, the exponential

decay rate, the induced $\mathscr{L}_2$-norm, and $\mathscr{H}_2$ performance — can be optimized. To test the controller design method, real-time experiments are performed on a 2-Degrees-Of-Freedom (2DOF) gyroscope setup.

- A discrete-time state-space LPV controller design method is proposed for the class of discrete-time LPV state-space plants affine in the scheduling parameters to avoid the issues related to the LPV controller discretization. As the controller parameters appear as decision variables in the convex optimization program, the controller structure specified by the user is preserved. Bounded scheduling parameter variations and scheduling parameter uncertainty coming from the sensor measurement error are treated in the design. $\mathscr{H}_2$ or induced l_2-norm performance can be optimized using an iterative convex optimization algorithm. A numerical comparison with an approach founded on similar premises is performed and a simpler controller with better value of l_2-norm performance is obtained.

The remainder of the thesis is organized as follows. Chapter 2 presents a method for the fixed-order gain-scheduled controller design based on the frequency-domain models and its application to the benchmark on adaptive regulation. Chapter 3 describes a method for the design of fixed-order $\mathscr{H}_\infty$ LPV controllers for LTI plants in the polynomial setting with a polytopic representation of the scheduling parameter space. A new fixed-order output-feedback LPV controller design method for continuous-time state-space LPV plant models with affine dependence on the scheduling parameter vector is presented in Chapter 4. In Chapter 5 a fixed-structure LPV controller design method for the class of discrete-time LPV state-space plants, affine in the scheduling parameter vector, is considered. Finally, Chapter 6 concludes the thesis and provides some perspectives for future work.

2 Fixed-order Gain-Scheduled Controller Design in Frequency Domain

2.1 Introduction

In [75], a fixed-order $\mathcal{H}_\infty$ controller design method for spectral models is proposed. In this chapter, the idea is extended to design of gain-scheduled $\mathcal{H}_\infty$ controllers. As already discussed, LPV controllers can guarantee the closed-loop stability for fast variation of the scheduling parameters. However, this may come with a detriment of performance because of the conservatism of existing LPV controller design methods. The method proposed in this chapter guarantees the stability and performance for frozen and slowly time-varying scheduling parameters.

The method is applied to the benchmark on adaptive regulation, which is performed on the active suspension experimental setup [76]. The goal of the benchmark is to reject the output disturbance which consists of multiple harmonics with time-varying frequencies. This leads to a primary control goal of strong attenuation of the closed-loop system in the frequency range of disturbance. It is important as well to minimize the transient effects and to ensure low amplification outside of the frequency range of interest, in order to avoid amplifying the measurement noise. Designed controller is scheduled in real time based on the disturbance model estimate, which is dependent on the disturbance frequency. Even though stability and good performance is guaranteed only for frozen values of the scheduling parameters, this application illustrates that both are preserved even for fast variations of scheduling parameters.

As no parametric model is needed for this controller design method, the approach can also be used for systems with pure time delay. Moreover, there is no under-modeling coming from the structural mismatch. Another positive feature of this method is that computation of the controller parameters and their interpolation are performed by one convex optimization. In this manner, the stability and performance are guaranteed for all the gridded scheduling parameter values, which may not be the case if an a posteriori interpolation is performed.

2.2 Preliminaries

First, the class of models that can be considered using the proposed approach is described. Next, the class of controllers treated by the approach is defined.

2.2.1 Class of models

The class of causal discrete-time SISO models with bounded infinity-norm is considered. It is assumed that the spectral model of the system $G(e^{-j\omega}, \boldsymbol{\theta})$ is available as a function of the scheduling parameter vector $\boldsymbol{\theta} = [\theta_1, \dots, \theta_{n_\theta}]^T$. The scheduling parameter vector $\boldsymbol{\theta}$ is assumed to belong to a bounded set $\Theta \in \mathcal{R}^{n_\theta}$. For example, Θ can be a hyperrectangle, which signifies that

$$\theta_i \in [\underline{\theta}_i, \overline{\theta}_i], \ i = 1, \dots, n_\theta. \tag{2.1}$$

However, other types of bounded sets can be considered as well. The bounded infinity norm condition can be relaxed in order to consider systems with poles on the unit circle. Since only the frequency-domain data are used in the design method, the extension to continuous-time systems is straightforward.

2.2.2 Class of controllers

Linearly parameterized discrete-time gain-scheduled controllers are treated:

$$K(z^{-1}, \boldsymbol{\rho}(\boldsymbol{\theta})) = \boldsymbol{\rho}^T(\boldsymbol{\theta})\boldsymbol{\phi}(z^{-1}), \tag{2.2}$$

where

$$\boldsymbol{\phi}^T(z^{-1}) = [\phi_1(z^{-1}), \phi_2(z^{-1}), \dots, \phi_n(z^{-1})] \tag{2.3}$$

represents the vector of n stable transfer functions, namely basis functions vector. It may be chosen from a set of generalized orthonormal basis functions, e.g. Laguerre basis [77]. Vector

$$\boldsymbol{\rho}^T(\boldsymbol{\theta}) = [\rho_1(\boldsymbol{\theta}), \rho_2(\boldsymbol{\theta}), \dots, \rho_n(\boldsymbol{\theta})] \tag{2.4}$$

represents the vector of controller parameters. Dependence of the controller parameters ρ_i on $\boldsymbol{\theta}$ is given by

$$\rho_i(\boldsymbol{\theta}) = \rho_{i,0} h_{i,0}(\boldsymbol{\theta}) + \sum_{j=1}^{n_\theta} \rho_{i,j} h_{i,j}(\boldsymbol{\theta}), \quad h_{i,0}(\boldsymbol{\theta}) = 1. \tag{2.5}$$

In the case of affine dependency of $\boldsymbol{\rho}$ on $\boldsymbol{\theta}$ functions $h_{i,j}(\boldsymbol{\theta})$ take values $h_{i,j}(\boldsymbol{\theta}) = \theta_j$ for $i = 1, \dots, n$ and $j = 1, \dots, n_\theta$.

2.3 Gain-scheduled $\mathcal{H}_\infty$ controller design

For simplicity, a single $\mathcal{H}_\infty$ constraint on the weighted sensitivity function is considered. The extension to the case of $\mathcal{H}_\infty$ constraints on several sensitivity functions is straightforward.

The main reason to use a linearly parameterized controller is that every point on the Nyquist diagram of the open-loop transfer function becomes a linear function of the vector of controller parameters $\boldsymbol{\rho}(\boldsymbol{\theta})$:

$$L(e^{-j\omega}, \boldsymbol{\rho}(\boldsymbol{\theta})) = K(e^{-j\omega}, \boldsymbol{\rho}(\boldsymbol{\theta}))G(e^{-j\omega}, \boldsymbol{\theta}) = \boldsymbol{\rho}^T(\boldsymbol{\theta})\boldsymbol{\phi}(e^{-j\omega})G(e^{-j\omega}, \boldsymbol{\theta}). \qquad (2.6)$$

This representation enables obtaining a parameterization of an inner convex approximation of the set of fixed-order gain-scheduled $\mathcal{H}_\infty$ controllers.

2.3.1 Design specifications

The nominal performance can be defined by [78]

$$\| W_1(z^{-1})S(z^{-1}, \boldsymbol{\rho}(\boldsymbol{\theta})) \|_\infty < 1, \qquad \forall \boldsymbol{\theta} \in \Theta, \qquad (2.7)$$

where $S(z^{-1}, \boldsymbol{\rho}(\boldsymbol{\theta})) = [1 + L(z^{-1}, \boldsymbol{\rho}(\boldsymbol{\theta}))]^{-1}$ is the sensitivity function and $W_1(z^{-1})$ represents the performance weighting filter. A fixed-order controller design method for systems with multiplicative and multimodel uncertainty is proposed in [75]. It is based on the linearization of this constraint around a known desired open-loop transfer function $L_d(z^{-1})$. The main benefit of this linearization is that it gives not only sufficient conditions for the nominal performance, but as well the conditions on $L_d(z^{-1})$ that guarantee the stability of the closed-loop system. The linearized constraints are given by [75]:

$$|W_1(e^{-j\omega})[1 + L_d(e^{-j\omega})]| - \mathrm{Re}\{[1 + L_d(e^{j\omega})][1 + L(e^{-j\omega}, \boldsymbol{\rho})]\} < 0, \forall \omega \in [0, \omega_N], \qquad (2.8)$$

where $\mathrm{Re}\{\cdot\}$ denotes the real part of the complex number, and ω_N represents the Nyquist frequency of the system.

These results are extended here to the case of gain-scheduled controller design. First, notice that the desired open-loop transfer function can be a function of $\boldsymbol{\theta}$ for the gain-scheduled controller design. This leads to the following constraints for the gain-scheduled controller design:

$$|W_1(e^{-j\omega})[1 + L_d(e^{-j\omega}, \boldsymbol{\theta})]| - \mathrm{Re}\{[1 + L_d(e^{j\omega}, \boldsymbol{\theta})][1 + L(e^{-j\omega}, \boldsymbol{\rho}(\boldsymbol{\theta}))]\} < 0, \forall \omega \in [0, \omega_N], \forall \boldsymbol{\theta} \in \Theta.$$
$$(2.9)$$

It has to be proven that the inequality in (2.7) is met if the above inequality is satisfied. Knowing that the real part of a complex number is always smaller than or equal to its absolute value,

from (2.9) can be concluded that

$$|W_1(e^{-j\omega})[1+L_d(e^{-j\omega},\boldsymbol{\theta})]| - |1+L_d(e^{j\omega},\boldsymbol{\theta})||1+L(e^{-j\omega},\boldsymbol{\rho}(\boldsymbol{\theta}))| < 0, \forall\omega \in [0,\omega_N], \forall\boldsymbol{\theta} \in \Theta. \quad (2.10)$$

If $L_d(z^{-1},\boldsymbol{\theta})$ is chosen so that it satisfies the Nyquist criterion for $\forall\boldsymbol{\theta} \in \Theta$, then $|1+L_d(e^{-j\omega},\boldsymbol{\theta})| = |1+L_d(e^{j\omega},\boldsymbol{\theta})| > 0$. Hence (2.10) is equivalent to

$$|W_1(e^{-j\omega})| < |1+L(e^{-j\omega},\boldsymbol{\rho}(\boldsymbol{\theta}))|, \quad \forall\omega \in [0,\omega_N], \forall\boldsymbol{\theta} \in \Theta, \quad (2.11)$$

which is equivalent to (2.7). Next, it can be shown that the number of encirclements of the critical point by $L(\boldsymbol{\theta})$ and $L_d(\boldsymbol{\theta})$ is equal. This is essential as it proves stability of the closed-loop system for frozen values of scheduling parameters.

Theorem 2.1 *Suppose that the following inequality*

$$|W_1(e^{-j\omega})[1+L_d(e^{-j\omega},\boldsymbol{\theta})]| - \mathrm{Re}\{[1+L_d(e^{j\omega},\boldsymbol{\theta})][1+L(e^{-j\omega},\boldsymbol{\rho}(\boldsymbol{\theta}))]\} < 0 \quad (2.12)$$

is satisfied for $\forall\omega \in [0,\omega_N], \forall\boldsymbol{\theta} \in \Theta$. If $L_d(e^{-j\omega},\boldsymbol{\theta})$ is such a transfer function that it satisfies Nyquist criterion for $\forall\boldsymbol{\theta} \in \Theta$, then transfer function $L(e^{-j\omega},\boldsymbol{\theta})$ is stable for $\forall\boldsymbol{\theta} \in \Theta$.

Proof. The lines of the proof in [75] are followed. Observe the inequality (2.12) for some $\boldsymbol{\theta}_1 \in \Theta$. It trivially implies:

$$\mathrm{Re}\{[1+L_d(e^{j\omega},\boldsymbol{\theta}_1)][1+L(e^{-j\omega},\boldsymbol{\rho}(\boldsymbol{\theta}_1))]\} > 0, \quad \forall\omega \in [0,\omega_N]. \quad (2.13)$$

If wno denotes the winding number around the origin of a transfer function, then the last inequality can equivalently be rewritten as

$$\mathrm{wno}\{[1+L_d(e^{j\omega},\boldsymbol{\theta}_1)][1+L(e^{-j\omega},\boldsymbol{\rho}(\boldsymbol{\theta}_1))]\} = 0. \quad (2.14)$$

The transfer functions $L_d(z^{-1},\boldsymbol{\theta}_1)$ and $L(z^{-1},\boldsymbol{\rho}(\boldsymbol{\theta}_1))$ are assumed to be causal. This implies that $L_d(e^{j\omega},\boldsymbol{\theta}_1)$ and $L(e^{-j\omega},\boldsymbol{\rho}(\boldsymbol{\theta}_1))$ are constant or zero on the part of Nyquist contour with infinite radius. Hence the wno depends only on the variations caused by the imaginary axis. Therefore

$$\mathrm{wno}\{1+L_d(e^{-j\omega},\boldsymbol{\theta}_1)\} = \mathrm{wno}\{1+L(e^{-j\omega},\boldsymbol{\rho}(\boldsymbol{\theta}_1))\}. \quad (2.15)$$

If $L_d(e^{-j\omega},\boldsymbol{\theta}_1)$ is chosen so that it satisfies the Nyquist criterion, $L(e^{-j\omega},\boldsymbol{\theta}_1)$ will satisfy it as well. This applies to $\forall\boldsymbol{\theta}_1 \in \Theta$. $\square$

The closed-loop stability is ensured in the case that $L_d(\boldsymbol{\theta})$ satisfies the Nyquist criterion for all values of $\boldsymbol{\theta}$ (e.g. for stable plant models this means that $L_d(\boldsymbol{\theta})$ should not turn around -1). On the other hand, if the plant model or the controller have unbounded infinity-norm (i.e. the poles on the unit circle), these poles should be included in $L_d(\boldsymbol{\theta})$ (see [75]) to ensure the satisfaction of Nyquist criterion for $L(\boldsymbol{\theta})$.
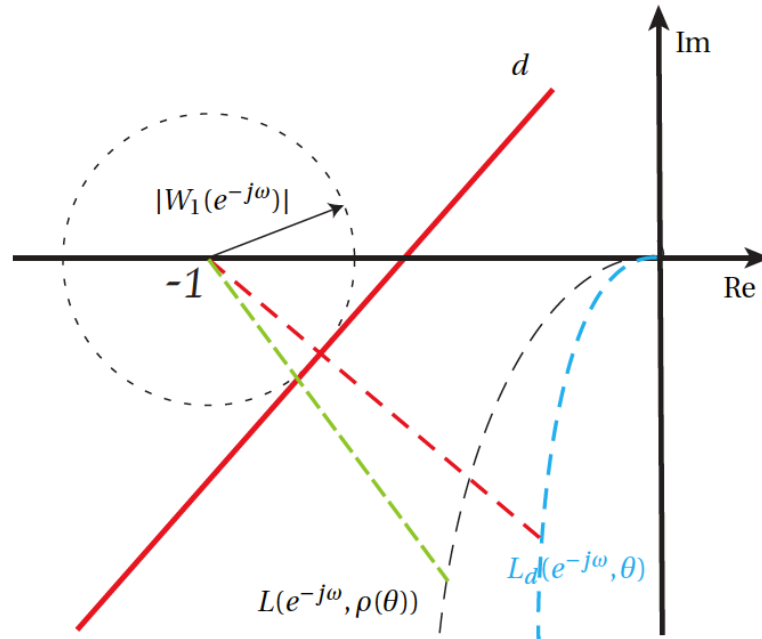
Figure 2.1 – Graphical interpretation of the performance condition (2.9)

The graphical interpretation of this method is given in Fig.2.1. It is well known that the $\mathcal{H}_\infty$ performance condition in (2.7) is satisfied if and only if there is no intersection between $L(e^{-j\omega}, \boldsymbol{\rho}(\boldsymbol{\theta}))$ and a circle centered at -1 with radius $|W_1(e^{j\omega})|$ [78]. It is clear that this condition is satisfied if $L(e^{-j\omega}, \boldsymbol{\rho}(\boldsymbol{\theta}))$ lies at the side of d that excludes -1 for all ω and $\boldsymbol{\theta}$, where d is tangent to the circle and orthogonal to the line connecting -1 to $L_d(e^{-j\omega}, \boldsymbol{\theta})$. The conservatism of the proposed approach depends on the choice of L_d [75]. It is clear that if $L_d = L$ there is no conservatism. Therefore, choosing L_d as close as possible to L reduces significantly this conservatism. In the case that $\|W_1(z^{-1})S(z^{-1}, \boldsymbol{\rho}(\boldsymbol{\theta}))\|_\infty$ is minimized as a performance criterion, an iterative approach can be used for the choice of L to reduce the conservatism. The idea is that at each iteration L of the previous iteration is used as L_d. This kind of iterative algorithm ensures that performance cost decreases over successive iterations, as the controller at the ith iteration also belongs to the new convex solution set generated by $L_d = L^{(i)}$.

2.3.2 Optimization problem

It can be proven that proposed iterative algorithm actually converges to the point satisfying the first-order necessary conditions of optimality. As the cost is decreasing, in practice this means that a local minimum or a saddle point is reached. The proof is based on the fact that the given algorithm can be considered as a particular instance of the Convex-Concave Optimization Program (CCOP) for which results on convergence exist in the literature. First, a short introduction to the convex-concave optimization paradigm is given.

In [79] the optimization program with cost equal to the difference of two convex functions and linear constraints is studied. It is proven that the local minimum can be found performing the successive convex approximations around the solution from the last iteration. This result is extended in [80], where except the cost function the constraints are as well considered to be equal to difference of some convex functions.

Lemma 2.1 *[80] Assume that the following optimization problem is to be solved:*

$$\underset{\boldsymbol{x}}{minimize} \quad f_0(\boldsymbol{x}) - g_0(\boldsymbol{x})$$
$$subject\ to \quad f_i(\boldsymbol{x}) - g_i(\boldsymbol{x}) \leq 0,\ i = 1,\dots,m, \tag{2.16}$$

where all functions $f_i(\boldsymbol{x})$ and $g_i(\boldsymbol{x})$, for $i = 0,\dots,m$, are convex in $\boldsymbol{x}$. The following algorithm can be applied to solve the given optimization problem:

Step 1: *set $k = 0$ and choose initial point $\boldsymbol{x}^{(0)}$;*

Step 2: *form $\hat{g}_i(\boldsymbol{x};\boldsymbol{x}^{(k)}) = g_i(\boldsymbol{x}^{(k)}) + \left[\nabla g_i(\boldsymbol{x}^{(k)})\right]^T (\boldsymbol{x} - \boldsymbol{x}^{(k)})$ for $i = 0,\dots,m$;*
solve for $\boldsymbol{x}^{(k+1)}$ the following convex optimization problem:

$$\underset{\boldsymbol{x}^{(k+1)}}{minimize} \quad f_0(\boldsymbol{x}) - \hat{g}_0(\boldsymbol{x};\boldsymbol{x}^{(k)})$$
$$subject\ to \quad f_i(\boldsymbol{x}) - \hat{g}_i(\boldsymbol{x};\boldsymbol{x}^{(k)}) \leq 0,\ i = 1,\dots,m; \tag{2.17}$$

Step 3: *if stopping criterion is satisfied exit; otherwise set $k = k + 1$ and jump to **Step 2**.*

The stopping criterion can for example be the lack of progress in the cost, i.e.

$$(f_0(\boldsymbol{x}^{(k)}) - g_0(\boldsymbol{x}^{(k)})) - (f_0(\boldsymbol{x}^{(k+1)}) - g_0(\boldsymbol{x}^{(k+1)})) \leq \epsilon_{\text{stop}}. \tag{2.18}$$

If such an algorithm is applied, it is guaranteed that the solution x^* corresponds to the local optimum, or saddle point, of the initial optimization problem.

This lemma directly leads to the proof of the convergence of the applied design algorithm.

Theorem 2.2 *Assume that the following optimization problem is given:*

$$\underset{\gamma,\boldsymbol{\rho}}{minimize} \quad \gamma$$
$$subject\ to \quad \|W_1(e^{-j\omega})S(e^{-j\omega},\boldsymbol{\rho}(\boldsymbol{\theta}))\|_\infty < \gamma, \qquad \forall \omega \in [0,\omega_N], \forall \boldsymbol{\theta} \in \Theta. \tag{2.19}$$

Let it be solved using the following optimization algorithm:

Step 1: *set $k = 0$ and choose $L_d(e^{-j\omega},\boldsymbol{\rho}(\boldsymbol{\theta}))$ satisfying the same assumptions as in Theorem 2.1; choose small $\epsilon_{stop} > 0$;*

Step 2: *if $k = 0$ use the initial $L_d(e^{-j\omega}, \boldsymbol{\theta})$; otherwise set*

$$L_d(e^{-j\omega}, \boldsymbol{\theta}) = (\boldsymbol{\rho}^{(k)})^T(\boldsymbol{\theta})\boldsymbol{\phi}(e^{-j\omega})G(e^{-j\omega}, \boldsymbol{\theta});$$

solve for $(\gamma_{\mathrm{inv}}, \boldsymbol{\rho})$ the following convex optimization problem:

$$\begin{aligned}
\underset{\gamma_{\mathrm{inv}}, \boldsymbol{\rho}}{minimize} \quad & -\gamma_{\mathrm{inv}} \\
subject\ to \quad & \gamma_{\mathrm{inv}}|W_1(e^{-j\omega})[1 + L_d(e^{-j\omega}, \boldsymbol{\theta})]| \\
& - \mathrm{Re}\{[1 + L_d(e^{j\omega}, \boldsymbol{\theta})][1 + L(e^{-j\omega}, \boldsymbol{\rho}(\boldsymbol{\theta}))]\} < 0, \forall \omega \in [0, \omega_N], \forall \boldsymbol{\theta} \in \Theta;
\end{aligned} \tag{2.20}$$

set $\gamma^{(k+1)} = \gamma_{\mathrm{inv}}^{-1}$ and $\boldsymbol{\rho}^{(k+1)} = \boldsymbol{\rho}$;

Step 3: *if $\gamma^{(k)} - \gamma^{(k+1)} < \epsilon_{stop}$ exit with $\boldsymbol{\rho}^* = \boldsymbol{\rho}^{(k+1)}$ and $\gamma^* = \gamma^{(k+1)}$; otherwise set $k = k + 1$ and jump to **Step 2**.*

Then, this algorithm converges to the point $(\gamma^*, \boldsymbol{\rho}^*)$ at which the first-order necessary conditions of optimality are satisfied.

Proof. Observe that γ_{inv} is a shorthand for γ^{-1}. The cost is a linear function of optimization variable vector $\boldsymbol{x}^T = [\gamma_{\mathrm{inv}}, \boldsymbol{\rho}^T]^T$, so it satisfies assumptions of the described algorithm. Next, observe for $\forall \omega \in [0, \omega_N]$ and $\forall \boldsymbol{\theta} \in \Theta$ functions

$$f(\omega, \boldsymbol{\theta}, \boldsymbol{x}) = \gamma_{\mathrm{inv}}|W_1(e^{-j\omega})| \text{ and } g(\omega, \boldsymbol{\theta}, \boldsymbol{x}) = |1 + L(e^{-j\omega}, \boldsymbol{\rho}(\boldsymbol{\theta}))|. \tag{2.21}$$

These two functions are convex. Next, as

$$\gamma_{\mathrm{inv}}|W_1(e^{-j\omega})| - |1 + L(e^{-j\omega}, \boldsymbol{\rho}(\boldsymbol{\theta}))| < 0 \Leftrightarrow \|W_1(e^{-j\omega})S(e^{-j\omega}, \boldsymbol{\rho}(\boldsymbol{\theta}))\|_\infty < \gamma \tag{2.22}$$

for $\forall \omega \in [0, \omega_N]$ and $\forall \boldsymbol{\theta} \in \Theta$, the inequality $f(\omega, \boldsymbol{\theta}, \boldsymbol{x}) - g(\omega, \boldsymbol{\theta}, \boldsymbol{x}) < 0$ is equivalent to the constraint of the original optimization problem.

The partial derivative of $g(\omega, \boldsymbol{\theta}, \boldsymbol{x})$ over $\rho_{i,j}$ for $i = 1, \dots, n$ and $j = 0, \dots, n_\theta$ at $\boldsymbol{\rho} = \hat{\boldsymbol{\rho}}$ is given by

$$\begin{aligned}
\left.\frac{\partial g(\omega, \boldsymbol{\theta})}{\rho_{i,j}}\right|_{\boldsymbol{\rho} = \hat{\boldsymbol{\rho}}} &= \frac{2\left[1 + \mathrm{Re}\{L(e^{-j\omega}, \hat{\boldsymbol{\rho}}(\boldsymbol{\theta}))\}\right]\mathrm{Re}\{h_{i,j}(\boldsymbol{\theta})\boldsymbol{\phi}(e^{-j\omega})G(e^{-j\omega}, \boldsymbol{\theta})\}}{2\sqrt{\left[1 + \mathrm{Re}\{L(e^{-j\omega}, \hat{\boldsymbol{\rho}}(\boldsymbol{\theta}))\}\right]^2 + \left[\mathrm{Im}\{L(e^{-j\omega}, \hat{\boldsymbol{\rho}}(\boldsymbol{\theta}))\}\right]^2}} + \\
&\quad + \frac{2\,\mathrm{Im}\{L(e^{-j\omega}, \hat{\boldsymbol{\rho}}(\boldsymbol{\theta}))\}\mathrm{Im}\{h_{i,j}(\boldsymbol{\theta})\boldsymbol{\phi}(e^{-j\omega})G(e^{-j\omega}, \boldsymbol{\theta})\}}{2\sqrt{\left[1 + \mathrm{Re}\{L(e^{-j\omega}, \hat{\boldsymbol{\rho}}(\boldsymbol{\theta}))\}\right]^2 + \left[\mathrm{Im}\{L(e^{-j\omega}, \hat{\boldsymbol{\rho}}(\boldsymbol{\theta}))\}\right]^2}}.
\end{aligned} \tag{2.23}$$

Next, let $L_d(z^{-1}, \boldsymbol{\theta}) = L(z^{-1}, \boldsymbol{\rho}^{(k)}(\boldsymbol{\theta}))$. Also, let L_d denote $L_d(e^{-j\omega}, \boldsymbol{\theta})$ and L denote $L(e^{-j\omega}, \boldsymbol{\rho}(\boldsymbol{\theta}))$

in the following equation. Using expressions (2.23) it can be proven that

$$
\begin{aligned}
g(\boldsymbol{x}^{(k)}) + \left[\nabla g(\boldsymbol{x}^{(k)})\right]^T (\boldsymbol{x} - \boldsymbol{x}^{(k)}) = \\
= \frac{[1 + \operatorname{Re}\{L_d\}]\,[\operatorname{Re}\{L\} - \operatorname{Re}\{L_d\}] + \operatorname{Im}\{L_d\}\,[\operatorname{Im}\{L\} - \operatorname{Im}\{L_d\}] + |1 + L_d|^2}{|1 + L_d|}.
\end{aligned}
\tag{2.24}
$$

After some simple manipulations with real and imaginary parts of L and L_d it can be proven that the linearized version of the constraint $f(\omega, \boldsymbol{\theta}, \boldsymbol{x}) - g(\omega, \boldsymbol{\theta}, \boldsymbol{x}) < 0$ is given by

$$
\gamma_{\mathrm{inv}} |W_1(e^{-j\omega})| - \frac{\operatorname{Re}\{[1 + L_d(e^{j\omega}, \boldsymbol{\theta})][1 + L(e^{-j\omega}, \boldsymbol{\rho}(\boldsymbol{\theta}))]\}}{|1 + L_d(e^{-j\omega}, \boldsymbol{\theta})|} < 0,
\tag{2.25}
$$

or equivalently

$$
\gamma_{\mathrm{inv}} |W_1(e^{-j\omega})[1 + L_d(e^{-j\omega}, \boldsymbol{\theta})]| - \operatorname{Re}\{[1 + L_d(e^{j\omega}, \boldsymbol{\theta})][1 + L(e^{-j\omega}, \boldsymbol{\rho}(\boldsymbol{\theta}))]\} < 0.
\tag{2.26}
$$

So, performing the linearization of constraints of the original optimization problem around the current solution $\boldsymbol{x}^{(k)}$ leads to constraints in algorithm proposed in the Theorem definition. However, this implies that the algorithm from the Theorem definition belongs to the class of algorithms described in Lemma 2.1. Hence the conclusion on convergence of the solution to the local minimum or saddle point is valid by Lemma 2.1. □

Remark 2.1 *Algorithm from Lemma 2.1 is initialized using some initial point $\boldsymbol{x}^{(0)}$. Here it would mean that stabilizing initial controller with parameter vector $\boldsymbol{\rho}$ and appropriate value of $\gamma^{(0)}$ have to be known. This is, however, not always the case in practice. Instead, algorithm in Theorem 2.2 is initialized using some reasonable choice of desired open-loop transfer function $L_d(z^{-1}, \boldsymbol{\theta})$. Based on it in the first iteration a feasible controller and appropriate performance cost may be obtained, and starting from the next iteration the algorithm exactly matches the structure from Lemma 2.1.*

Remark 2.2 *The constraints in (2.9) should be satisfied for $\forall \omega \in [0, \omega_N]$ and for $\forall \boldsymbol{\theta} \in \Theta$. This leads to an infinite number of constraints that is numerically intractable. A practical approach is to choose finite grids for ω and the scheduling parameter $\boldsymbol{\theta}$ and find a feasible solution for the grid points. This leads to a large number of linear constraints that can be handled efficiently by linear programming solvers. By increasing the number of scheduling parameters, the number of constraints will drastically increase, which will in turn elevate the optimization time. In this case a scenario approach can be used to guarantee feasibility of the optimization problem with a predefined probability level when only constraints for a finite number of randomly chosen scheduling parameters [81] are satisfied. Some of the effects of gridding in frequency and additional constraints that can be imposed for ensuring good behavior between the grid points are described in [82].*
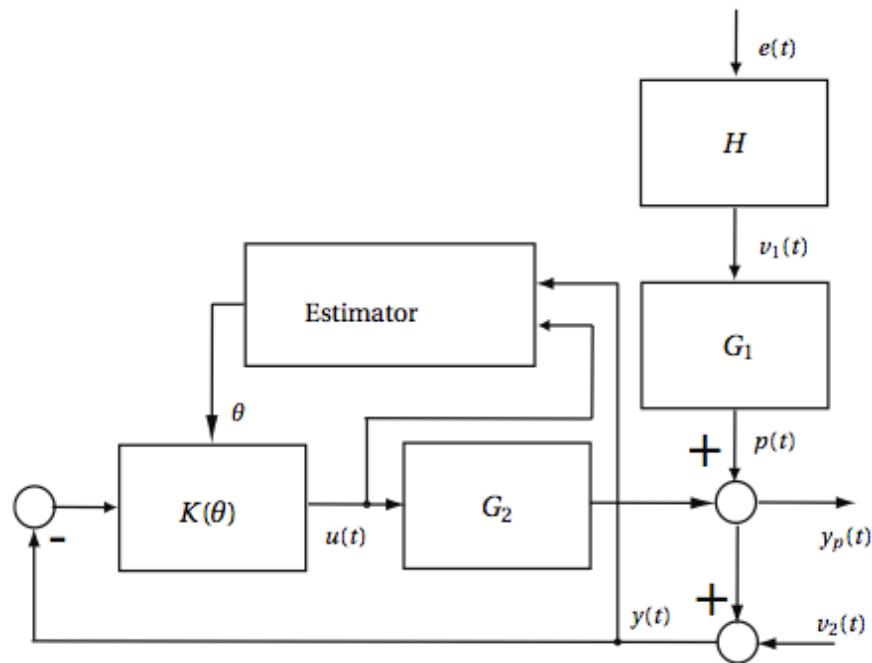
Figure 2.2 – Block diagram of the active suspension system

2.4   Active Suspension Benchmark

The objective of the benchmark is to design a controller for the rejection of unknown/time-varying multiple narrow band disturbances located in a given frequency region. The proposed controllers are applied to the active suspension system of the Control Systems Department in Grenoble (GIPSA - lab) [76]. The block diagram of the active suspension system together with the proposed gain scheduled controller is shown in Fig. 2.2.

The system is excited by a sinusoidal disturbance $v_1(t)$ generated using a computer-controlled shaker. Disturbance $v_1(t)$ can be represented as a white noise signal $e(t)$ filtered through the disturbance model H. The transfer function G_1 between the disturbance input and the residual force in open-loop, $y_p(t)$, is called the primary path. The signal $y(t)$ is a measured voltage that represents the residual force, affected by the measurement noise. The secondary path is the transfer function G_2 between the output of the controller $u(t)$ and the residual force in open-loop. The control input drives an inertial actuator through a power amplifier. The sampling frequency for both identification and control is 800Hz, as chosen by the benchmark organizers. The magnitude Bode diagram of the primary and the secondary path models sampled at 800Hz are shown in Fig. 2.3. It can be noticed that several high resonance modes are present in the system.

The disturbance is supposed to consist of one to three sinusoids. This leads to three different levels of benchmark, depending on the number of sinusoids in the disturbance. Disturbance

Bode Diagram
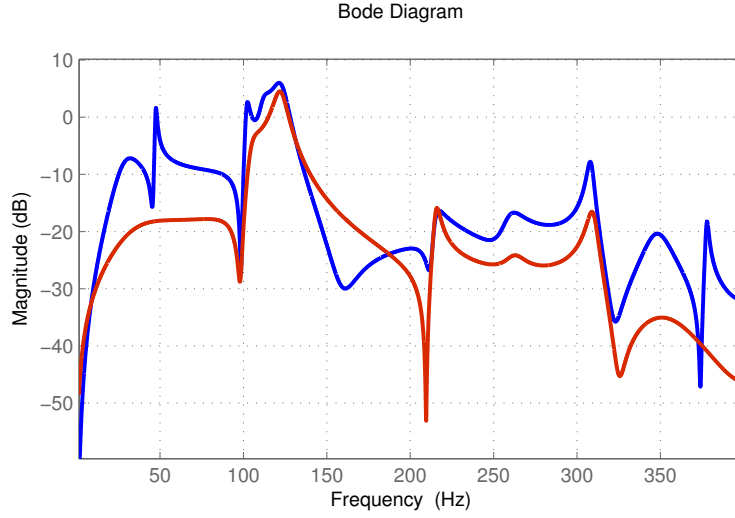
Figure 2.3 – Frequency response of the primary (red) and the secondary path (blue)

frequencies are unknown in advance, but known lie in an interval from 50 to 95Hz. The controller should reject the disturbance as fast as possible. The control structure and the design method are explained in detail for Level 1. The extension to the other levels is straightforward.

2.4.1 Controller design for benchmark Level 1

An $\mathcal{H}_\infty$ gain-scheduled controller, based on the internal model principle to ensure the asymptotic disturbance rejection, is considered. The following structure is proposed:

$$K(z^{-1},\theta) = [K_0(z^{-1}) + \theta K_1(z^{-1})] M(z^{-1},\theta) \tag{2.27}$$

where K_0 and K_1 are FIR filters of order n and

$$H(z^{-1},\theta) = \frac{1}{1 + \theta z^{-1} + z^{-2}} \tag{2.28}$$

is the disturbance model of a sinusoidal disturbance with frequency $f_1 = \cos^{-1}(-\theta/2)/2\pi$. The transient response can be improved by the minimization of the infinity norm of the transfer function HG_1S between the disturbance and the output. However, it is often difficult to obtain a good model of the disturbance path in reality, so the primary path model G_1 cannot be used in the controller design. To overcome this, in the optimization it is replaced by a constant gain. This approximation is actually very reasonable as in the disturbance frequency range gain of G_1 is almost constant, as it can be observed in Figure 2.3. On the other hand, in order to increase the robustness and prevent the activity of the command input at frequencies where the gain of the secondary path is low, the infinity norm of the input sensitivity function $\|KS\|_\infty$ should be kept low. A constraint on the maximum of the modulus of the sensitivity function

$\|S\|_\infty < 2$ (6dB) is considered according to the benchmark requirements in order to prevent the amplification of the noise.

A gain-scheduled controller is designed using the following steps:

1. A very fine frequency grid of a resolution 0.5 rad/s (i.e. 5027 frequency points) is considered due to high resonance modes in the secondary path model.

2. The interval of the disturbance frequencies is divided in 46 points (a resolution of 1Hz). This corresponds to 46 points in the interval $[-1.8478, -1.4686]$ to which the scheduling parameter θ belongs.

3. The following optimization problem is solved:

$$\min \gamma$$
$$\gamma^{-1}\left[|H(e^{-j\omega_k},\theta_i)| + |K(e^{-j\omega_k},\boldsymbol{\rho}(\theta_i))|\right] \times |1 + L_d(e^{-j\omega_k},\theta_i)| -$$
$$- R_e\{[1 + L_d(e^{j\omega_k},\theta_i)][1 + L(e^{-j\omega_k},\boldsymbol{\rho}(\theta_i))]\} < 0,$$
$$\qquad\qquad\qquad\qquad\qquad\qquad\qquad\qquad\qquad\qquad (2.29)$$
$$0.5|1 + L_d(e^{-j\omega_k},\theta_i)| - R_e\{[1 + L_d(e^{j\omega_k},\theta_i)][1 + L(e^{-j\omega_k},\boldsymbol{\rho}(\theta_i))]\} < 0,$$
$$\text{for } k = 1,\dots,5027, \quad i = 1,\dots,46.$$

The first constraint represents the convexification of $\||HS| + |KS|\|_\infty < \gamma$, while the second one that of $\|S\|_\infty < 2$. This is a convex optimization problem for fixed γ and can be solved by an iterative bisection algorithm.

Remarks:

- The controller order (the order of the FIR models for K_0 and K_1 in (2.27)) is chosen equal to 10 (the controller order is increased gradually to obtain acceptable results). Note that it is much less than the order of the plant model, which is equal to 26.

- The desired open-loop transfer functions are chosen as $L_d(\theta_i) = K_{ini}(\theta_i)G_2$, where $K_{ini}(\theta_i)$ are stabilizing controllers computed by the pole placement technique.

- For convenience, the internal model is considered as a part of the plant model, i.e. $G(\theta) = H(\theta)G_2$, and after the controller design, it is returned to the controller.

- After 7 iterations for the bisection algorithm $\gamma_{\min} = 1.68$ is obtained. The total computation time is about 11 minutes on a personal computer (16GB of DDR3 RAM memory at 1600MHz and processor Intel Core i7 running at 3.4GHz).
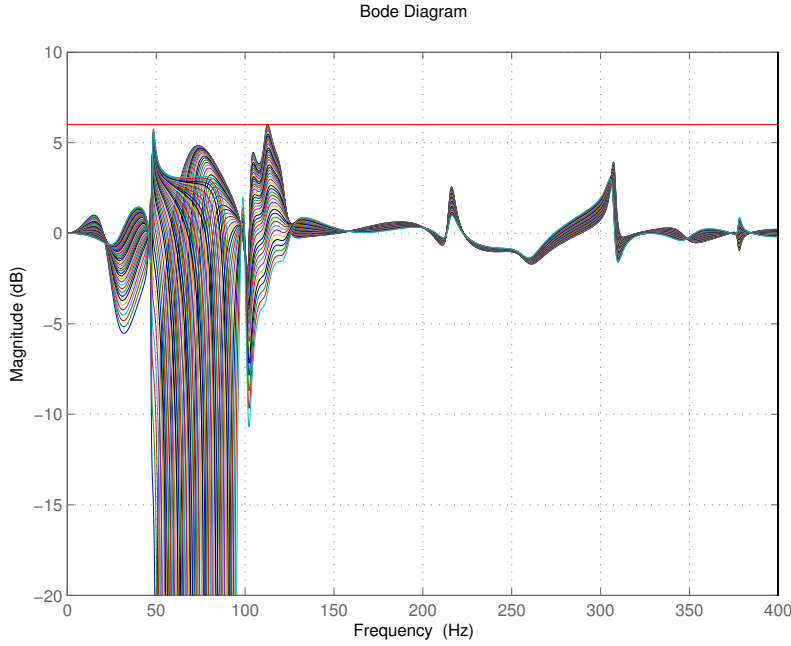
Figure 2.4 – Magnitude plot of the output sensitivity functions S
for disturbance frequencies from 50Hz to 95Hz

The parameters of the final designed gain-scheduled controller with structure (2.27) are:

$$
\begin{aligned}
K_0(z^{-1}) &= 3.669 - 2.311z^{-1} - 0.7776z^{-2} + 0.7171z^{-3} + 3.424z^{-4} - 5.402z^{-5} \\
&\quad + 5.077z^{-6} - 5.143z^{-7} + 4.637z^{-8} - 2.01z^{-9} + 0.5125z^{-10}, \\
K_1(z^{-1}) &= 2.241 - 1.293z^{-1} - 0.7633z^{-2} + 0.4309z^{-3} + 2.673z^{-4} - 3.921z^{-5} \\
&\quad + 3.117z^{-6} - 2.638z^{-7} + 2.476z^{-8} - 1.15z^{-9} + 0.3444z^{-10}.
\end{aligned}
$$

This gain-scheduled controller gives very good transient performance and satisfies the constraint on the maximum modulus of the sensitivity function for all values of the scheduling parameter. Figure 2.4 and Fig. 2.5 show the magnitude of the output sensitivity function S and the input sensitivity function KS, respectively, for 46 gridded values of the disturbance frequency. One can observe very good attenuation at the disturbance frequencies and the satisfaction of the modulus margin of at least 6dB for all disturbance frequencies.

Bode Diagram
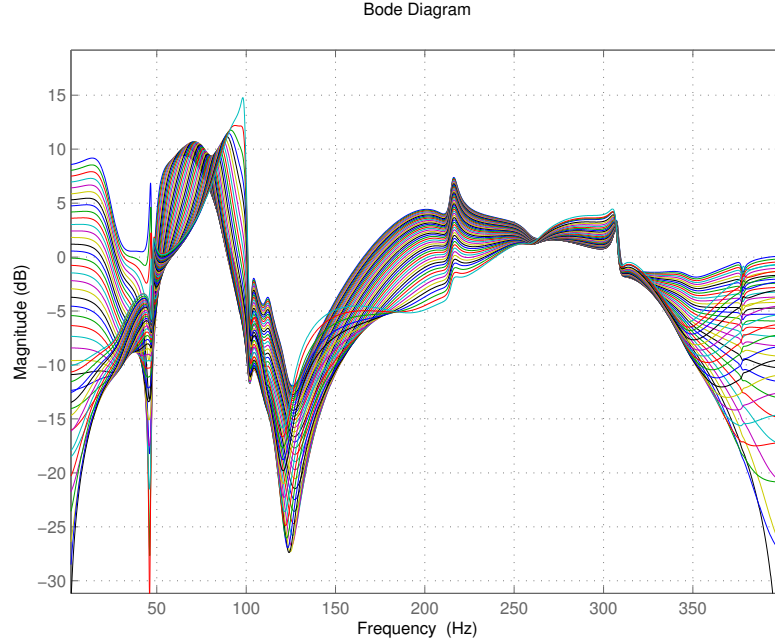
Figure 2.5 – Magnitude plot of the input sensitivity functions KS
for disturbance frequencies from 50Hz to 95Hz

2.4.2   Controller design for benchmark Level 2

In this level of the benchmark, two sinusoidal disturbances should be rejected. The structure of the gain scheduled controller is given by (z^{-1} is omitted):

$$K(\theta_1, \theta_2) = (K_0 + \theta_1 K_1 + \theta_2 K_2) H(\theta_1, \theta_2) \tag{2.30}$$

where K_0, K_1 and K_2 are the 8th order FIR filters and

$$H(\theta_1, \theta_2) = \frac{1}{1 + \theta_1 z^{-1} + \theta_2 z^{-2} + \theta_1 z^{-3} + z^{-4}}. \tag{2.31}$$

By considering a hard constraint on the magnitude of the sensitivity function $\|(1+K(\theta_1,\theta_2)G_2)^{-1}\|_\infty <$ 2.24 (7dB) the optimization becomes infeasible. Therefore, the following soft constraint is considered for optimization:

$$|H(\theta_1,\theta_2)(1 + K(\theta_1,\theta_2)G_2)^{-1}| + |(1 + K(\theta_1,\theta_2)G_2)^{-1}| < \gamma, \quad \forall \omega, \forall \theta_1, \forall \theta_2, \tag{2.32}$$

and γ is minimized. The first term on the left hand side represents the approximation of the disturbance path impulse response (approximating the unknown transfer function G_1 by gain of 1). By minimizing its ∞-norm the transient time is indirectly reduced, with a tradeoff between fast response and robustness, coming from the second term.

As there are two scheduling parameters at this level of benchmark, a resolution of 1Hz for each sinusoidal disturbance leads to $46^2/2 = 1058$ grid points. This increases the number of constraints by a factor of 23 with respect to that of Level 1. Moreover, the resolution of the frequency grid step is reduced from 0.5 rad/s to 0.2 rad/s, which further increases the number of constraints. The number of variables is also increased, so instead of 22 from level 1 now there are in total 27 variables (the coefficients of three FIR filters of order 8). In order to obtain a faster optimization problem, the scenario approach is used. From the set of 1058 frequency pairs, 50 samples are chosen randomly and the constraints are considered just for these frequencies. The stability of the closed-loop system is verified a posteriori for all 1058 frequency pairs. This makes the probability of stability constraint violation (between the grid points) very low. The computed controller, however, destabilizes the real system for disturbance frequency pair (50-70)Hz. The main reason for this is the modeling error for the secondary path model around 50Hz. Therefore, a new model for the secondary path provided by the benchmark organizers with smaller modeling error around 50Hz is used for the controller design. A new controller is designed using the scenario approach and $\gamma_{\min} = 10.62$ is achieved after 11 iterations, with a total computation time of about 15 minutes.

The controller parameters are:

$$K_0(z^{-1}) = -4.835 + 43.93z^{-1} - 98.74z^{-2} + 96.2z^{-3}$$
$$- 0.3158z^{-4} - 100.8z^{-5} + 117.5z^{-6} - 64.79z^{-7} + 16.35z^{-8},$$

$$K_1(z^{-1}) = -24.02 + 122.4z^{-1} - 226.7z^{-2} + 204.9z^{-3}$$
$$- 52.21z^{-4} - 71.05z^{-5} + 80.54z^{-6} - 36.53z^{-7} + 8.671z^{-8},$$

$$K_2(z^{-1}) = -16.05 + 77.44z^{-1} - 139.6z^{-2} + 124.7z^{-3}$$
$$- 37.19z^{-4} - 28.47z^{-5} + 31.64z^{-6} - 11.83z^{-7} + 2.561z^{-8}.$$

Figures 2.6 and 2.7 show the magnitude of the output and input sensitivity functions, respectively, for *known* disturbance frequencies taken from the following set:

$$\mathscr{F} = \{(50,70),(55,75),(60,80),(65,85),(70,90)\}$$

The attenuation of at least 40 dB is obtained for all frequencies but the maximum of the output sensitivity function is greater than 7 dB in some frequencies.

2.4.3 Controller design for benchmark Level 3

Although good performance can be obtained for linear controller design for every triplet of disturbance frequencies, a simple gain-scheduled controller that satisfies all constraints could
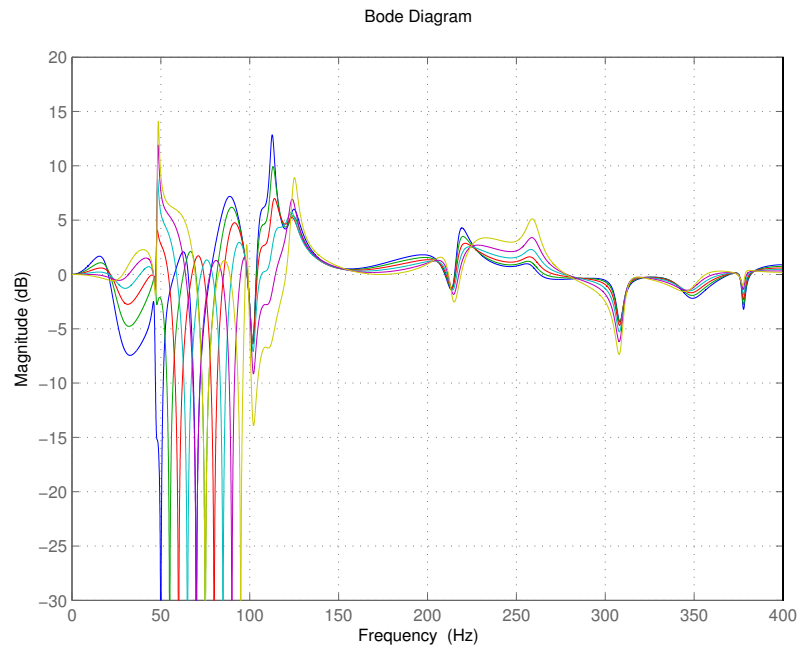
Figure 2.6 – Magnitude of the output sensitivity function for disturbance frequencies in $\mathscr{F}$
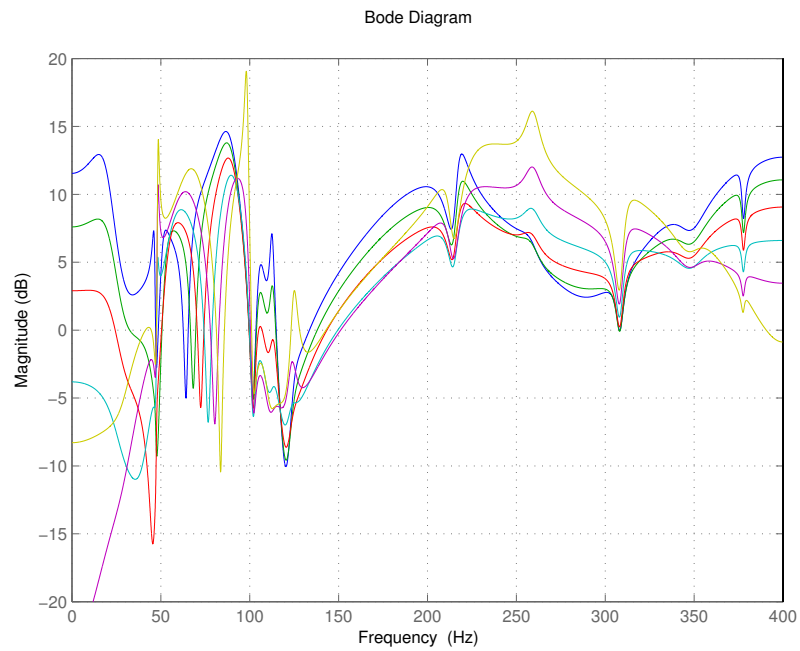
Figure 2.7 – Magnitude of the input sensitivity function for disturbance frequencies in $\mathscr{F}$

not be obtained by the proposed approach. In fact the optimization problem becomes infeasible for affine dependence of the controller parameters on the scheduling parameters. If the constraints are relaxed, the resulting stabilizing controller does not lead to good performance even for known disturbance frequencies.

It is important to emphasize that there is no theoretical limitation for having three or even more disturbance frequencies. However, increasing the number of frequencies increases the complexity of the optimization problem. This problem could be fixed by designing better initial controllers for each fixed disturbance frequency and use of these controllers for computing L_d. In addition, the basis functions can be altered to produce the desired effect. The participation was taken only in the first and the second level of the benchmark for the reason of approaching benchmark deadline.

2.4.4 Estimator design

The scheduling parameter θ used in the internal model of disturbance in (2.28) is estimated using a parameter adaptation algorithm. To estimate the parameters of the disturbance model, the disturbance signal $p(t)$ has to be known (see Fig. 2.2). If $p(t)$ is modeled as the output of an ARMA model with white noise as input, then

$$D_p(q^{-1})p(t) = N_p(q^{-1})e(t), \tag{2.33}$$

where $e(t)$ is a zero mean white noise with unknown variance. Estimation of the parameters of N_p and D_p could be performed by the standard *Recursive Extended Least Squares* method [83]. Since $p(t)$ is not available, it is estimated using the measured signal $y(t)$ and the known model of the secondary path. Fig. 2.2 leads to:

$$p(t) = y(t) - \frac{q^{-d}B(q^{-1})}{A(q^{-1})}u(t) - v_2(t), \tag{2.34}$$

where $\dfrac{q^{-d}B(q^{-1})}{A(q^{-1})}$ is the parametric model of the secondary path G_2. Since $v_2(t)$ is a zero mean noise signal, unbiased estimate of $p(t)$ is given as

$$\bar{p}(t) = y(t) + [A(q^{-1}) - 1][y(t) - \bar{p}(t)] - B(q^{-1})u(t - d).$$

For the asymptotic rejection of a sinusoidal disturbance, there is no need to identify the whole model of the disturbance path, i.e. HG_1 as shown in Figure 2.2. The information needed for the controller scheduling is the frequency of the disturbance. So, by setting $D_p(q^{-1}, \theta) = 1 - \theta q^{-1} + q^{-2}$ (for Level 1) and $N_p(q^{-1}) = 1 + c_1 q^{-1} + c_2 q^{-2}$, a simple parameter

estimation algorithm can be developed. Let the following be defined:

$$
\begin{aligned}
z(t+1) &= \bar{p}(t+1) + \bar{p}(t-1) & \text{(2.35)} \\
\boldsymbol{\psi}^T(t) &= [-\bar{p}(t), \varepsilon(t), \varepsilon(t-1)]^T & \text{(2.36)} \\
\boldsymbol{\Upsilon}^T(t) &= [\theta, c_1, c_2]^T & \text{(2.37)}
\end{aligned}
$$

where $\varepsilon(t) = z(t) - \hat{z}(t)$ is the a posteriori prediction error. Then the following recursive adaptation algorithm can be used to estimate the scheduling parameter θ:

$$
\begin{aligned}
\varepsilon^\circ(t+1) &= z(t+1) - \hat{\boldsymbol{\Upsilon}}(t)\boldsymbol{\psi}(t) \\
\varepsilon(t+1) &= \frac{\varepsilon^\circ(t+1)}{1 + \boldsymbol{\psi}_f^T(t)F(t)\boldsymbol{\psi}_f(t)} \\
\hat{\boldsymbol{\Upsilon}}(t+1) &= \hat{\boldsymbol{\Upsilon}}(t) + F(t)\boldsymbol{\psi}_f(t)\varepsilon(t+1) \\
F(t+1) &= \frac{1}{\lambda_1(t)}\left[F(t) - \frac{F(t)\boldsymbol{\psi}_f^T(t)\boldsymbol{\psi}_f(t)F(t)}{\dfrac{\lambda_1(t)}{\lambda_2(t)} + \boldsymbol{\psi}_f^T(t)F(t)\boldsymbol{\psi}_f(t)}\right]
\end{aligned}
$$

(2.38)

where $\boldsymbol{\psi}_f(t) = \frac{1}{N_p(q^{-1})}\boldsymbol{\psi}(t)$, $\varepsilon^\circ(t)$ is the *a priori* prediction error and $\lambda_1(t)$ and $\lambda_2(t)$ define the variation profile of the adaptation gain $F(t)$. Filtered observation vector $\boldsymbol{\psi}_f(t)$ is used to ensure the stability and convergence properties of the adaptation algorithm [83]. The other condition for the convergence, namely the richness of excitation, is satisfied as long as disturbance is not zero. A constant trace algorithm [83] is used for the adaptation gain.

The same recursive adaptation algorithm is used for Level 2 of the benchmark with the difference that the order of the disturbance model and consequently the number of the scheduling parameters is increased (θ is replaced by a vector $[\theta_1, \theta_2]^T$).

2.5 Simulation and experimental results

The simulation results are presented for three different tests of each benchmark level: simple step test, step changes in frequencies test and chirp test, according to the benchmark requirements. Simulations are performed on the simulator provided by the benchmark organizers.

2.5.1 Simple step test

The simulation and experimental results for Level 1 are given in Table 2.1 and Table 2.2, respectively. The first column gives the global attenuation in dB. It is the ratio of the energy of the disturbance in open-loop to that in closed-loop computed in steady state (last three seconds of the experiment). The second column shows the attenuation at the disturbance
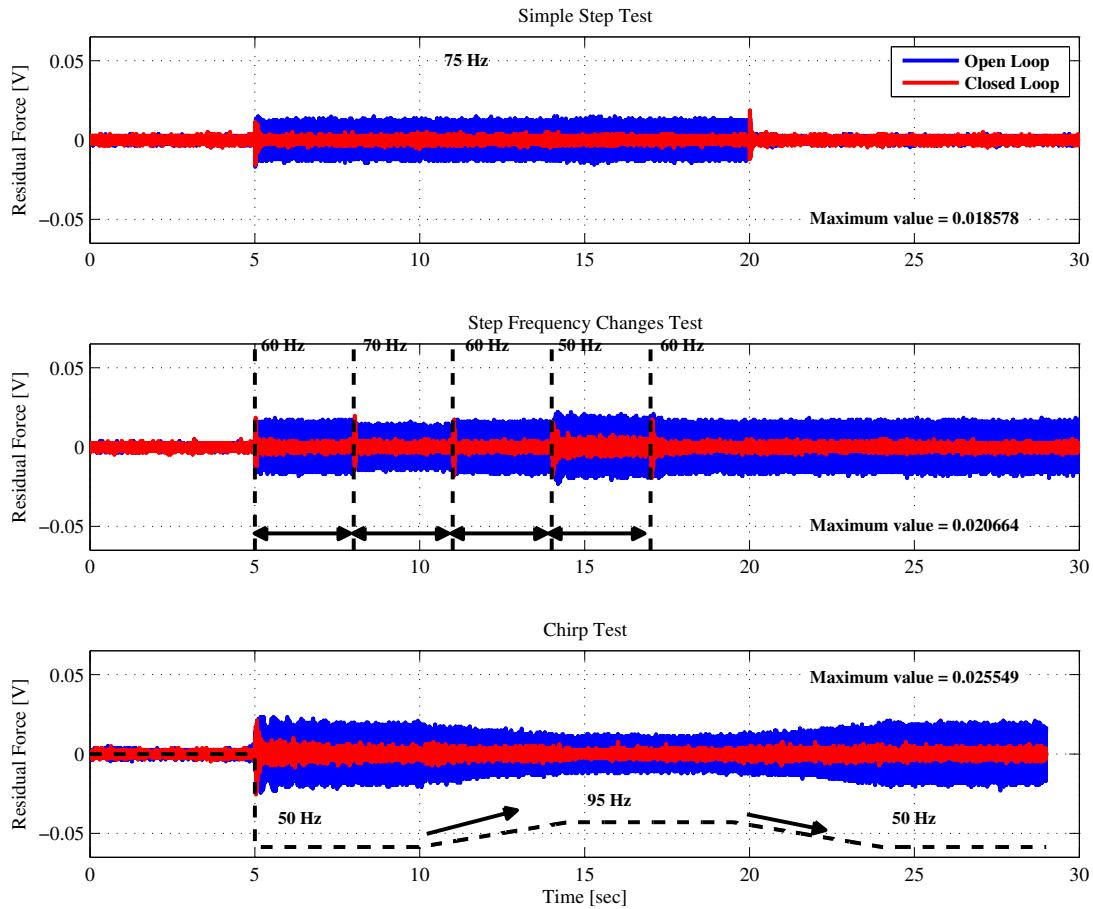
Figure 2.8 – Experimental time-domain responses for different Level 1 tests

frequency. The maximum amplification of the disturbance at other frequencies is computed and shown in the third column together with the frequency at which it occurs. The two-norm of the transient response of the residual force is given in the forth column and the two-norm at the steady state (last three seconds) in the fifth column. The peak value of the transient response is given in the 6th column, and a BSI index for transient duration in the 7th column (100% means that the transient duration is less than 2s and 0% corresponds to more than 4s). The results show good coherence between the simulation and experimental results. There is a discrepancy between the simulation and experimental results for the disturbance frequency of 50Hz probably, which may come from the modeling error around this frequency of the secondary-path model used in the simulator of the benchmark.

The simulation results for simple step test of Level 2 are given in Table 2.3 and the experimental results in Table 2.4. For Level 1 tests, apart from the disturbance at 50Hz, disturbances at other frequencies are rejected. The global attenuation of more than 30 dB is met in simulation for
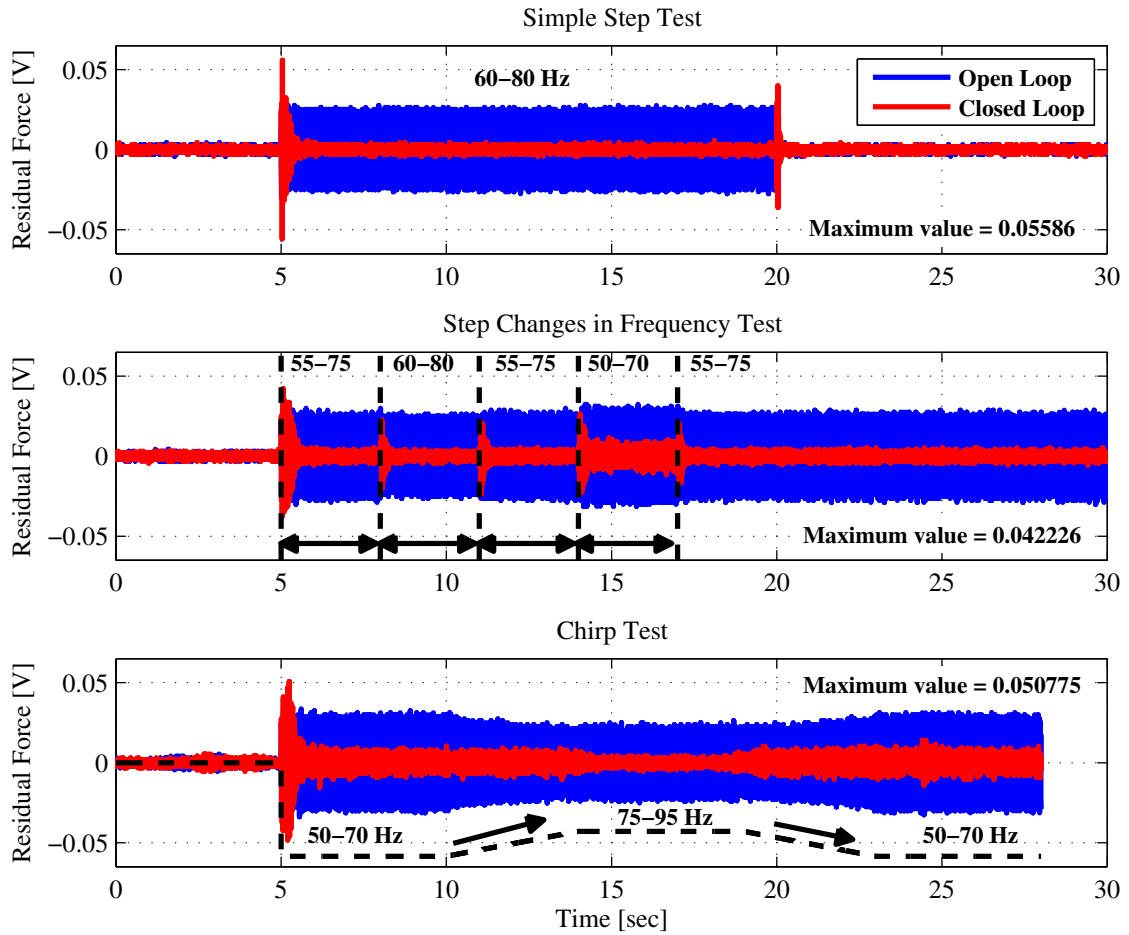
Figure 2.9 – Experimental time-domain responses for different Level 2 tests

Frequency (Hz)	Global (dB)	Dist. Atte. (dB)	Max. Amp. (dB@Hz)	Norm^2 Trans. ($\times 10^{-3}$)	Norm^2 Res. ($\times 10^{-3}$)	Max. Val. ($\times 10^{-3}$)	BSI (%)
50	30.0539	22.1214	9.6674@ 53.12	13.4803	6.0275	19.2347	100.00
55	33.0839	39.1389	5.7785@ 114.06	11.2054	4.2825	21.5834	100.00
60	32.9298	40.6649	5.2791@78.12	9.1452	4.3614	21.5092	100.00
65	33.1775	39.2777	5.4087@73.43	7.9451	4.3065	19.5405	100.00
70	33.5947	47.4173	4.6449@51.56	7.9827	4.1534	22.6636	100.00
75	34.2959	42.8627	3.6597@ 50.00	8.1354	3.9172	22.5296	100.00
80	34.8302	45.3628	3.8744@50.00	8.0156	3.6393	21.3056	100.00
85	34.5090	43.2440	4.0071@50.00	8.6001	3.6477	23.4386	100.00
90	32.3077	39.3682	4.4651@50.00	12.5930	3.8676	25.5074	100.00
95	23.9978	23.8150	4.9679@50.00	15.5999	4.4858	29.8633	100.00

Table 2.1 – Simple step test (Simulation) - Level 1
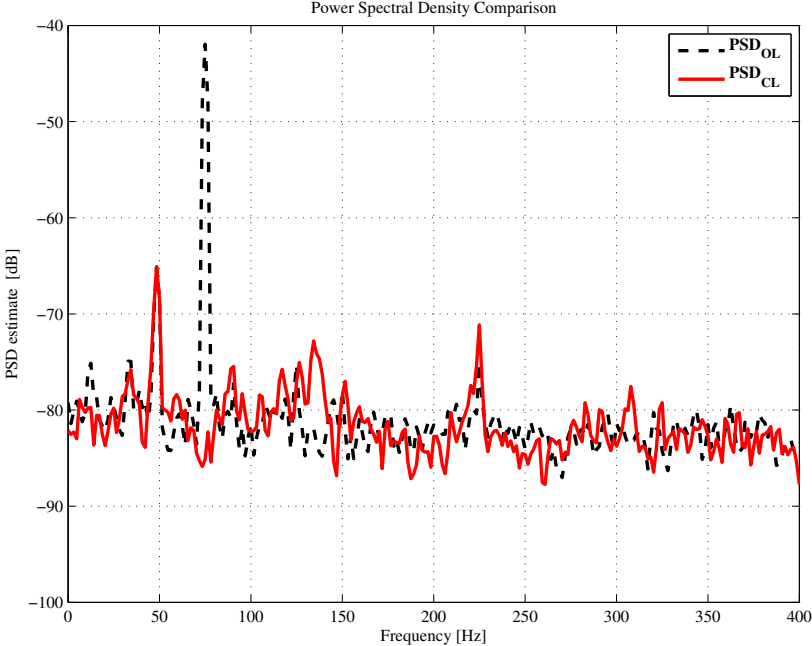
Figure 2.10 – Power spectral density for the real-time simple step test
with disturbance frequency of 75Hz
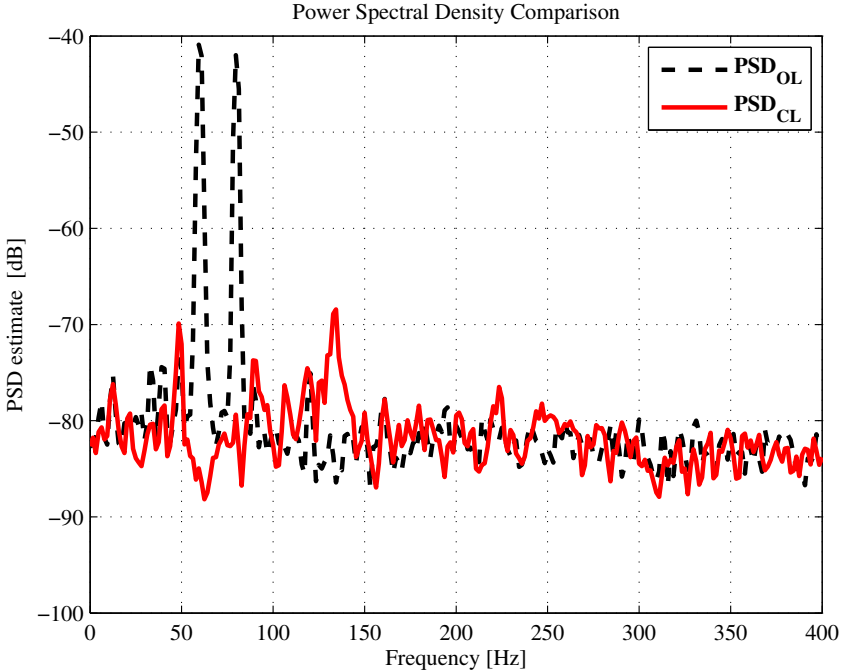
Figure 2.11 – Power spectral density for the Level 2 real-time simple step test
with disturbance frequencies of 60 and 80Hz

Frequency (Hz)	Global (dB)	Dist. Atte. (dB)	Max. Amp. (dB@Hz)	Norm^2 Trans. ($\times 10^{-3}$)	Norm^2 Res. ($\times 10^{-3}$)	Max. Val. ($\times 10^{-3}$)	BSI (%)
50	32.1963	26.0390	13.19@117.19	28.7275	9.8031	22.2959	83.88
55	32.9624	41.5091	11.66@125.00	13.7586	5.6248	18.5939	100.00
60	33.7955	41.3196	11.59@70.31	9.9979	5.1623	17.3711	97.99
65	32.5293	45.4435	9.54@134.37	9.8304	5.0178	19.3765	100.00
70	30.0156	42.6926	11.41@134.37	9.3400	5.5506	20.6127	95.06
75	30.9359	43.1902	9.74@137.50	7.7819	4.4682	15.7354	100.00
80	29.6325	44.9083	9.43@137.50	8.5284	5.0297	21.8171	100.00
85	28.3826	38.3824	7.63@118.75	8.0995	5.7268	20.5997	100.00
90	28.2388	37.0264	10.02@135.94	8.8059	5.0778	23.0987	100.00
95	28.8061	37.0992	7.36@114.06	8.5047	4.6892	22.2701	100.00

Table 2.2 – Simple step test (Experimental results) - Level 1

all frequencies. However, in real experiments the performance for the disturbance frequency pair (50-70)Hz deteriorates comparing to the one in simulation. The main reason is that the estimated parameters in the adaptation algorithm do not converge to the true values (a linear controller with known disturbance frequencies performs very well in simulation as well as in real experiments). For the other disturbance frequencies the transient behavior in simulation and experimental results are close and mostly satisfy the specifications. In practice there always exists a small bias that degrades the performance. This effect can be reduced by adding a small damping to the internal model of the disturbance. This way, a small error in the scheduling parameters will have less effect in the performance, but at a cost of having less attenuation for the exact parameter estimates.

Although the maximum amplification of disturbance in simulation is close to that of linear controller, higher values are obtained in real experiments. This probably comes from the modeling error around 129-137 Hz.

The real-time response from the simple step test with disturbance frequency of 75Hz is shown in the first plot of Figure 2.8. Similarly, in Figure 2.9 the first plot presents the simple step test response for the Level 2 disturbance frequency combination of 60 and 80Hz. Figure 2.10 illustrates the comparison between the open-loop (dashed) and closed-loop power spectral density for the real-time simple step test with single disturbance frequency of 75Hz. Strong attenuation (around 45dB) at 75Hz and low (or no) amplification at other frequencies can be observed. Similar conclusion can be drawn from Figure 2.11 for the simple step test of Level 2 with disturbance frequencies of 60 and 80Hz.

Frequency (Hz)	Global (dB)	Dist. Atte. (dB)-(dB)	Max. Amp. (dB@Hz)	Norm^2 Trans. ($\times 10^{-3}$)	Norm^2 Res. ($\times 10^{-3}$)	Max. Val. ($\times 10^{-3}$)	BSI (%)
50-70	35.5110	27.42 - 23.00	11.28@114.06	87.6744	6.4925	61.5624	100.00
55-75	38.6182	33.68 - 33.59	9.59@114.06	67.8341	4.6086	59.1878	100.00
60-80	39.8107	41.80 - 37.09	6.84@114.06	53.7933	3.9936	53.7369	100.00
65-85	39.9478	49.57 - 43.77	6.37@50.00	64.8855	3.8930	68.9495	100.00
70-90	38.4478	54.70 - 47.07	9.09@50.00	80.7946	4.2437	76.4654	100.00
75-95	35.1036	48.74 - 36.81	11.17@50.00	95.3054	4.7593	72.0523	100.00

Table 2.3 – Simple step test (Simulation) - Level 2

Frequency (Hz)	Global (dB)	Dist. Atte. (dB)-(dB)	Max. Amp. (dB@Hz)	Norm^2 Trans. ($\times 10^{-3}$)	Norm^2 Res. ($\times 10^{-3}$)	Max. Val. ($\times 10^{-3}$)	BSI (%)
50-70	24.6660	20.58 - 17.49	18.06@131.25	144.4955	34.0463	50.7286	100.00
55-75	36.9297	34.20 - 30.54	18.88@129.69	174.1515	6.4665	86.2932	100.00
60-80	39.9376	44.32 - 37.43	18.00@134.37	64.0941	4.0669	55.8595	100.00
65-85	32.5931	37.85 - 32.34	14.65@ 135.94	47.4775	8.2762	54.6568	100.00
70-90	36.3403	55.54 - 47.05	14.41@ 137.50	52.3746	4.7614	63.1648	100.00
75-95	33.7952	43.26 - 36.27	13.07@ 137.50	116.2289	5.7348	86.3334	50.78

Table 2.4 – Simple step test (Experimental results) - Level 2

2.5.2 Step changes in frequencies test

For Level 1 of the benchmark, three sequences of step changes in the frequency of the disturbance are considered. These sequences are defined as follows:

Sequence 1 : $60 \rightarrow 70 \rightarrow 60 \rightarrow 50 \rightarrow 60$
Sequence 2 : $75 \rightarrow 85 \rightarrow 75 \rightarrow 65 \rightarrow 75$
Sequence 3 : $85 \rightarrow 95 \rightarrow 85 \rightarrow 75 \rightarrow 85$

Similarly, for Level 2, two sequences of the step changes in the disturbance frequencies are defined (see the first column of Table 2.5). The transient performance in simulation for Level 1 and Level 2 are given in Table 2.5 and the experimental results in Table 2.6. It can be observed that good performance is obtained for all disturbance frequency pairs except for (50-70) in the real experiment.

The second plot of Figures 2.8 and 2.9 presents the real-time response for the first disturbance frequency sequence of the step changes in frequencies test for Levels 1 and 2, respectively.

2.5.3 Chirp test

For Level 1 of the benchmark a chirp signal that starts from 50Hz and goes to 95Hz and returns to 50Hz with a variation rate of 10 Hz/s is applied as the disturbance signal. For Level 2 the disturbance frequencies change from (50-70)Hz to (75-95)Hz with a variation rate of 5 Hz/s and return to (50-70)Hz. The maximum value and the two-norm of the disturbance response in simulation and in the real-time experiment are given in Table 2.7. The experimental results of the chirp disturbance responses for Levels 1 and 2 are given in Figures 2.8 and 2.9, respectively.

	SEQUENCE - 1		
	Frequency	**Norm² Trans.**	**Max. Val.**
	(Hz)	$(\times 10^{-3})$	$(\times 10^{-3})$
	60→70	7.9407	20.7565
	70→60	8.3077	16.5109
	60→50	10.2125	13.4903
	50→60	7.3136	15.6196
	SEQUENCE - 2		
	Frequency	**Norm² Trans.**	**Max. Val.**
Level 1	**(Hz)**	$(\times 10^{-3})$	$(\times 10^{-3})$
	75→85	7.2684	13.9343
	85→75	8.7004	17.0025
	75→65	7.6486	17.0491
	65→75	7.8875	15.2766
	SEQUENCE - 3		
	Frequency	**Norm² Trans.**	**Max. Val.**
	(Hz)	$(\times 10^{-3})$	$(\times 10^{-3})$
	85→95	8.3668	20.2567
	95→85	9.5780	18.5376
	85→75	7.3373	17.1218
	75→85	8.0514	17.4093
	SEQUENCE - 1		
	Frequency	**Norm² Trans.**	**Max. Val.**
	(Hz)	$(\times 10^{-3})$	$(\times 10^{-3})$
	[55-75] → [60-80]	10.0628	22.8093
	[60-80] → [55-75]	16.3247	21.5839
Level 2	**[55-75] → [50-70]**	20.0613	18.7106
	[50-70] → [55-75]	10.0798	17.8500
	SEQUENCE - 2		
	Frequency	**Norm² Trans.**	**Max. Val.**
	(Hz)	$(\times 10^{-3})$	$(\times 10^{-3})$
	[70-90] → [75-95]	11.5762	18.1048
	[75-95] → [70-90]	13.9285	22.5232
	[70-90] → [65-85]	12.0298	23.1736
	[65-85] → [70-90]	10.8733	20.8162

Table 2.5 – Step changes in frequencies test (Simulation)

		SEQUENCE - 1	
	Frequency (Hz)	**Norm^2 Trans. ($\times 10^{-3}$)**	**Max. Val. ($\times 10^{-3}$)**
Level 1	**60→70**	9.8243	19.7289
	70→60	9.8454	18.2445
	60→50	22.6091	18.2210
	50→60	13.8104	19.4511
		SEQUENCE - 2	
	Frequency (Hz)	**Norm^2 Trans. ($\times 10^{-3}$)**	**Max. Val. ($\times 10^{-3}$)**
	75→85	8.5829	15.7833
	85→75	10.1036	17.3218
	75→65	9.9323	19.7391
	65→75	10.1643	19.72531
		SEQUENCE - 3	
	Frequency (Hz)	**Norm^2 Trans. ($\times 10^{-3}$)**	**Max. Val. ($\times 10^{-3}$)**
	85→95	8.5971	15.8359
	95→85	9.8947	17.2523
	85→75	9.1527	16.0698
	75→85	9.1745	17.0129
Level 2		SEQUENCE - 1	
	Frequency (Hz)	**Norm^2 Trans. ($\times 10^{-3}$)**	**Max. Val. ($\times 10^{-3}$)**
	[55-75] → **[60-80]**	13.7017	22.5980
	[60-80] → **[55-75]**	18.0644	23.9297
	[55-75] → **[50-70]**	51.0763	26.2669
	[50-70] → **[55-75]**	14.2444	20.1445
		SEQUENCE - 2	
	Frequency (Hz)	**Norm^2 Trans. ($\times 10^{-3}$)**	**Max. Val. ($\times 10^{-3}$)**
	[70-90] → **[75-95]**	13.0523	18.9047
	[75-95] → **[70-90]**	12.7703	21.6059
	[70-90] → **[65-85]**	15.5371	20.3018
	[65-85] → **[70-90]**	13.3272	18.9160

Table 2.6 – Step changes in frequencies test (Experimental results)

	Error	
	Maximum Value ($\times 10^{-3}$)	**Mean Square Value ($\times 10^{-6}$)**
Level 1 - Simulation	6.40	3.5910
Level 1 - Experimental	7.54	4.5412
Level 2 - Simulation	10.12	10.5170
Level 2 - Experimental	11.56	11.8759

Table 2.7 – Chirp Changes

2.6 Conclusions

A new method for fixed-order gain-scheduled $\mathscr{H}_\infty$ controller design is proposed and applied to the active suspension benchmark. It is shown that one or two unknown sinusoidal disturbances can be rejected using the gain-scheduled controller and an adaptation algorithm that estimates the internal model of the disturbance. The proposed gain-scheduled controller design method is able to satisfy all frequency-domain constraints. However, the results are slightly deteriorated in simulation and real experiments. The main reasons are the followings:

- During the convergence of the scheduling parameter, the whole system becomes non-linear and the desired performance is not necessarily achieved.

- Even at the steady state, there is always an estimation error in the scheduling parameter.

- The modeling error in the secondary-path model is not considered in the design.

As presented in [14], method described here leads to the least complex control strategy of all the benchmark participants. The approach proposed here is the only of the benchmark solutions not using the Youla-Kučera parameterization as the basis for the control strategy [15, 16, 17, 18, 19, 20, 21]. The Youla-Kučera parameterization leads to the controller order equal to that of the augmented plant, and here the order of the plant model is already high. In [14] a comparison of the control algorithm execution times in the real-time experiments is provided. It can be observed that the methods [17, 21] have comparable execution times to this method, even though based on the Youla-Kučera parameterization. A reason is that an important portion of the execution time is spent on calculations related to adaptation.

The fact that the proposed method uses frequency domain model for design is very reasonable for this application, as the majority of the performance specifications are defined in the frequency domain. Of course, a reliable parametric model is still necessary for the adaptation loop. This method is as well the only one that ensures specification on the output sensitivity transfer function in the design phase. A good attenuation of the disturbance and low amplification of noise are achieved in the real-time experiments, with performance comparable to other participants. In terms of the time-domain performance, i.e. transient duration, obtained performance is excellent. However, the benchmark criterion altered after the controller design, so this fact is not at all appreciated by the final benchmark performance indices.

Although the proposed method could consider the modeling error in the design, it has not been taken to account for few reasons. First, it was supposed that the provided model for the benchmark is very close to the real system and modeling error can be neglected. Second, considering the unmodeled dynamics makes the optimization method more complicated (number of constraints increases). Finally, robust controllers in general lead to conservative solutions which impact negatively the control system performance.

There are two main issues related to the gain-scheduled controller design using the frequency response model, and they are somewhat related. The first issue is the computational burden caused by the constraint sampling both in the frequency domain and the scheduling parameter space. The other one is a lack of guarantee of stability and performance for all the values of scheduling parameters, not just those treated in design. Evidently, denser sampling in the scheduling parameter space approximately resolves the second issue, but at the high computation cost. A method for the design of fixed-order LPV controllers with the transfer function representation is proposed in the next chapter, where these issues are overcome through the use of LMIs.

3 Fixed-order LPV Controller Design for Plants with Transfer Function Description

3.1 Introduction

Gain-scheduled controller design method based on the frequency response models has an advantage that no parametric model is needed. However, this leads to a disadvantage which is the computational burden caused by gridding in the frequency domain. As optimization constraints are sampled in the scheduling parameter space, the method guarantees stability and performance just for scheduling parameter values treated in design. To overcome these issues, a method for the design of fixed-order LPV controllers with the transfer function representation is proposed. Unlike in the method presented in the previous chapter, the LPV controller parameterization considered in this approach leads to design variables in both the numerator and denominator of the controller. As the motivating application is the rejection of the multi-sinusoidal disturbances with time-varying frequencies, the LPV controller design is performed for LTI plants with a transfer function model. Closed-loop stability and $\mathcal{H}_\infty$ performance are characterized using LMIs for all fixed values of scheduling parameters.

3.2 Preliminaries

In [84], plants with a polytopic uncertainty description are treated:

$$\mathcal{G} = \left(\sum_{i=1}^{q} \lambda_i N_i \right) \left(\sum_{i=1}^{q} \lambda_i M_i \right)^{-1}, \tag{3.1}$$

where $\lambda_i \geq 0$, $\sum_{i=1}^{q} \lambda_i = 1$ and q is the number of the polytope's vertices. Transfer functions N_i and M_i are co-prime and belong to $\mathcal{R}\mathcal{H}_\infty$, the set of all proper stable rational transfer functions with bounded infinity norm. Controller being designed can be parameterized as $K = XY^{-1}$, with $X, Y \in \mathcal{R}\mathcal{H}_\infty$. The theory proposed there works for both discrete-time and continuous-time systems, with some minor differences. This chapter is focused on discrete-time systems, but the transition to the continuous-time is straightforward.

As a basis for the characterization of designed controllers, the following theorem is used.

Theorem 3.1 *[84] The set of all stabilizing controllers for the polytopic system defined in (3.1) is given by*

$$\{K = XY^{-1}|M_i Y + N_i X \in \mathscr{S}, i = 1,\ldots,q\}, \tag{3.2}$$

where $\mathscr{S}$ denotes the convex set of all Strictly Positive Real (SPR) transfer functions.

The main gain coming from the polytopic representation of the plant is the fact that ensuring the stability and $\mathscr{H}_\infty$ performance for every vertex of the polytope implies the same for every model inside the polytope. This means that the infinite number of optimization constraints for the whole polytope is replaced by a finite number of them.

In this chapter a SISO LTI plant G given by its rational transfer function representation is considered:

$$G = NM^{-1}, \tag{3.3}$$

where co-prime transfer functions N and M belong to $\mathscr{R}\mathscr{H}_\infty$. It is assumed that the scheduling parameter vector $\boldsymbol{\theta}$, coming for example from the time-varying disturbance model, belongs to the polytope with vertices $\boldsymbol{\theta}_{(i)}$, $i = 1,\ldots,q$. Hence every allowable $\boldsymbol{\theta}$ can be represented as

$$\boldsymbol{\theta} = \sum_{i=1}^{q} \lambda_i \boldsymbol{\theta}_{(i)}. \tag{3.4}$$

The class of LPV controllers that can be treated by this approach is characterized by the polytopic representation

$$X(\boldsymbol{\lambda}) = \sum_{i=1}^{q} \lambda_i X_i, \qquad Y(\boldsymbol{\lambda}) = \sum_{i=1}^{q} \lambda_i Y_i, \tag{3.5}$$

where $X_i = X(\boldsymbol{\theta}_{(i)})$ and $Y_i = Y(\boldsymbol{\theta}_{(i)})$ belong to $\mathscr{R}\mathscr{H}_\infty$. This representation covers a wide class of dependencies of the controller on the scheduling parameters. The following theorem parameterizes polytopic LPV controllers stabilizing the closed-loop system for every value of scheduling parameter vector $\boldsymbol{\theta}$.

Theorem 3.2 *The set of all stabilizing polytopic LPV controllers for the LTI plant $G = NM^{-1}$ is given by:*

$$\mathscr{K} : \{K = X_i Y_i^{-1} \text{ for } i = 1,\ldots,q | F_i \in \mathscr{S}\}, \tag{3.6}$$

where $F_i = MY_i + NX_i$.

Proof: The same line of thought is used as in [84] for the proof of Theorem 3.1.

Sufficiency: First, from Theorem 3.1 it can be concluded that the closed-loop system for every vertex controller is stable. Then, the convex combination of the transfer functions F_i is obtained as

$$
\begin{aligned}
F(\boldsymbol{\lambda}) &= \sum_{i=1}^{q} \lambda_i (MY_i + NX_i) = M\left(\sum_{i=1}^{q} \lambda_i Y_i\right) + N\left(\sum_{i=1}^{q} \lambda_i X_i\right) \\
&= MY(\boldsymbol{\lambda}) + NX(\boldsymbol{\lambda}).
\end{aligned}
\tag{3.7}
$$

The transfer function $F(\boldsymbol{\lambda})$ is also SPR, since the sum of SPR transfer functions weighted by nonnegative weights is SPR. Hence, the plant is stabilized by every controller from the polytope $K(\boldsymbol{\lambda}) = X(\boldsymbol{\lambda})Y^{-1}(\boldsymbol{\lambda})$.

Necessity: Assume that there exists a polytopic LPV controller stabilizing the plant G, given by its vertices $K_i^* = X_i^*(Y_i^*)^{-1}$, and that for it $F_i \in \mathscr{S}$ is not satisfied. A polytope of stable characteristic polynomials with vertices c_i can be constructed from the plant G and the vertex controllers K_i^*. For such a polynomial polytope it is proven [85] that the phase difference between its elements is less than π. So, according to Theorem 2.1 of [86] (for discrete-time systems, for continuous-time systems Theorem 3.1 of the same paper) there always exists a polynomial or transfer function d such that c_i/d is SPR for $i = 1,\ldots,q$. As a result, there exists a transfer function

$$
L = (MY_i^* + NX_i^*)^{-1} c_i/d
\tag{3.8}
$$

such that $(MY_i^* + NX_i^*)L$ is SPR for $i = 1,\ldots,q$. Note that L does not depend on i because the numerator of $(MY_i^* + NX_i^*)$ is equal to c_i and cancels it out in the expression for L. Finally, the polytopic LPV controller

$$
K(\boldsymbol{\lambda}) = \left(\sum_{i=1}^{q} \lambda_i X_i\right)\left(\sum_{i=1}^{q} \lambda_i Y_i\right)^{-1}
\tag{3.9}
$$

belongs to $\mathscr{K}$ taking $X_i = X_i^* L$ and $Y_i = Y_i^* L$. $\qquad\square$

3.3 Convex set of stabilizing LPV controllers

The first goal is to propose the parameterization of LPV controllers for which the stability of the closed-loop system is guaranteed with every controller (3.5) corresponding to some value of the scheduling parameter from the assumed polytope. To do so, a suitable controller structure must be chosen. Using the fact that every controller in the polytope should depend affinely on the scheduling parameter vector, vertex controllers can be presented in the form

$$
X_i(\boldsymbol{\theta}_{(i)}, z) = \boldsymbol{x}(\boldsymbol{\theta}_{(i)})^T \boldsymbol{\phi}(z), \quad Y_i(\boldsymbol{\theta}_{(i)}, z) = \boldsymbol{y}(\boldsymbol{\theta}_{(i)})^T \boldsymbol{\phi}(z),
\tag{3.10}
$$

where $x(\theta_{(i)})$ and $y(\theta_{(i)})$ are vectors of the controller parameters, affine with respect to the scheduling parameters. A good choice of basis function vectors ϕ are orthonormal basis functions such as Kautz, Laguerre or generalized orthonormal functions [87].

The SPR condition in (3.6) can be represented as a set of infinitely many constraints in the frequency domain:

$$\text{Re}\{M(e^{-j\omega})Y_i(e^{-j\omega}) + N(e^{-j\omega})X_i(e^{-j\omega})\} > 0, \ \forall\omega \in [0,\omega_N], \text{ for } i = 1,\dots,q \tag{3.11}$$

with $\text{Re}\{\cdot\}$ representing the real part of a complex number, and ω_N the Nyquist frequency of the system. To solve this problem numerically, frequency gridding is necessary. As a result, constraint violation between the grid frequencies could occur.

To avoiding gridding constraints in the frequency domain, the SPR condition in (3.6) can alternatively be presented using the Kalman-Yakubovich-Popov (KYP) lemma. For the discrete-time systems, the KYP lemma states that the transfer function $F_i(z) = C_i(zI - A)^{-1}B + D_i$ belongs to $\mathscr{S}$ if and only if there exists a matrix $P_i = P_i^T > 0$ such that

$$\begin{bmatrix} A^T P_i A - P_i & A^T P_i B - C_i^T \\ B^T P_i A - C_i & B^T P_i B - (D_i + D_i^T) \end{bmatrix} < 0. \tag{3.12}$$

If (A, B, C_i, D_i) is chosen as a controllable canonical realization of $F_i = MY_i + NX_i$, then the controller and the plant parameters which are in the numerator of F_i appear only in C_i and D_i. Hence, the inequality (3.12) becomes an LMI with respect to P_i, C_i and D_i. Matrices A and B are the same for all the vertices because of the properties of controllable canonical form and the fact that denominators of all transfer functions F_i are the same (where also the fact that all the transfer functions X_i and Y_i have the same poles is used). Unknown controller parameter vectors $x(\theta_{(i)})$ and $y(\theta_{(i)})$, appearing in matrices C_i and D_i, are found as a feasible point of the LMI constraints. Note that these constraints lead to the guarantee of stability only for frozen values of scheduling parameter.

Remark 3.1 *The issue of the state-space realization of the LPV model given in the polynomial setting is the reason why stability of the closed-loop system is discussed only for frozen values of scheduling parameters. In [88] it is shown that if the theory of state-space realization of LTI systems is applied directly to LPV models in polynomial setting, the issue of "dynamic dependence" of the model on scheduling parameter arises. For the discrete-time LPV models in polynomial setting this means that not only current values of the scheduling parameter, but some previous values as well, enter the state-space matrices. Hence, the realization theory applied here corresponds exactly only to the LTI case, i.e. to frozen values of scheduling parameters. In practice this means that the stability guarantee obtained here is similar to the one in the previous chapter, which applies only to slowly varying scheduling parameters. The main difference is that there guarantee is given only for sampled values of scheduling parameters, while here it is for all frozen values.*

3.4 $\mathcal{H}_\infty$ **performance constraints**

The $\mathcal{H}_\infty$ performance of the weighted closed-loop transfer functions is considered for fixed values of the parameter $\boldsymbol{\lambda}$. The motivation lies in the previously mentioned problem of sinusoidal disturbance rejection. If, for example, it is supposed that the frequency of the sinusoidal disturbance is fixed over some period, the goal during that time is to reject the disturbance without amplifying the noise too much in other frequencies. To ensure this, the controller is designed by shaping the frequency response of the output sensitivity function S using the performance filter W_1. The output sensitivity function S is defined as the transfer function from the output disturbance to the output of the closed-loop system and is given by the expression

$$S = (1 + GK)^{-1} = MY(MY + NX)^{-1}. \tag{3.13}$$

The following should be ensured for S:

$$\|W_1 S\|_\infty = \left\| \frac{W_1 MY}{MY + NX} \right\|_\infty < \gamma, \tag{3.14}$$

where γ is a bound on the $\mathcal{H}_\infty$ norm of the weighted output sensitivity function. As it can be observed, the controller parameters appear both in the numerator and denominator of the transfer function $W_1 S$. The application of Bounded Real Lemma on the state-space representation of the weighted sensitivity function would result in a non-convex optimization problem, because of the product of controller and Lyapunov function parameters. To convexify this performance constraint, the relation between the Bounded Real Lemma and the Positive Real Lemma can be employed [89, 90].

In [91] it is shown that Inequality (3.14) is satisfied if and only if the following stands:

$$H_\infty = \frac{(MY + NX) - \gamma^{-1} W_1 MY}{(MY + NX) + \gamma^{-1} W_1 MY} \in \mathcal{S}. \tag{3.15}$$

Therefore, the set of all controllers for which the inequality $\|W_1 S\|_\infty < \gamma$ is satisfied is given by

$$\mathcal{K}_{s_\infty} : \{K = XY^{-1} | H_\infty \in \mathcal{S}\}. \tag{3.16}$$

To enable the calculation of the controller parameters, the set $\mathcal{K}_{s_\infty}$ is represented via LMIs. Let H_∞ in (3.15) be defined as the ratio of two co-prime transfer functions

$$H_\infty = H_n / H_d,$$

where H_n and H_d are given by

$$
\begin{aligned}
H_n &= (MY + NX) - \gamma^{-1} W_1 MY \\
H_d &= (MY + NX) + \gamma^{-1} W_1 MY.
\end{aligned}
\tag{3.17}
$$

Then, the set of all stabilizing controllers that ensure inequality (3.14) is given by:

$$
\mathcal{K}_{s_\infty} : \{K = XY^{-1} | H_n \text{ and } H_d \text{ are CL-SPR}\},
\tag{3.18}
$$

where CL-SPR stands for Common Lyapunov - SPR. Two transfer functions are said to be CL-SPR if they satisfy the inequality of KYP lemma with the same Lyapunov matrix P [91].

Using the fact that transfer functions H_n and H_d have the same denominators, their controllable canonical realizations can be represented as (A, B, C_n, D_n) and (A, B, C_d, D_d), respectively. Then, the condition that the transfer functions H_n and H_d are CL-SPR is expressed using the following set of matrix inequalities:

$$
\begin{bmatrix}
A^T PA - P & A^T PB - C_n^T \\
B^T PA - C_n & B^T PB - (D_n + D_n^T)
\end{bmatrix} < 0,
\tag{3.19}
$$

$$
\begin{bmatrix}
A^T PA - P & A^T PB - C_d^T \\
B^T PA - C_d & B^T PB - (D_d + D_d^T)
\end{bmatrix} < 0.
\tag{3.20}
$$

To allow design of controllers with a polytopic structure, the LMIs have to be adapted in a similar manner to the stability constraints. First, for the controller representing the polytope vertex i, the transfer functions H_{n_i} and H_{d_i} are defined by

$$
\begin{aligned}
H_{n_i} &= (MY_i + NX_i) - \gamma^{-1} W_1 MY_i, \\
H_{d_i} &= (MY_i + NX_i) + \gamma^{-1} W_1 MY_i.
\end{aligned}
\tag{3.21}
$$

Let controllable canonical representations of these two transfer functions be labeled as (A, B, C_{n_i}, D_{n_i}) and (A, B, C_{d_i}, D_{d_i}), respectively, where A and B are the same for all the vertices (similar reasoning as for the stability constraints in 3.12).

Writing inequalities (3.19) and (3.20) for every H_{n_i} and H_{d_i} ensures that the $\mathcal{H}_\infty$ performance is guaranteed for the closed-loop system with every polytope vertex controller:

$$
\begin{bmatrix}
A^T P_i A - P_i & A^T P_i B - C_{n_i}^T \\
B^T P_i A - C_{n_i} & B^T P_i B - (D_{n_i} + D_{n_i}^T)
\end{bmatrix} < 0,
\tag{3.22}
$$

$$\begin{bmatrix} A^T P_i A - P_i & A^T P_i B - C_{d_i}^T \\ B^T P_i A - C_{d_i} & B^T P_i B - (D_{d_i} + D_{d_i}^T) \end{bmatrix} < 0. \tag{3.23}$$

But, if this is satisfied, all the transfer functions H_{n_i} and H_{d_i} are SPR. By taking the convex combination of all the transfer functions H_{n_i}, a new SPR transfer function is obtained:

$$H_n(\boldsymbol{\lambda}) = \sum_{i=1}^q \lambda_i H_{n_i} = \sum_{i=1}^q \lambda_i [(MY_i + NX_i) - \gamma^{-1} W_1 MY_i].$$

It can be rewritten as

$$H_n(\boldsymbol{\lambda}) = M \sum_{i=1}^q \lambda_i Y_i + N \sum_{i=1}^q \lambda_i X_i - \gamma^{-1} W_1 M \sum_{i=1}^q \lambda_i Y_i. \tag{3.24}$$

This means that for any controller from the polytope $K(\boldsymbol{\lambda})$ the transfer function $H_n(\boldsymbol{\lambda})$ is SPR. In a similar manner it can be concluded that, for the controller $K(\boldsymbol{\lambda})$, the transfer function $H_d(\boldsymbol{\lambda})$ is SPR. Therefore for any controller belonging to the polytope (3.5), hence for every value of the scheduling parameter, the $\mathscr{H}_\infty$ constraint in (3.14) is satisfied.

Remark 3.2 *The fact that the transfer functions H_{n_i} and H_{d_i} are SPR leads to the conclusion that the transfer function $H_i = H_{n_i} + H_{d_i}$ is SPR as well. But, using the expressions for H_{n_i} and H_{d_i}, it can be concluded that $H_i = 2(MY_i + NX_i)$ is SPR. Then, according to Section 3.2, the closed-loop system is stabilized for every controller from the polytope. In practice this means that if LMIs (3.22) and (3.23) are set as a design constraints, no separate set of LMIs defined by (3.12) for stability is needed.*

Remark 3.3 *The results can be extended to the case of an uncertain plant model with polytopic uncertainty. Let the uncertain polytopic plant model be given by*

$$G(\eta) = N(\eta) M^{-1}(\eta),$$

where $N(\eta) = \sum_{j=1}^p \eta_j N_j$, $M(\eta) = \sum_{j=1}^p \eta_j M_j$, $\eta_j \geq 0$, $\sum_{j=1}^p \eta_j = 1$, and N_j and M_j belong to $\mathscr{RH}_\infty$. Assume that a stabilizing LPV controller, described by (3.5), needs to be designed for such a system. Then the LMI (3.12) (or (3.22) and (3.23) for both stability and performance) needs to be set as a design constraint for every possible combination of vertices of two polytopes, i.e. the SPRness of

$$F_{i,j} = M_j Y_i + N_j X_i$$

for $i = 1, \ldots, q$ and $j = 1, \ldots, p$ needs to be assured. It is easy to show, by taking convex combinations of these pq LMIs, that the stability (and in a similar manner performance as well) of any model from the plant uncertainty polytope is guaranteed by application of any controller from the LPV controller polytope.
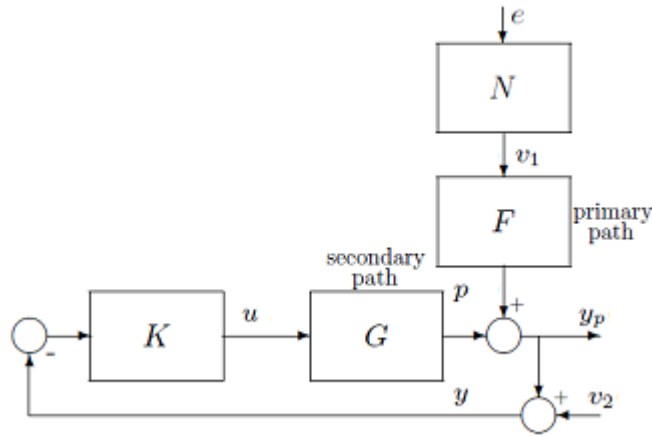
Figure 3.1 – Block diagram of the active suspension system

Remark 3.4 *All of the results can easily be extended to the continuous-time case. The only difference is that the LMIs of the KYP lemma should be expressed for continuous-time systems.*

3.5 Simulation results

As a test system, a simple model of the active suspension system in the Control Systems Department in Grenoble (GIPSA - lab) is used. A detailed description of the system is given in [92]. The proposed method is used to design a controller capable of rejecting a sinusoidal disturbance with a time-varying frequency. The disturbance frequency is known to lie in the interval between 45 and 105Hz, and the sampling frequency for both data acquisition and control is set to 800Hz. The block diagram of the active suspension system is shown in Figure 3.1. It is important to emphasize that the active suspension system described here is not the same as the one in Chapter 2. The reason is that the original system got broken before the tests for the Benchmark were performed. In this example the model of the original setup is still used, unlike in Chapter 2.

The sinusoidal disturbance $v_1(t)$ can be represented as a white noise e filtered through the disturbance model N. The transfer function G_d between the disturbance input and the open-loop system output $y_p(t)$ is called the primary path. The measured output affected by the measurement noise is denoted by $y(t)$ and it is fed back to the controller. The secondary path denotes the transfer function G between the output of controller $u(t)$ and the system output in the open loop. Both the primary (red line in Figure 3.2) and the secondary path (blue line) contain several high-resonant modes in the disturbance frequency region, as it can be observed on the amplitude Bode diagram of the identified test model.

By the application of the internal model principle, the controller is parameterized as a function of the disturbance frequency. Note that the denominator of the discrete-time model (with T_s
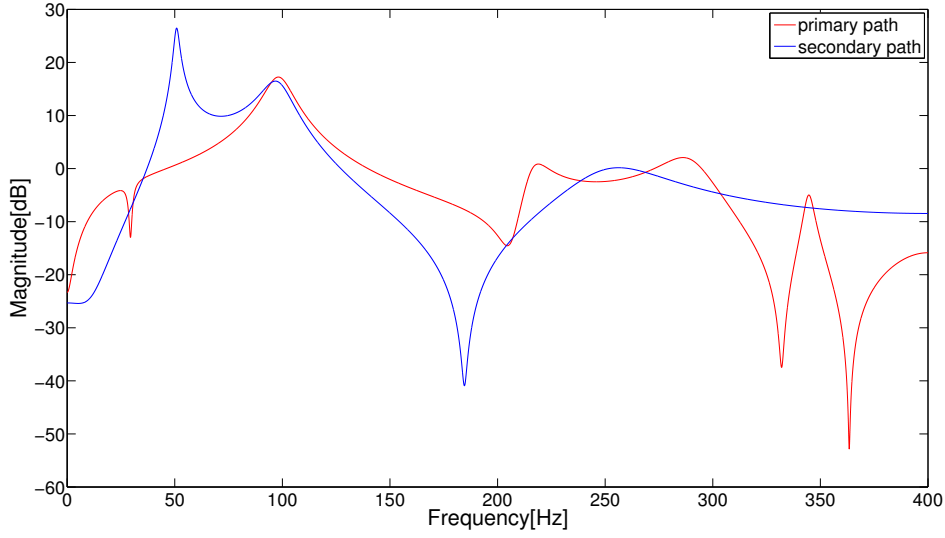
Figure 3.2 – Frequency response of the primary and secondary path

as the sampling period) of the sinusoidal disturbance with frequency ω (in rad/s) is given by

$$D_s(z,\omega) = z^2 - 2\cos(T_s\omega)z + 1.$$

For a given disturbance frequency interval $[\omega_1, \omega_2]$, this can be rewritten as a linear function of one parameter $\theta \in [\theta_1, \theta_2]$, with $\theta_1 = -2\cos(T_s\omega_1)$ and $\theta_2 = -2\cos(T_s\omega_2)$. This means that θ enters the denominator of the controller in an affine fashion. The controller for $\theta = \theta_1$ is denoted by $K_1(z) = X_1(z)Y_1^{-1}(z)$, and the one for $\theta = \theta_2$ as $K_2(z) = X_2(z)Y_2^{-1}(z)$, where $Y_i(z) = Y_f(z)(z^2 + \theta_i z + 1))$. Then the stabilizing controller for any $\theta \in [\theta_1, \theta_2]$ that incorporates $z^2 + \theta z + 1$ in the denominator is given by

$$K(z,\lambda) = [\lambda X_1(z) + (1-\lambda)X_2(z)][\lambda Y_1(z) + (1-\lambda)Y_2(z)]^{-1}, \tag{3.25}$$

where $\lambda = (\theta_2 - \theta)(\theta_2 - \theta_1)^{-1}$.

Due to the "waterbed effect", the amplification at other frequencies has to be allowed in order to have strong attenuation at the disturbance frequency, and yet to preserve the stability of the closed-loop system. To guarantee that the noise at other frequencies will not be strongly amplified, the performance constraint $\|S\|_\infty < 6\text{dB}$ is set using the performance filter $W_1 = 0.5$. The value of 6dB is a general practical recommendation [83]. For each of the polytope vertices (for the limiting frequencies of 45 and 105Hz) two appropriate LMIs (3.22) and (3.23) are set to ensure the performance. Yalmip [93] is used as a Matlab interface for defining the appropriate convex optimization problem. The chosen SDP solver is SDPT3 [94].

For the sake of simplicity, the denominators of the transfer functions $X_1(z)$, $X_2(z)$, $Y_1(z)$ and
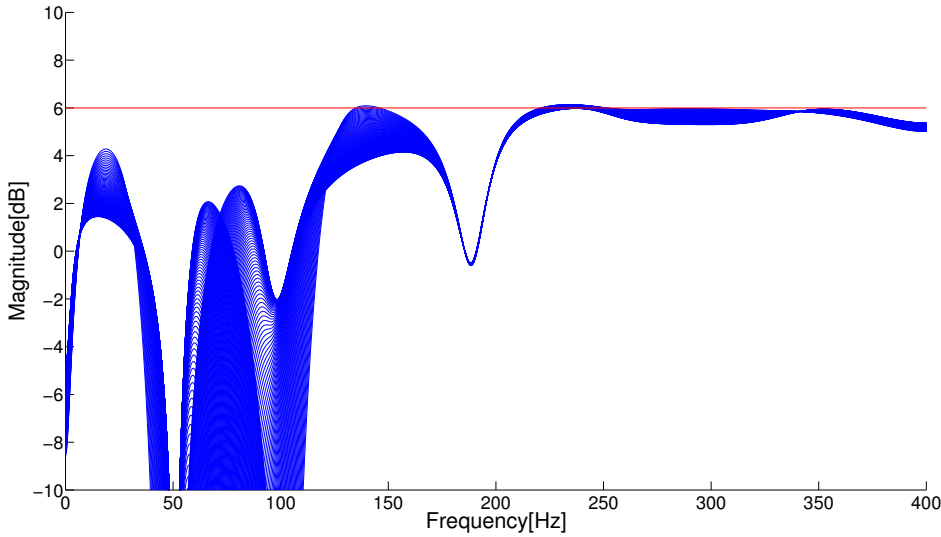
Figure 3.3 – Joint sensitivity plot for a fine grid of θ

$Y_2(z)$ are set to have all poles at 0.2 (the sensitivity of the design approach to this choice is not high). The numerators of these transfer functions, as well as two Lyapunov matrices P_1 and P_2, represent the optimization variables in this problem (bearing in mind that $Y_1(z)$ and $Y_2(z)$ have a fixed part $D_s(z,\theta)$ for $\theta \in \{\theta_1, \theta_2\}$). The exact problem to be solved is given as $\|W_1(z)S(z,\theta)\|_\infty < \gamma$, for $\theta \in \{\theta_1, \theta_2\}$ and fixed γ. The optimal γ is the minimal value for which the problem can be solved. To find the optimal γ, the bisection algorithm is used. If it can be solved for $\gamma = 1$ it means that the desired performance level can be obtained.

As a representative solution to the given problem a 10th order controller is chosen. The optimal γ obtained is 1.03 (for the purpose of comparison, for the 6th order controller the optimal γ equals 1.16, and for the 12th order one the optimal γ is 0.95). Solving the problem takes around 5 seconds per iteration of the bisection algorithm. Figure 3.3 depicts superimposed Bode amplitude plots of the transfer function S for a fine grid of disturbance frequencies θ between 45 and 105Hz (a grid step of 0.5Hz was used). It can be observed in the upper part of the graph that the performance constraint is satisfied. In the lower part asymptotic rejection in the area of disturbance frequencies can be observed, which comes from the presence of the disturbance model in the denominator of the LPV controller.

To illustrate the performance of the controller, simulations are performed on the plant model. Since the objective of this method is controller design for the rejection of a sinusoidal disturbance with time-varying, but known, frequency, estimation of the disturbance frequency is omitted in the simulation. For the purpose of simulation, the disturbance frequency is directly fed to the controller. This corresponds to the situation when it is possible to measure the disturbance (or a signal correlated to it) and directly obtain the disturbance frequency.
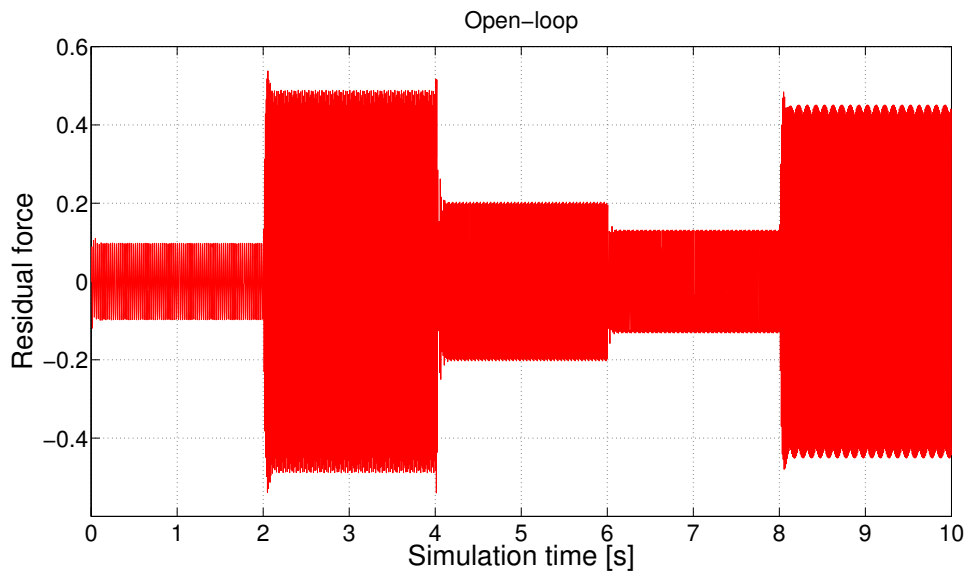
Figure 3.4 – Open-loop response to step changes in the disturbance frequency

The initial disturbance frequency is set to 45Hz, and every 2 seconds is altered via a step change to 105Hz, 75Hz, 60Hz and 90Hz, respectively. In Figure 3.4, the open-loop simulation response to such a disturbance is represented in red. The blue plot in Figure 3.5 depicts the closed-loop response to the same disturbance. Both plots are shown on the same scale, so the asymptotic rejection can easily be noticed. For a closer view of the transient after the change of the disturbance frequency, the open-loop and closed-loop responses from 2.0 to 2.1 seconds are superimposed in Figure 3.6. The closed-loop transient after each frequency change is rather short and the peak value is smaller than in the open-loop case.

3.6 Conclusions

A fixed-order LPV controller design method, with a primary focus on the problem of rejection of a frequency-varying sinusoidal disturbance, is proposed in this chapter. Different sets of LMIs for ensuring the closed-loop system stability for the fixed values of the scheduling parameter and desired $\mathcal{H}_\infty$ performance are proposed. Simulations results show that sensitivity function shaping ensures good performance for fixed values of the scheduling parameter, and that stability of the closed-loop system is preserved during the scheduling parameter variations. However, the method cannot guarantee the closed-loop system stability during fast scheduling parameter variations. The other issue is extension of the method to the MIMO systems. In the next chapter a state-space LPV controller design method is proposed to resolve these issues.
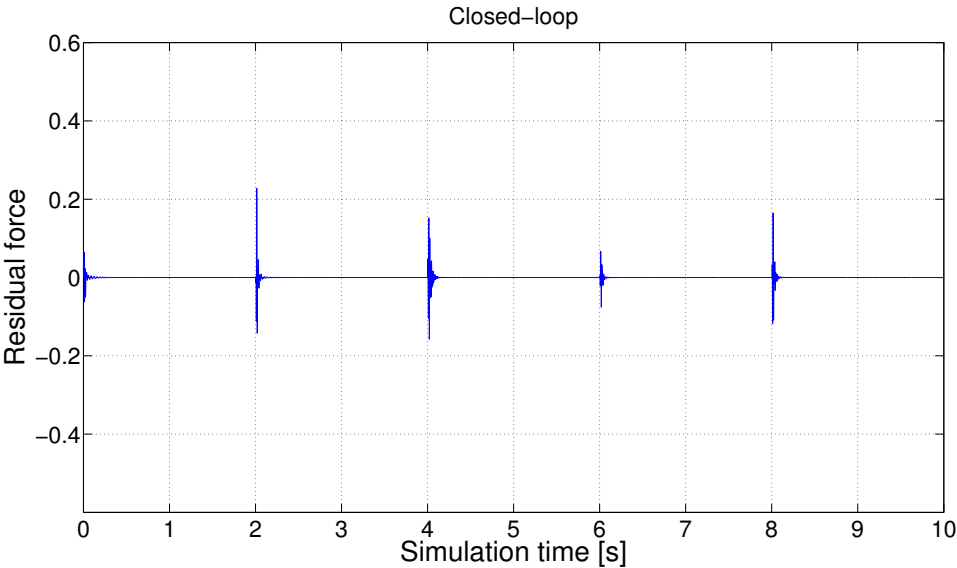
Figure 3.5 – Closed-loop response to step changes in the disturbance frequency
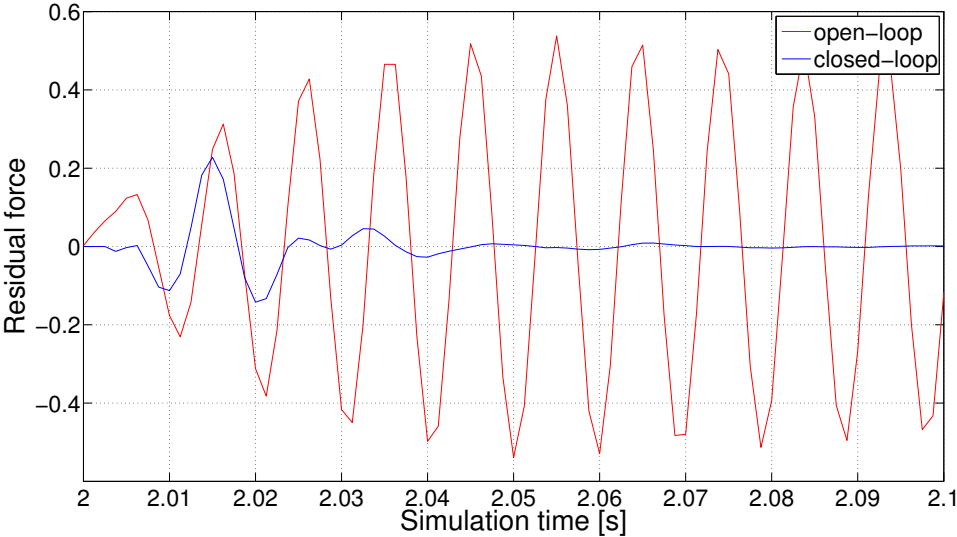
Figure 3.6 – Comparison of the open-loop and closed-loop response

4 Fixed-structure LPV Controller Design for Continuous-time LPV Systems

4.1 Introduction

In the previous chapter, a method for designing fixed-order LPV controllers in the transfer function setting is presented. Even though the transfer function structure is often used in practice, the advantages are lost in case that controller design is performed for a MIMO system. Also, dependency of the LPV transfer function on scheduling parameter vector can be much more complex than in the state-space setting. For example, a simple affine dependence of the state matrix could lead to an LPV transfer function with polynomial dependence on scheduling parameter vector. Hence, the procedure for designing LPV controllers in the state-space setting is proposed.

A fixed-order output-feedback LPV controller design method for continuous-time state-space LPV plant models with an affine dependence on the scheduling parameter vector is presented in this chapter. Bounds on the scheduling parameter vector and its variation rate are exploited in design through the use of affine PDLFs. The exponential decay rate, $\mathscr{H}_\infty$ and $\mathscr{H}_2$ performance constraints are expressed through a set of LMIs. Controller design algorithms based on these constraints are discussed. Simulation example and the application of the proposed method to a 2DOF gyroscope experimental setup are described.

4.2 Problem Formulation

4.2.1 Plant model

A class of continuous-time LPV systems with the following model $G(\boldsymbol{\theta}(t))$ is considered:

$$
\begin{aligned}
\dot{\mathbf{x}}_g(t) &= A_g(\boldsymbol{\theta}(t))\mathbf{x}_g(t) + B_u(\boldsymbol{\theta}(t))\mathbf{u}(t) + B_w(\boldsymbol{\theta}(t))\mathbf{w}(t) \\
\mathbf{z}(t) &= C_z(\boldsymbol{\theta}(t))\mathbf{x}_g(t) + D_{zu}(\boldsymbol{\theta}(t))\mathbf{u}(t) + D_{zw}(\boldsymbol{\theta}(t))\mathbf{w}(t) \\
\mathbf{y}(t) &= C_y\mathbf{x}_g(t) + D_{yw}\mathbf{w}(t).
\end{aligned}
\tag{4.1}
$$

The state vector belonging to $\mathbb{R}^n$ is denoted by $\mathbf{x}_g(t)$, $\mathbf{u}(t)$ is the control input vector belonging to $\mathbb{R}^{n_u}$, $\mathbf{z}(t)$ from $\mathbb{R}^{n_z}$ is the vector of performance outputs, $\mathbf{y}(t)$ from $\mathbb{R}^{n_y}$ is the vector of measured outputs and $\mathbf{w}(t)$ from $\mathbb{R}^{n_w}$ denotes the vector of external inputs, such as references or disturbances. The vector $\boldsymbol{\theta}(t) = [\theta_1(t), \ldots, \theta_{n_\theta}(t)]^T$ represents the vector of scheduling parameters. The plant model is taken to be strictly proper, which is a characteristic of all physical systems. Proper models can easily be converted to strictly proper models by using a high bandwidth filter for output sensors.

One important subclass of LPV systems, related to many practical problems, are LPV systems with affine structure. They are characterized through the affine dependence of state-space matrices on the scheduling parameter vector:

$$A_g(\boldsymbol{\theta}(t)) = A_{g_0} + \sum_{i=1}^{n_\theta} \theta_i(t) A_{g_i}, \tag{4.2}$$

similarly for other matrices dependent on $\boldsymbol{\theta}(t)$. To keep the affine dependence of the closed-loop matrices on the scheduling parameter vector, only one of the matrices B_u or C_y can be scheduling parameter dependent. For the same reason matrix D_{yw} is assumed to be independent of the scheduling parameter vector. Results are developed for C_y and D_{yw} independent of $\boldsymbol{\theta}$, but similar results can easily be presented for other combinations satisfying given limitation.

In many applications, the scheduling parameter vector $\boldsymbol{\theta}(t)$ belongs to hyperrectangle $\Theta \in \mathbb{R}^{n_\theta}$:

$$\theta_i(t) \in [\underline{\theta}_i, \overline{\theta}_i], \ i = 1, \ldots, n_\theta. \tag{4.3}$$

The set of vertices of Θ is denoted by Θ_v.

Remark 4.1 *If the structure of the plant is such that the dependence of the closed-loop matrices on the scheduling parameter vector is not affine, but for example a higher order polynomial, the method should be extended to treat polynomial dependence of closed-loop matrices on the scheduling parameter vector. The evident benefit of such an extension is a possibility of covering the larger class of LPV plants. The other benefit would be a possibility to use PDLFs with higher order polynomial dependence on the scheduling parameter vector. However, the price that would be paid is elevated computation time, because the polynomial relaxation techniques heavily increases the number of matrix constraints. This would increase the complexity of presentation as well. For this reason, only affine dependence of plant and controller matrices and PDLF on the scheduling parameter vector is considered.*

4.2.2 Controller structure

The goal of this chapter is to provide a parameterization of a set of fixed-order LPV dynamic output feedback controllers $K(\boldsymbol{\theta}(t), \dot{\boldsymbol{\theta}}(t))$ that stabilize the plant $G(\boldsymbol{\theta}(t))$. The structure of the

LPV controller $K(\boldsymbol{\theta}(t), \dot{\boldsymbol{\theta}}(t))$ is given by

$$
\begin{aligned}
\dot{\mathbf{x}}_c(t) &= A_c(\boldsymbol{\theta}(t), \dot{\boldsymbol{\theta}}(t))\mathbf{x}_c(t) + B_c(\boldsymbol{\theta}(t), \dot{\boldsymbol{\theta}}(t))\mathbf{y}(t) \\
\mathbf{u}(t) &= C_c\mathbf{x}_c(t) + D_c\mathbf{y}(t),
\end{aligned}
\tag{4.4}
$$

where $\mathbf{x}_c(t)$ represents states of controller. Similar to $\boldsymbol{\theta}(t)$, it is supposed that $\dot{\boldsymbol{\theta}}(t)$ belongs to a hyperrectangle $\Delta \in \mathbb{R}^{n_\theta}$, i.e.

$$
\dot{\theta}_i(t) \in [\underline{\delta}_i, \overline{\delta}_i], \; i = 1, \dots, n_\theta.
\tag{4.5}
$$

The set of vertices of Δ is denoted by Δ_v.

Dependence of the controller matrices on the scheduling parameter vector $\boldsymbol{\theta}(t)$ and its variation rate $\dot{\boldsymbol{\theta}}(t)$ is affine, as for the plant, with matrix $A_c(\boldsymbol{\theta}(t), \dot{\boldsymbol{\theta}}(t))$ given by

$$
A_c(\boldsymbol{\theta}(t), \dot{\boldsymbol{\theta}}(t)) = A_{c_0} + \sum_{i=1}^{n_\theta} \theta_i(t) A_{c_i} + \sum_{i=1}^{n_\theta} \dot{\theta}_i(t) A_{cd_i},
\tag{4.6}
$$

and accordingly for $B_c(\boldsymbol{\theta}(t), \dot{\boldsymbol{\theta}}(t))$. Again, in order to to keep the affine dependence of the closed-loop matrices on the scheduling parameter vector, matrices C_c and D_c are assumed to be independent of the scheduling parameter. Other combinations are possible based on the plant matrices.

Remark 4.2 *It is important to emphasize at this stage that in practice $\dot{\boldsymbol{\theta}}(t)$ is not always measurable. Some of the LPV controller design methods in literature are limited by this issue [59, 60, 62], as LPV controllers designed using these methods inherently depend on $\dot{\boldsymbol{\theta}}(t)$. For the approach presented here this does not pose a problem, as it can be circumvented by setting to zero the terms of $K(\boldsymbol{\theta}(t), \dot{\boldsymbol{\theta}}(t))$ related to $\dot{\boldsymbol{\theta}}(t)$.*

4.2.3 Closed-loop system structure

Merging the plant model and the controller structure leads to the following closed-loop system representation:

$$
\begin{aligned}
\begin{bmatrix} \dot{\mathbf{x}}_g(t) \\ \dot{\mathbf{x}}_c(t) \end{bmatrix} &= \begin{bmatrix} A_g(\boldsymbol{\theta}(t)) + B_u(\boldsymbol{\theta}(t))D_cC_y & B_u(\boldsymbol{\theta}(t))C_c \\ B_c(\boldsymbol{\theta}(t), \dot{\boldsymbol{\theta}}(t))C_y & A_c(\boldsymbol{\theta}(t), \dot{\boldsymbol{\theta}}(t)) \end{bmatrix} \begin{bmatrix} \mathbf{x}_g(t) \\ \mathbf{x}_c(t) \end{bmatrix} \\
&\quad + \begin{bmatrix} B_w(\boldsymbol{\theta}(t)) + B_u(\boldsymbol{\theta}(t))D_cD_{yw} \\ B_c(\boldsymbol{\theta}(t), \dot{\boldsymbol{\theta}}(t))D_{yw} \end{bmatrix} \mathbf{w}(t) \\
\mathbf{z}(t) &= \begin{bmatrix} C_z(\boldsymbol{\theta}(t)) + D_{zu}(\boldsymbol{\theta}(t))D_cC_y & D_{zu}(\boldsymbol{\theta}(t))C_c \end{bmatrix} \begin{bmatrix} \mathbf{x}_g(t) \\ \mathbf{x}_c(t) \end{bmatrix} \\
&\quad + \begin{bmatrix} D_{zw}(\boldsymbol{\theta}(t)) + D_{zu}(\boldsymbol{\theta}(t))D_cD_{yw} \end{bmatrix} \mathbf{w}(t)
\end{aligned}
\tag{4.7}
$$

It can be noticed that the closed-loop matrices depend affinely on both $\boldsymbol{\theta}(t)$ and $\dot{\boldsymbol{\theta}}(t)$. To shorten the presentation, in the rest of the text the closed-loop matrices are denoted by $A_{cl}(\boldsymbol{\theta}(t),\dot{\boldsymbol{\theta}}(t))$, $B_{cl}(\boldsymbol{\theta}(t),\dot{\boldsymbol{\theta}}(t))$, $C_{cl}(\boldsymbol{\theta}(t))$ and $D_{cl}(\boldsymbol{\theta}(t))$, and the closed-loop state vector by $\mathbf{x} = [\mathbf{x}_g^T(t)\ \mathbf{x}_c^T(t)]^T$. Hence (4.7) can be rewriten as

$$
\begin{aligned}
\dot{\mathbf{x}}(t) &= A_{cl}(\boldsymbol{\theta}(t),\dot{\boldsymbol{\theta}}(t))\mathbf{x}(t) + B_{cl}(\boldsymbol{\theta}(t),\dot{\boldsymbol{\theta}}(t))\mathbf{w}(t) \\
\mathbf{z}(t) &= C_{cl}(\boldsymbol{\theta}(t))\mathbf{x}(t) + D_{cl}(\boldsymbol{\theta}(t))\mathbf{w}(t).
\end{aligned}
\tag{4.8}
$$

4.2.4 Stability conditions

A method for verifying the stability of a dynamical system is to search for the existence of an appropriate Lyapunov function. In literature, the predominant choice of a Lyapunov function candidate for an LPV system is a Lyapunov function that is quadratic in the state:

$$
V(\mathbf{x}(t)) = \mathbf{x}^T(t)P(t)\mathbf{x}(t).
\tag{4.9}
$$

The matrix $P(t)$ should be independent of the scheduling parameter vector $\boldsymbol{\theta}(t)$ if $\boldsymbol{\theta}(t)$ can vary infinitely fast. However, this assumption is too restrictive for many practical systems. Hence, it is reasonable to assume that certain bounds on $\dot{\boldsymbol{\theta}}(t)$ can be defined in advance. In this case, the use of scheduling parameter independent Lyapunov matrix $P(t) = P$ could be too conservative. Hence, a PDLF with affine dependence on the scheduling parameter vector is considered:

$$
V(\mathbf{x}(t)) = \mathbf{x}^T(t)P(\boldsymbol{\theta}(t))\mathbf{x}(t), P(\boldsymbol{\theta}(t)) = P_0 + \sum_{i=1}^{n_\theta} \theta_i(t)P_i,
\tag{4.10}
$$

where $P(\boldsymbol{\theta}(t)) > 0$ for $\forall \boldsymbol{\theta}(t) \in \Theta$.

Given that $V(\mathbf{x}(t))$ is quadratic in $\mathbf{x}(t)$ and $P(\boldsymbol{\theta}(t))$ is positive definite, it can be concluded that $V(\mathbf{x}(t))$ is strictly positive for all non-zero state vectors $\mathbf{x}(t)$ and zero only for $\mathbf{x}(t) = 0$. Another condition for $V(\mathbf{x}(t))$ to be a Lyapunov function for the LPV system (4.7) is the negativeness of its derivative for all non-zero $\mathbf{x}(t)$ [95]:

$$
\begin{aligned}
\dot{V}(\mathbf{x}(t)) &= \frac{dV}{dt}\left[\mathbf{x}^T(t)P(\boldsymbol{\theta}(t))\mathbf{x}(t)\right] \\
&= \dot{\mathbf{x}}^T(t)P(\boldsymbol{\theta}(t))\mathbf{x}(t) + \mathbf{x}^T(t)P(\boldsymbol{\theta}(t))\dot{\mathbf{x}}(t) + \mathbf{x}^T(t)\dot{P}(\boldsymbol{\theta}(t))\mathbf{x}(t) < 0.
\end{aligned}
\tag{4.11}
$$

In combination with the dynamic equation of the unforced system $\dot{\mathbf{x}}(t) = A_{cl}(\boldsymbol{\theta}(t),\dot{\boldsymbol{\theta}}(t))\mathbf{x}(t)$ the following expression for $\dot{V}(\mathbf{x}(t))$ is obtained:

$$
\dot{V}(\mathbf{x}(t)) = \mathbf{x}^T(t)[A_{cl}^T(\boldsymbol{\theta}(t),\dot{\boldsymbol{\theta}}(t))P(\boldsymbol{\theta}(t)) + P(\boldsymbol{\theta}(t))A_{cl}(\boldsymbol{\theta}(t),\dot{\boldsymbol{\theta}}(t)) + \dot{P}(\boldsymbol{\theta}(t))]\mathbf{x}(t),
\tag{4.12}
$$

where

$$\dot{P}(\boldsymbol{\theta}(t)) = \sum_{i=1}^{n_\theta} \dot{\theta}_i(t) P_i = P(\dot{\boldsymbol{\theta}}(t)) - P_0.$$

Therefore, the sufficient condition for the LPV system stability using quadratic PDLF affine in $\boldsymbol{\theta}(t)$ is given by the following matrix inequality:

$$A_{cl}^T(\boldsymbol{\theta}(t), \dot{\boldsymbol{\theta}}(t)) P(\boldsymbol{\theta}(t)) + P(\boldsymbol{\theta}(t)) A_{cl}(\boldsymbol{\theta}(t), \dot{\boldsymbol{\theta}}(t)) + \dot{P}(\boldsymbol{\theta}(t)) < 0, \forall \boldsymbol{\theta}(t) \in \Theta \wedge \forall \dot{\boldsymbol{\theta}}(t) \in \Delta. \quad (4.13)$$

It can be observed that the left hand side of the inequality is polynomial in $(\boldsymbol{\theta}(t), \dot{\boldsymbol{\theta}}(t))$. In general, the infinite number of inequalities in (4.13) cannot be replaced by a finite inequality set without loosing the full guarantee on stability or without introducing some conservatism. On the other hand, the controller parameters in $A_{cl}(\boldsymbol{\theta}(t), \dot{\boldsymbol{\theta}}(t))$ are multiplied by Lyapunov matrix parameters $P(\boldsymbol{\theta}(t))$ which makes the above inequality bilinear in optimization variables. Hence, the goal of this chapter is to replace the given infinite set of bilinear matrix inequalities with a finite set of linear matrix inequalities in which $A_{cl}(\boldsymbol{\theta}(t), \dot{\boldsymbol{\theta}}(t))$ is decoupled from $P(\boldsymbol{\theta}(t))$. In the rest of this chapter the dependence of $\boldsymbol{\theta}(t)$ and $\dot{\boldsymbol{\theta}}(t)$ on time is implied.

4.3 Fixed-order LPV Controller Design

The goal is to give a parameterization of an inner convex approximation of the feasible set of the stability condition (4.13) for affine LPV state-space plants by decoupling $A_{cl}(\boldsymbol{\theta}, \dot{\boldsymbol{\theta}})$ from $P(\boldsymbol{\theta})$. In the transfer function setting the use of central polynomial enables decoupling [38, 96]. Similar effect is achieved here by introducing two additional matrix parameters. The first parameter M should enable decoupling of matrices $A_{cl}(\boldsymbol{\theta}, \dot{\boldsymbol{\theta}})$ and $P(\boldsymbol{\theta})$, through relating indirectly stability of M to stability of $A_{cl}(\boldsymbol{\theta}, \dot{\boldsymbol{\theta}})$. The second parameter is the similarity transformation matrix T, which should provide an additional degree of freedom. A method for the robust controller design for systems with polytopic uncertainty structure, which uses a similar idea to obtain an inner convex approximation of the stabilizing controller set, is presented in [97].

To proceed, first some useful definitions and lemmas are presented. The KYP lemma, already mentioned in Chapter 3, for continuous-time systems states that the transfer function $H(s) = C(sI - A)^{-1} B + D$ is SPR if and only if there exists a matrix $P = P^T > 0$ such that

$$\begin{bmatrix} A^T P + PA & PB - C^T \\ B^T P - C & -D - D^T \end{bmatrix} < 0. \quad (4.14)$$

The SPRness of the system implies stability in Lyapunov sense, as it ensures that $A^T P + PA$ is negative definite. The following lemma relates the SPRness of a transfer function with the SPRness of its inverse.

Lemma 4.1 *These two statements are equivalent:*

1) $H(s) = \left[\begin{array}{c|c} A & B \\ \hline C & I \end{array}\right]$ is SPR.

2) $H^{-1}(s) = \left[\begin{array}{c|c} A - BC & B \\ \hline -C & I \end{array}\right]$ is SPR.

Proof. According to the KYP lemma and using the Schur complement lemma [98], Statement 1 is equivalent to the existence of $P = P^T > 0$ such that

$$A^T P + PA + \frac{1}{2}(PB - C^T)(B^T P - C) < 0. \tag{4.15}$$

This inequality can be rearranged to

$$(A - BC)^T P + P(A - BC) + \frac{1}{2}(PB + C^T)(B^T P + C) < 0, \tag{4.16}$$

which is equivalent to Statement 2. □

The following consequence of Lemma 4.1 is of great importance for the desired parameterization of a fixed-order LPV controller set.

Lemma 4.2 *The following matrix inequalities are equivalent:*

$$\begin{bmatrix} M^T P + PM & P - M^T + (T^{-1}AT)^T \\ P - M + T^{-1}AT & -2I \end{bmatrix} < 0 \Leftrightarrow \tag{4.17}$$

$$\begin{bmatrix} A^T P_T + P_T A & P_T - A^T X + M_T^T \\ P_T - XA + M_T & -2X \end{bmatrix} < 0, \tag{4.18}$$

where $P_T = T^{-T} P T^{-1}$, $M_T = T^{-T} M T^{-1}$ and $X = T^{-T} T^{-1}$.

Proof. Set $A := T^{-1}AT$, $B := I$ and $C := T^{-1}AT - M$ for the transfer function $H(s)$ in Lemma 4.1. Writing the KYP lemma in the matrix form for the transfer function $H^{-1}(s)$ provides exactly (4.17). Next, writing the KYP lemma matrix inequality for $H(s)$, which is equivalent to (4.17) by Lemma 4.1, and pre- and post-multiplication of the left-hand side by block diagonal matrix blkdiag(T^{-T}, T^{-T}) and its transpose lead to (4.18). As pre- an post-multiplication by a non-singular matrix and its transpose do not change the sign definiteness of a matrix expression, the equivalence is preserved. □

The next lemma enables the representation of the convex set of controllers through a finite number of LMIs.

Lemma 4.3 *Consider a symmetric matrix L which is affine in the parameter vector ϕ, i.e.*

$$L(\boldsymbol{\phi}) = L_0 + \sum_{i=1}^{n_\phi} \phi_i L_i, \tag{4.19}$$

where $\boldsymbol{\phi}$ belongs to the polytope Φ, and the finite set of vertices of Φ is denoted by $\Phi_v = \{\phi_{v_1},\dots,\phi_{v_q}\}$. Then the infinite set of matrix inequalities

$$L(\boldsymbol{\phi}) < 0, \forall \boldsymbol{\phi} \in \Phi \tag{4.20}$$

is equivalent to the finite set of matrix inequalities

$$L(\boldsymbol{\phi}) < 0, \forall \boldsymbol{\phi} \in \Phi_v. \tag{4.21}$$

The proof is easily derived using convex combinations of the vertices.

Based on these lemmas, the following fixed-order LPV controller parameterization is given.

Theorem 4.1 *Suppose that the LPV plant model is given by (4.1) and (4.2) and that the scheduling parameters and their variation rates belong to hyperrectangles Θ and Δ (as in (4.3) and (4.5)), with Θ_v and Δ_v denoting the vertex sets of Θ and Δ. Then, given matrices M and T, the controller in (4.4) stabilizes the LPV model for any allowable scheduling parameter trajectory if*

$$\begin{bmatrix} M^T P(\boldsymbol{\theta}) + P(\boldsymbol{\theta})M + P(\dot{\boldsymbol{\theta}}) - P(0) & (*) \\ P(\boldsymbol{\theta}) - M + T^{-1}A_{cl}(\boldsymbol{\theta},\dot{\boldsymbol{\theta}})T & -2I \end{bmatrix} < 0, \tag{4.22}$$

$$P(\boldsymbol{\theta}) > 0 \quad , \quad \forall \boldsymbol{\theta} \in \Theta_v, \forall \dot{\boldsymbol{\theta}} \in \Delta_v.$$

Symbol $(*)$ substitutes the terms which ensure the symmetry of the matrix.

Proof. First notice that the left-hand side of (4.22) can be represented as a symmetric matrix expression affine in vector $\phi^T = [\boldsymbol{\theta}^T, \dot{\boldsymbol{\theta}}^T]$. As ϕ belongs to the polytope Φ given by $\Phi = \Theta \times \Delta$, based on Lemma 4.3, it can be concluded that the matrix inequality (4.22) is valid for all $\boldsymbol{\theta} \in \Theta$ and $\dot{\boldsymbol{\theta}} \in \Delta$. Next, observe Lemma 4.2 and notice that the addition of a term $P(\dot{\boldsymbol{\theta}}) - P_0$ to the upper left blocks of both matrices by Schur complement lemma does not spoil the equivalence. Therefore, using the shorthands $P_T = T^{-T}PT^{-1}$, $M_T = T^{-T}MT^{-1}$ and $X = T^{-T}T^{-1}$, matrix inequality (4.22) leads to

$$\begin{bmatrix} A_{cl}^T(\boldsymbol{\theta},\dot{\boldsymbol{\theta}})P_T(\boldsymbol{\theta}) + P_T(\boldsymbol{\theta})A_{cl}(\boldsymbol{\theta},\dot{\boldsymbol{\theta}}) + P_T(\dot{\boldsymbol{\theta}}) - P_T(0) & (*) \\ P_T(\boldsymbol{\theta}) - XA_{cl}(\boldsymbol{\theta},\dot{\boldsymbol{\theta}}) + M_T & -2X \end{bmatrix} < 0, \tag{4.23}$$

$$P_T(\boldsymbol{\theta}) > 0 \quad , \quad \forall \boldsymbol{\theta} \in \Theta, \forall \dot{\boldsymbol{\theta}} \in \Delta.$$

The application of the Schur complement lemma on (4.23) leads to

$$A_{cl}^T(\boldsymbol{\theta},\dot{\boldsymbol{\theta}})P_T(\boldsymbol{\theta}) + P_T(\boldsymbol{\theta})A_{cl}(\boldsymbol{\theta},\dot{\boldsymbol{\theta}}) + P_T(\dot{\boldsymbol{\theta}}) - P_T(0) < 0 \tag{4.24}$$

for $\forall \boldsymbol{\theta} \in \Theta$ and $\forall \dot{\boldsymbol{\theta}} \in \Delta$. Hence, the system is stabilized for bounded scheduling parameter variations. $\qquad\square$

Remark 4.3 *As in (4.22) the controller and Lyapunov matrices appear affinely, it is a set of LMIs as long as the matrix parameters M and T are fixed. A proposition for their choice is given in the next subsection.*

The set of LMIs in (4.22) guarantees stability of the closed-loop system for a bounded scheduling parameter variation rate. A good exponential stability decay-rate for the closed-loop system can be ensured as well.

Corollary 4.1 *Using the same set of assumptions as in Theorem 4.1, the following finite set of matrix inequalities*

$$\begin{bmatrix} M^T P(\boldsymbol{\theta}) + P(\boldsymbol{\theta})M + P(\dot{\boldsymbol{\theta}}) - P(0) + \sigma P(\boldsymbol{\theta}) & (*) \\ P(\boldsymbol{\theta}) - M + T^{-1}A_{cl}(\boldsymbol{\theta},\dot{\boldsymbol{\theta}})T & -2I \end{bmatrix} < 0, \tag{4.25}$$

$$P(\boldsymbol{\theta}) > 0 \quad , \quad \forall \boldsymbol{\theta} \in \Theta_\nu, \forall \dot{\boldsymbol{\theta}} \in \Delta_\nu,$$

describes the convex set of LPV controllers stabilizing the LPV plant and ensuring the exponential stability decay-rate α such that $0 < \alpha < \sigma$ and

$$\|\mathbf{x}(t)\| \le c \|\mathbf{x}(0)\| e^{-2\alpha t} \tag{4.26}$$

for some $c > 0$. The value of $\sigma > 0$ can be maximized by the bisection algorithm.

Proof. Based on Theorem 4.10 from [95], if

$$A_{cl}^T(\boldsymbol{\theta},\dot{\boldsymbol{\theta}})P_T(\boldsymbol{\theta}) + P_T(\boldsymbol{\theta})A_{cl}(\boldsymbol{\theta},\dot{\boldsymbol{\theta}}) + P_T(\dot{\boldsymbol{\theta}}) - P_T(0) \le -k\alpha I, \tag{4.27}$$

and $P_T(\boldsymbol{\theta}) \le kI$, then the inequality in (4.26) holds for any $t > 0$ and initial state $\mathbf{x}(0)$, with $k > 0$ and $\alpha > 0$. Similarly to the proof to Theorem 4.1, it can be concluded that (4.25) is equivalent to

$$\begin{bmatrix} A_{cl}^T(\boldsymbol{\theta},\dot{\boldsymbol{\theta}})P_T(\boldsymbol{\theta}) + P_T(\boldsymbol{\theta})A_{cl}(\boldsymbol{\theta},\dot{\boldsymbol{\theta}}) + P_T(\dot{\boldsymbol{\theta}}) - P_T(0) + \sigma P_T(\boldsymbol{\theta}) & (*) \\ P_T(\boldsymbol{\theta}) - X A_{cl}(\boldsymbol{\theta},\dot{\boldsymbol{\theta}}) + M_T & -2X \end{bmatrix} < 0, \tag{4.28}$$

$$P_T(\boldsymbol{\theta}) > 0 \quad , \quad \forall \boldsymbol{\theta} \in \Theta, \forall \dot{\boldsymbol{\theta}} \in \Delta.$$

This implies

$$A_{cl}^T(\boldsymbol{\theta},\dot{\boldsymbol{\theta}})P_T(\boldsymbol{\theta}) + P_T(\boldsymbol{\theta})A_{cl}(\boldsymbol{\theta},\dot{\boldsymbol{\theta}}) + P_T(\dot{\boldsymbol{\theta}}) - P_T(0) \le -\sigma P_T(\boldsymbol{\theta}). \tag{4.29}$$

Since $P_T(\boldsymbol{\theta}) > 0$, there always exists some $k > 0$ such that $P_T(\boldsymbol{\theta}) \le kI$, which in turn implies $\sigma P_T(\boldsymbol{\theta}) \le \sigma kI$ and $-\sigma P_T(\boldsymbol{\theta}) \ge -\sigma kI$. Therefore, it can be concluded that there exists α such that $0 < \alpha < \sigma$ and $-\sigma P_T(\boldsymbol{\theta}) \le -\alpha kI$. $\square$

Remark 4.4 *If in (4.25) the term $\sigma P(\boldsymbol{\theta})$ is replaced by σI, the maximum of σ is a lower bound*

for the decay-rate α and it can be obtained without performing the bisection algorithm.

4.4 Algorithms for Fixed-order Controller Design

The matrix parameters M and T play a crucial role in this approach to a fixed-order LPV controller design. Yet, there exists no evident manner in which their values can be assigned. To resolve this issue, in the rest of this section three different algorithms for the fixed-order controller design are proposed. They all use matrix inequalities presented in the previous chapter as a basis for design. Another common feature is iterative convex optimization solving, with initialization based on the design of some fixed-order LTI controllers.

4.4.1 Algorithm 1: "The gain-scheduling based algorithm"

This algorithm is inspired by the classical gain-scheduled controller design methods. Suppose that for each $\boldsymbol{\theta} \in \Theta_\nu$ a fixed-order LTI controller ("vertex controller") is available such that it stabilizes the LPV model for the frozen scheduling parameter vector value $\boldsymbol{\theta}$. These vertex controllers may be computed using some of the existing LTI controller design approaches in the form of Matlab® toolboxes such as `hinfstruct` [99], `HIFOO` [100] and `FDRC` [101]. In the second phase, the classical gain-scheduling approaches would interpolate these controllers over the whole scheduling parameter space. The next step is calculation of matrices M_T and X. Based on the initial controllers, the vertex closed-loop matrices $A_{cl_j}^{(0)}, j = 1, \ldots, 2^{n_\theta}$ can be calculated. Then, the following semi-definite programming problem with 2^{n_θ} LMI constraints can be proposed to find appropriate values of M_T and X:

$$\begin{bmatrix} (A_{cl_j}^{(0)})^T P_{T_j} + P_{T_j} A_{cl_j}^{(0)} & (*) \\ P_{T_j} + M_T - X A_{cl_j}^{(0)} & -2X \end{bmatrix} < 0, \quad j = 1, \ldots, 2^{n_\theta}. \tag{4.30}$$

From matrix X the similarity transform matrix T can be reconstructed by Cholesky factorization, and afterwards M is calculated as $M = T^T M_T T$. Next, a stabilizing fixed-order LPV controller can be obtained from (4.22) using the values of M and T.

If a feasible solution is obtained for this convex optimization problem, design process is finished. For some plants and choice of initial controllers the convex problem (4.30) may turn out to be infeasible. In this case one of two following algorithms can be applied, where the choice depends on the preference of the user.

4.4.2 Algorithm 2: "The decay-rate based algorithm"

The second algorithm is based on the idea of initialization through the use of the gain-scheduled controller. It can be used in the case that the first algorithm fails, or in the case that user wishes to optimize the exponential decay rate. The main idea is to increase the domain of stability through the use of the exponential decay rate. If initially a stabilizing LPV controller

cannot be obtained, then the design problem is relaxed through negative values of exponential decay rate.

First, a set of controllers is designed for all vertices of the polytope Θ, then appropriate vertex closed-loop matrices $A_{cl_j}^{(0)}, j = 1,\ldots,2^{n_\theta}$ are designed based on them. The following SDP problem is solved next:

$$
\begin{bmatrix} (A_{cl_j}^{(0)})^T P_{T_j} + P_{T_j} A_{cl_j}^{(0)} + \sigma P_{T_j} & (*) \\ P_{T_j} + M_T - X A_{cl_j}^{(0)} & -2X \end{bmatrix} < 0. \tag{4.31}
$$

If this problem is feasible, considering M_T, X, σ and $P_T^{(j)}$, for $j = 1,\ldots,2^{n_\theta}$ as optimization variables, the values of M_T and X are chosen so that the value of σ is maximized using the bisection algorithm.

In the next step, a fixed-order LPV controller can be designed based on calculated values of M and T from (4.25). In order to optimize the value of the decay-rate parameter σ, obtained LPV controller can be used to calculate new values of M_T and X. This leads to a new LPV controller. This procedure is repeated until σ converges. The algorithm can be summarized as follows:

Step 1: choose small $\epsilon > 0$; design the initial controllers $K_i^{(0)}, i = 1,\ldots,2^{n_\theta}$ for $\boldsymbol{\theta}_v \in \Theta_v$; set $k = 1$

Step 2: for $\forall \boldsymbol{\theta}_v \in \Theta_v$ calculate $A_{cl}(\boldsymbol{\theta}_v)$ using $K^{(k-1)}$; set (4.28) for $\forall (\boldsymbol{\theta}, \boldsymbol{\theta}^+) \in \Omega_v$ using $A_{cl}(\boldsymbol{\theta})$ and find feasible X, M_T and $P_T(\theta)$ while maximizing σ by bisection; reconstruct T from $X = T^{-T} T^{-1}$ and subsequently $M = T^T M_T T$;

Step 3: set (4.25) for $\forall (\boldsymbol{\theta}, \boldsymbol{\theta}^+) \in \Omega_v$ using M and T obtained in ***Step 2*** and search for feasible $K^{(k)}$, $P_T(\boldsymbol{\theta})$ and maximal (by bisection) $\sigma^{(k)}$;

Step 4: if $\sigma^{(k)} - \sigma^{(k-1)} > \epsilon$ set $k = k + 1$ and jump to ***Step 2***; otherwise stop.

Equivalence of (4.25) and (4.28) ensures that as a worst case in Step 3 we obtain the same controller and $\sigma^{(k)}$ as those applied in Step 2 are obtained. Therefore stability indicator (and exponential decay parameter) $\sigma^{(k)}$ is monotonically non-increasing in this synthesis procedure.

Remark 4.5 *It is important to keep in mind that the Step 2 slightly differs for the first iteration ($k = 0$) and other iterations ($k > 0$). This difference stems from the fact that in the first iteration initial LTI controllers are used for calculation of A_{cl}, and in the latter ones the LPV controller from the previous iteration.*

A negative value of σ can be obtained in the first iteration, if no stabilizing controller can be found for given values of M and T. However, by further application of the proposed algorithm

value of σ increases, hence it is reasonable to assume that after few iterations stability is achieved. If this does not happen, and no other initial controllers are available, there is still an option to use the third algorithm.

4.4.3 Algorithm 3: "The stretching algorithm"

Suppose that a single initial controller $K^{(0)}$ is available for the centre of hyperrectangle Θ, i.e. $\boldsymbol{\theta} = \mathbf{0}$. Since this is a single LTI system, one of the above-mentioned fixed-order LTI controller design methods can be used to design $K^{(0)}$. The next step is a choice of decoupling and transformation matrices. Based on $K^{(0)}$ system matrix $A_{cl}^{(0)}$ can be calculated. By introducing $A_{cl}^{(0)}$ into (4.23), feasible X, M_T and P_T are obtained. Note that for a single LTI system feasibility is always guaranteed, as $A_{cl}^{(0)}$ is a system matrix of a stable closed-loop system. Values of matrix parameters M and T are obtained from M_T and X, so the controller design phase can be performed. Since matrices M and T are obtained based only on a local information (i.e. controller $K^{(0)}$), it is possible that the LPV controller design based on them does not lead directly to an LPV controller stabilizing the plant for all $(\boldsymbol{\theta}, \dot{\boldsymbol{\theta}}) \in \Omega$, where $\Omega = \Theta \times \Delta$. To overcome this, the idea is to calculate first a controller for the "scaled down Ω", i.e. to perform the design for the set $\Omega(\alpha)$ obtained by scaling the set Ω by factor α around the origin. If the vertex set of $\Omega(\alpha)$ is denoted by $\Omega_v(\alpha)$, the design constraint set is given by

$$\begin{bmatrix} M^T P(\boldsymbol{\theta}) + P(\boldsymbol{\theta})M + P(\dot{\boldsymbol{\theta}}) - P(0) & (*) \\ P(\boldsymbol{\theta}) - M + T^{-1} A_{cl}(\boldsymbol{\theta}, \dot{\boldsymbol{\theta}})T & -2I \end{bmatrix} < 0, \quad P(\boldsymbol{\theta}) > 0, \quad \forall (\boldsymbol{\theta}, \dot{\boldsymbol{\theta}}) \in \Omega_v(\alpha). \qquad (4.32)$$

Since α appears linearly in all $\theta \in \Omega_v(\alpha)$, the maximum feasible $\alpha^{(1)}$ can be obtained by the bisection algorithm. If $\alpha^{(1)} \geq 1$, designed LPV controller $K^{(1)}$ stabilizes the original LPV system, and the design process is finished. In the case that $\alpha^{(1)} < 1$, the step of calculating new values of M and T should be performed, this time using the controller $K^{(1)}$ on $\Omega_v(\alpha^{(1)})$ set. Next, a new controller design step is taken, which leads to new LPV controller $K^{(2)}$ stabilizing $\Omega_v(\alpha^{(2)})$, where $\alpha^{(2)} > \alpha^{(1)}$. This iterative process should be performed until $\alpha^{(k)} \geq 1$ is obtained, after some k iterations.

The algorithm can be summarized with following 4 steps:

Step 1: choose small $\alpha_{tol} > 0$; set $k = 1$;
    design the initial LTI controller $K^{(0)}$ corresponding to $\alpha^{(0)} = 0$

Step 2: for $\forall (\boldsymbol{\theta}, \dot{\boldsymbol{\theta}}) \in \Omega_v(\alpha^{(k-1)})$ calculate $A_{cl}(\boldsymbol{\theta}, \dot{\boldsymbol{\theta}})$ using $K^{(k-1)}(\boldsymbol{\theta}, \dot{\boldsymbol{\theta}})$;
    set (4.23) for $\forall (\boldsymbol{\theta}, \dot{\boldsymbol{\theta}}) \in \Omega_v(\alpha^{(k-1)})$ using $A_{cl}(\boldsymbol{\theta}, \dot{\boldsymbol{\theta}})$ and find feasible X, M_T and $P_T(\boldsymbol{\theta})$;
    reconstruct T from $X = T^{-T} T^{-1}$ and subsequently $M = T^T M_T T$.

Step 3: set $\alpha_{min} = \alpha^{(k-1)}$ and $\alpha_{max} = 1.0$;
    while $(\alpha_{max} - \alpha_{min} > \alpha_{tol})$ do

    (i) $\alpha^{(k)} = (\alpha_{max} + \alpha_{min})/2$;

(ii) set (4.22) for $\forall (\boldsymbol{\theta}, \dot{\boldsymbol{\theta}}) \in \Omega_v(\alpha^{(i)})$ using M and T and search for feasible $K^{(k)}(\boldsymbol{\theta}, \dot{\boldsymbol{\theta}})$ and $P_T(\boldsymbol{\theta})$

(ii) if no feasible point in **(ii)** set $\alpha_{max} = \alpha^{(k)}$; otherwise $\alpha_{min} = \alpha^{(k)}$

Step 4: if $\alpha^{(k)} - \alpha^{(k-1)} > \alpha_{tol}$ set $k = k + 1$ and jump to **Step 2**; otherwise stop.

4.5 Design of Fixed-Order LPV Controllers with Induced $\mathscr{L}_2$-norm and $\mathscr{H}_2$ Performance Specifications

4.5.1 Induced $\mathscr{L}_2$-norm performance constraints

In the LPV literature, induced $\mathscr{L}_2$-norm performance is usually examined through the extension of Bounded Real Lemma to LPV systems. Based on [59], the induced $\mathscr{L}_2$-norm performance level γ for the closed-loop system (4.8) is the minimum γ for which there exists a Lyapunov function $P(\boldsymbol{\theta})$ such that

$$\begin{bmatrix} A_{cl}^T(\boldsymbol{\theta}, \dot{\boldsymbol{\theta}})P(\boldsymbol{\theta}) + P(\boldsymbol{\theta})A_{cl}(\boldsymbol{\theta}, \dot{\boldsymbol{\theta}}) + P(\dot{\boldsymbol{\theta}}) - P(0) & P(\boldsymbol{\theta})B_{cl}(\boldsymbol{\theta}, \dot{\boldsymbol{\theta}}) & C_{cl}^T(\boldsymbol{\theta}) \\ B_{cl}^T(\boldsymbol{\theta}, \dot{\boldsymbol{\theta}})P(\boldsymbol{\theta}) & -\gamma I & D_{cl}^T(\boldsymbol{\theta}) \\ C_{cl}(\boldsymbol{\theta}) & D_{cl}(\boldsymbol{\theta}) & -\gamma I \end{bmatrix} < 0, \qquad (4.33)$$

is satisfied for $\forall \boldsymbol{\theta} \in \Theta, \forall \dot{\boldsymbol{\theta}} \in \Delta$.

Similar to the case of stabilizing controller design, the goal is to obtain matrix constraints that decouple $A_{cl}(\boldsymbol{\theta}, \dot{\boldsymbol{\theta}})$ and $P_T(\boldsymbol{\theta})$. In [102] LMI conditions are proposed for the analysis of performance of polytopic uncertain systems. Based on these conditions, the following theorem can be used for the fixed-order controller design with guaranteed level of induced $\mathscr{L}_2$-norm performance.

Theorem 4.2 *Suppose that the LPV plant model is given by (4.1) and (4.2) and that the scheduling parameters and their variation rates belong to hyperrectangles Θ and Δ (as in (4.3) and (4.5)), with Θ_v and Δ_v denoting the vertex sets of Θ and Δ. Then, given matrices M and X, the controller in (4.4) and (4.6) stabilizes the LPV plant and provides the level γ of induced $\mathscr{L}_2$-norm performance for any allowable scheduling parameter trajectory if*

$$\begin{bmatrix} -M^T A_{cl}(\boldsymbol{\theta}, \dot{\boldsymbol{\theta}}) - A_{cl}^T(\boldsymbol{\theta}, \dot{\boldsymbol{\theta}})M + P(\dot{\boldsymbol{\theta}}) - P(0) & (*) & (*) & (*) \\ P(\boldsymbol{\theta}) + X^T A_{cl}(\boldsymbol{\theta}, \dot{\boldsymbol{\theta}}) + M & -X - X^T & (*) & (*) \\ -B_{cl}^T(\boldsymbol{\theta}, \dot{\boldsymbol{\theta}})M & B_{cl}^T(\boldsymbol{\theta}, \dot{\boldsymbol{\theta}})X & -\gamma I & (*) \\ C_{cl}(\boldsymbol{\theta}) & 0 & D_{cl}(\boldsymbol{\theta}) & -\gamma I \end{bmatrix} < 0, \qquad (4.34)$$

$$P(\boldsymbol{\theta}) > 0, \quad \forall \boldsymbol{\theta} \in \Theta_v, \forall \dot{\boldsymbol{\theta}} \in \Delta_v.$$

Proof. Observe the matrix

$$
L_\infty^T(\boldsymbol{\theta}) = \begin{bmatrix} I & A_{cl}^T(\boldsymbol{\theta},\dot{\boldsymbol{\theta}}) & 0 & 0 \\ 0 & B_{cl}^T(\boldsymbol{\theta},\dot{\boldsymbol{\theta}}) & I & 0 \\ 0 & 0 & 0 & I \end{bmatrix}.
\tag{4.35}
$$

Note that the matrix $L_\infty(\boldsymbol{\theta})$ is of a full row rank, which implies that it is of a full rank. Hence, the pre-multiplication of (4.34) by $L_\infty^T(\boldsymbol{\theta})$ and post-multiplication by $L_\infty(\boldsymbol{\theta})$ preserves the positive-definiteness of the resulting lower dimensional matrix. But, this resulting matrix is exactly the one on the left-hand side of (4.33) [102]. This concludes the proof. $\qquad\square$

To apply this theorem for the fixed-order controller design with guaranteed level of induced $\mathscr{L}_2$-norm performance, an algorithm similar to one of those presented for the stabilizing controller design can be used here. In the case that the stabilizing LPV controller is already available, it can be used for the initialization of the algorithm. The important difference is that instead of alternating between two different sets of LMIs, here a single LMI constraint set (4.34) is used in both steps of the algorithm iterate. In one step controller variables would be fixed, and optimization performed over the others (including M and X), and in the other step matrices M and X would be fixed. Notice as well that X it is not necessarily symmetric.

4.5.2 $\mathscr{H}_2$ performance constraints

Based on [103], the $\mathscr{H}_2$ performance for an LPV system can be examined in the following manner. The $\mathscr{H}_2$ performance level η for the closed-loop system (4.8) is a minimum η for which exists a Lyapunov function $P(\boldsymbol{\theta})$ and symmetric matrix $W(\boldsymbol{\theta})$ such that

$$
\begin{bmatrix} A_{cl}^T(\boldsymbol{\theta},\dot{\boldsymbol{\theta}})P(\boldsymbol{\theta}) + P(\boldsymbol{\theta})A_{cl}(\boldsymbol{\theta},\dot{\boldsymbol{\theta}}) + P(\dot{\boldsymbol{\theta}}) - P(0) & C_{cl}^T(\boldsymbol{\theta}) \\ C_{cl}(\boldsymbol{\theta}) & -I \end{bmatrix} < 0,
$$

$$
\begin{bmatrix} W(\boldsymbol{\theta}) & B_{cl}^T(\boldsymbol{\theta},\dot{\boldsymbol{\theta}})P(\boldsymbol{\theta}) \\ P(\boldsymbol{\theta})B_{cl}(\boldsymbol{\theta},\dot{\boldsymbol{\theta}}) & P(\boldsymbol{\theta}) \end{bmatrix} > 0,
\tag{4.36}
$$

$$
\text{trace}(W(\boldsymbol{\theta})) \le \eta^2
$$

is fulfilled for $\forall \boldsymbol{\theta} \in \Theta, \forall \dot{\boldsymbol{\theta}} \in \Delta$.

As for the fixed-order induced $\mathscr{L}_2$-norm performance controller design, for the $\mathscr{H}_2$ LPV fixed-order controller design using the convex optimization tools the matrix conditions are needed in which $A_{cl}(\boldsymbol{\theta},\dot{\boldsymbol{\theta}})$ and $P_T(\boldsymbol{\theta})$, and $B_{cl}(\boldsymbol{\theta},\dot{\boldsymbol{\theta}})$ and $P(\boldsymbol{\theta})$ as well, are decoupled. In [104], LMI conditions are presented for the analysis of $\mathscr{H}_2$ performance of polytopic uncertain systems. Motivated by these conditions, the following theorem is proposed for the fixed-order controller design with guaranteed level of $\mathscr{H}_2$ performance.

Theorem 4.3 *Suppose the LPV plant model is given by (4.1) and (4.2) and that the scheduling parameters and their variation rates belong to hyperrectangles Θ and Δ (as in (4.3) and (4.5)), with Θ_v and Δ_v denoting the vertex sets of Θ and Δ. Then, given matrices M, X, M_B and X_B, the controller in (4.4) and (4.6) stabilizes the LPV plant and provides the level η of $\mathcal{H}_2$ performance for any allowable scheduling parameter trajectory if*

$$\begin{bmatrix} -A_{cl}^T(\boldsymbol{\theta},\dot{\boldsymbol{\theta}})M - M^T A_{cl}(\boldsymbol{\theta},\dot{\boldsymbol{\theta}}) + P(\dot{\boldsymbol{\theta}}) - P(0)) & (*) & (*) \\ PT(\boldsymbol{\theta}) + X^T A_{cl}(\boldsymbol{\theta},\dot{\boldsymbol{\theta}}) + M & -X - X^T & (*) \\ C_{cl}(\boldsymbol{\theta}) & 0 & -I \end{bmatrix} < 0,$$

$$\begin{bmatrix} -W(\boldsymbol{\theta}) + B_{cl}^T(\boldsymbol{\theta},\dot{\boldsymbol{\theta}})M_B + M_B^T B_{cl}(\boldsymbol{\theta},\dot{\boldsymbol{\theta}}) & -M_B^T + B_{cl}^T(\boldsymbol{\theta},\dot{\boldsymbol{\theta}})X_B^T \\ -M_B + X_B B_{cl}(\boldsymbol{\theta},\dot{\boldsymbol{\theta}}) & P(\boldsymbol{\theta}) - (X_B + X_B^T) \end{bmatrix} < 0, \tag{4.37}$$

$$trace(W(\boldsymbol{\theta})) \le \eta^2, \quad P(\boldsymbol{\theta}) > 0, \quad \forall \boldsymbol{\theta} \in \Theta_v, \forall \dot{\boldsymbol{\theta}} \in \Delta_v.$$

Proof. Application of the Schur complement lemma around the bottom right block of the first inequality in (4.37) leads to

$$\begin{bmatrix} -A_{cl}^T(\boldsymbol{\theta},\dot{\boldsymbol{\theta}})M - M^T A_{cl}(\boldsymbol{\theta},\dot{\boldsymbol{\theta}}) + P(\dot{\boldsymbol{\theta}}) - P(0) + C_{cl}^T(\boldsymbol{\theta})C_{cl}(\boldsymbol{\theta}) & P(\boldsymbol{\theta}) + A_{cl}^T(\boldsymbol{\theta},\dot{\boldsymbol{\theta}})X + M^T \\ P(\boldsymbol{\theta}) + X^T A_{cl}(\boldsymbol{\theta},\dot{\boldsymbol{\theta}}) + M & -X - X^T \end{bmatrix} < 0. \tag{4.38}$$

Pre-multiplication of this inequality by $\begin{bmatrix} I & -A_{cl}^T(\boldsymbol{\theta},\dot{\boldsymbol{\theta}}) \end{bmatrix}$ and post-multiplication by its transpose lead to

$$A_{cl}^T(\boldsymbol{\theta},\dot{\boldsymbol{\theta}})P(\boldsymbol{\theta}) + P(\boldsymbol{\theta})A_{cl}(\boldsymbol{\theta},\dot{\boldsymbol{\theta}}) + P(\dot{\boldsymbol{\theta}}) - P(0) + C_{cl}^T(\boldsymbol{\theta})C_{cl}(\boldsymbol{\theta}) < 0, \tag{4.39}$$

which is by Schur complement lemma equivalent to the first inequality in (4.36).

Next, consider pre- and post-multiplication of the second inequality in (4.37) by $\begin{bmatrix} I & B_{cl}^T(\boldsymbol{\theta},\dot{\boldsymbol{\theta}}) \end{bmatrix}$ and its transpose. This leads to

$$B_{cl}^T(\boldsymbol{\theta},\dot{\boldsymbol{\theta}})P(\boldsymbol{\theta})B_{cl}(\boldsymbol{\theta},\dot{\boldsymbol{\theta}}) - W(\boldsymbol{\theta}) < 0, \tag{4.40}$$

which is by Schur complement lemma equivalent to the second inequality in (4.36). This concludes the proof. $\square$

Based on this theorem, proposed design algorithms can be employed for fixed-order controller design with guaranteed level of $\mathcal{H}_2$ performance. Stabilizing fixed-order LPV controller can be used here for the initialization as well. Note that algorithms for the stabilizing fixed-order LPV controller design have to be altered in order to be applied here. The reason is that 4, instead of 2, additional matrix parameters appear: M, X, M_B and X_B. This means that in the first phase of Algorithm 1 (or Step 2 of Algorithms 2 and 3) the controller variables are fixed, while the

optimization is performed over M, X, M_B and X_B (and the other optimization variables). In the second phase of Algorithm 1 (Step 3 of Algorithms 2 and 3) matrices M, X, M_B and X_B are fixed and optimization is performed to obtain new fixed-order LPV controller.

4.6 Applications

4.6.1 Simulation results

The efficiency of the proposed method is verified on the simulation example taken from [62]. The simulation plant represents a simple two-disc system with the following LPV model

$$\dot{\mathbf{x}}_g = \begin{bmatrix} 0 & 0 & 1 & 0 \\ 0 & 0 & 0 & 1 \\ \theta_1 - \dfrac{k_0}{m_1} & \dfrac{k_0}{m_1} & \dfrac{b_0}{m_1} & 0 \\ \dfrac{k_0}{m_2} & \theta_2 - \dfrac{k_0}{m_2} & 0 & \dfrac{b_0}{m_2} \end{bmatrix} \mathbf{x}_g + \begin{bmatrix} 0 \\ 0 \\ \dfrac{0.1}{m_1} \\ 0 \end{bmatrix} \mathbf{u} \tag{4.41}$$

$$\mathbf{y} = \begin{bmatrix} 0 & 1 & 0 & 0 \end{bmatrix} \mathbf{x}_g,$$

with constants $k_0 = 200N/m$, $b_0 = 1kg/s$, $m_1 = 1kg$ and $m_2 = 0.5kg$. The scheduling parameters θ_1 and θ_2 belong to the intervals $[0,9]$ and $[0,25]$, respectively. For bounds on the scheduling parameter variation rate the reasonable values of $[\underline{\delta}_1, \overline{\delta}_1] = [-30,30]\dfrac{rad}{s^2}$ and $[\underline{\delta}_2, \overline{\delta}_2] = [-50,50]\dfrac{rad}{s^2}$ are chosen. Analyzing the plant for frozen values of $\boldsymbol{\theta}$, it can be observed that for $[\theta_1, \theta_2] = [0,0]$ there is one pole at 0, and for the other 3 vertices of the hyperrectangle Θ, the open-loop system is unstable. The aim is to compute a second-order LPV controller that guarantees the exponential stability of the closed-loop system with a good decay rate.

In order to optimize the closed-loop decay rate, the Algorithm 2 is employed for the controller design. The first step is to design simple initial controllers for 4 vertices of Θ. As a tool, the Frequency-domain Robust Controller Design Toolbox [105] is used. In order to show that simple tuning of initial controllers gives good results some PID controllers are designed, as this is still the first choice of control engineers in practice [106]. The controllers are designed by an open-loop shaping method that guarantees a maximum of 4.5 for the magnitude of the

sensitivity function. In this manner the following controllers are obtained:

$$
\begin{aligned}
K_1^0(s) &= -828.73\frac{(s+0.3278)(s+5.32)}{s(s+50)} \quad \text{for } \boldsymbol{\theta} = [0,\ 0]^T \\
K_2^0(s) &= -992.27\frac{(s+0.5496)(s+17.19)}{s(s+50)} \quad \text{for } \boldsymbol{\theta} = [0,\ 25]^T \\
K_3^0(s) &= -919.68\frac{(s+0.7045)(s+15.4)}{s(s+50)} \quad \text{for } \boldsymbol{\theta} = [9,\ 0]^T \\
K_4^0(s) &= -948.97\frac{(s+0.1187)(s+24.58)}{s(s+50)} \quad \text{for } \boldsymbol{\theta} = [9,\ 25]^T.
\end{aligned}
$$

Obviously, if a unique Lyapunov matrix P for 4 closed-loop systems based on these 4 controllers can be obtained, then any interpolation between these controllers would produce an LPV controller stabilizing the LPV plant for any possible variation of $\boldsymbol{\theta}$. Hence, there would be no need to continue with design if just a stabilizing LPV controller is needed. However, examining the system of 4 LMIs in unknown matrix P gives no feasible solution. Therefore, it is reasonable to design an LPV controller for given bounds on the scheduling parameter variation rate.

Using initial controllers, the decoupling matrix M is obtained from 4 LMIs in (4.30) related to the 4 vertices of Θ. The matrix T is chosen to be fixed and equal to I in all the simulations in this subsection. The next step is to verify the existence of an affine LPV controller $K(\boldsymbol{\theta})$ and an affine Lyapunov matrix $P(\boldsymbol{\theta})$ in (4.22). All controller state-space matrices, i.e. A_c, B_c, C_c and D_c are chosen to depend affinely on $\boldsymbol{\theta}$. Note that since matrices B_g and C_g are independent of $\boldsymbol{\theta}$, this choice still ensures that A_{cl} is affine with respect to $\boldsymbol{\theta}$. The number of LMIs appearing here is 16, representing the number of vertices of the polytope $\Theta \times \Delta$. For solving the described semidefinite programming problem, SDPT3 [94] can be used as a solver, with YALMIP [93] as a Matlab environment for describing convex programming problems. The maximum value of σ obtained by the bisection algorithm is 0.6789. The state-space description of the resulting controller K_1 is:

$$
\begin{aligned}
A_c(\boldsymbol{\theta}) &= \begin{bmatrix} -3.9959 & -0.9679 \\ -1.1207 & -46.2523 \end{bmatrix} + \theta_1 \begin{bmatrix} -0.0994 & 0.2436 \\ -0.2160 & -0.0359 \end{bmatrix} \\
&\quad + \theta_2 \begin{bmatrix} 0.1112 & 0.0277 \\ 0.2213 & -0.0066 \end{bmatrix} \\
B_c(\boldsymbol{\theta}) &= \begin{bmatrix} 10.7943 \\ 177.6351 \end{bmatrix} + \theta_1 \begin{bmatrix} -1.0236 \\ 0.0678 \end{bmatrix} + \theta_2 \begin{bmatrix} -0.1847 \\ -0.0736 \end{bmatrix} \\
C_c^T(\boldsymbol{\theta}) &= \begin{bmatrix} 12.2934 \\ 109.0334 \end{bmatrix} + \theta_1 \begin{bmatrix} 2.7138 \\ -2.6864 \end{bmatrix} + \theta_2 \begin{bmatrix} -1.0924 \\ -0.2185 \end{bmatrix} \\
D_c(\boldsymbol{\theta}) &= -639.2795 + 5.5746\theta_1 - 3.5194\theta_2.
\end{aligned}
$$

Remark 4.6 *The results can be improved if a decoupling matrix M is chosen again, based on the*
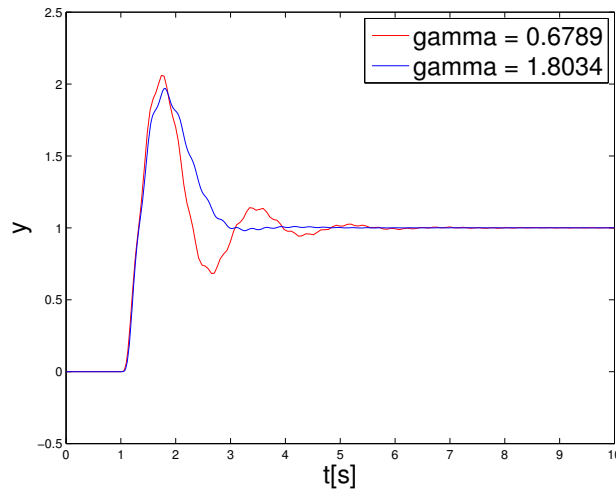
Figure 4.1 – Step response for two different LPV controllers. Red line: using initial PID controllers; Blue line: after 5 iterations.

LPV controller K_1. For this purpose, $A^0_{cl_j}$ are computed based on K_1 and the convex optimization problem in (4.28) is solved. This way, a new decoupling matrix M_1 is obtained that leads to a new controller K_2 with $\sigma = 1.0769$. If 4 more iterations of Algorithm 2 are run, the controller K_6 with $\sigma = 1.8034$ is found. To see how an increased value of σ affects the response of the system, simulations with a step signal as a reference for the closed-loop system with LPV controllers K_1 and K_6 are performed. In both cases the step is applied at $t = 1s$, while θ_1 and θ_2 take the following exponential trajectories:

$$\theta_i = \left\{ \begin{array}{l} \overline{\theta}_i\,,\ t < 1 \\ \overline{\theta}_i e^{-(t-1)/\tau_i}\,,\ t \geq 1 \end{array} \right. , i = 1,2.$$

which corresponds to moving exponentially from $\theta_1 = 9$ and $\theta_2 = 25$ to $\theta_1 = 0$ and $\theta_2 = 0$, respectively. Taking the equation of parameter trajectories into account, it can be concluded that the absolute value of the variation rate of θ_i is maximum for $t = 1s$ where it reaches the value θ_i/τ_i. So, to bring the system to the design limits $\tau_i = \overline{\theta}_i/\overline{\delta}_i$ is chosen, i.e. $\tau_1 = 0.3s$ and $\tau_2 = 0.5s$. Figure 4.1 illustrates the step response for K_1 (red) and K_6 (blue). The second one is much less oscillatory (no undershoot and shorter settling time). Note that the open-loop model is unstable and an overshoot of 100% with a second order controller is a reasonable response very close to the limit of achievable performance.

Remark 4.7 *As previously explained, this approach allows us to obtain controllers that depend on both $\boldsymbol{\theta}$ and $\dot{\boldsymbol{\theta}}$, if variation rate measurements are also available. This provides some additional degrees of freedom that may lead to better decay-rate performance. For this example using the same initial M a new controller $K(\boldsymbol{\theta}, \dot{\boldsymbol{\theta}})$ can be designed with only a small improvement in*

Figure 4.2 – Quanser gyroscope experimental platform [107].

σ (=0.7117), which does not significantly change the closed-loop performance.

Remark 4.8 *In this approach, some of the poles of the controller can be fixed to a predefined value. For example, to ensure the integral action of the LPV controllers to track the step for frozen values of scheduling parameter, one column (or row) of the matrices A_{k_i} could simply be constrained to be identically equal to zero.*

4.6.2 Experimental results

In this section, the application of the proposed method to a 2DOF gyroscope experimental setup is described. The focus is on the LPV modeling of the experimental setup, initial LTI controller and desired LPV controller design, and experimental results obtained from the application of LPV controller on the setup.

Experimental setup description

The gyroscope experimental setup used for performing control experiments described in this section is presented in Figure 4.2. The system consists of three frames (red, blue and grey

Figure 4.3 – Axis of the rotating coordinate frame.

one), and a brass disk. Figure 4.3 illustrates the reference frame xyz that rotates together with the brass disk and the blue frame. The brass disk rotates around the axis x passing through its center and perpendicular to the disk. Axis y represents the axis around which blue frame rotates together with brass disk. Red frame rotates around the axis Z of the inertial reference frame (not to be confused with axis z). In the experiment described here, the grey frame is fixed.

The angular positions of the disk, blue and red frame are measured using quadrature encoders. Three DC motors are used to actuate the disk, the blue and the red frame about the axis x, y and Z, respectively. Data acquisition is performed using the National Instruments DAQ card and Mac Pro computer. A power amplifier is used to convert the voltage output of the DAQ card to current signals applied to the DC motors. A specific LabView virtual instrument is designed for real-time communication and control. Its role is to acquire all the measurements from the DAQ card and condition them properly, to serve as a user interface, and to calculate control signals and store all the relevant data from the experiment.

Experimental setup modeling

Nonlinear model and approximation.   First-principle modeling of the 2DOF gyroscope is explained in details in [108]. The model takes the following form:

$$J_y \ddot{\phi} - J_x^d \dot{v} \dot{\psi} \cos\phi + (J_z - J_x) \dot{\psi}^2 \sin\phi \cos\phi = M_b \tag{4.42}$$
$$(J_Z^r + J_z \cos^2\phi + J_x \sin^2\phi) \ddot{\psi} + J_x^d \dot{v} \dot{\phi} \cos\phi + 2(J_x - J_z) \dot{\psi} \dot{\phi} \sin\phi \cos\phi = M_r.$$

Dependence of all the signals on time is implied.

Angle v denotes the angular position of the disk around its axis of rotation x. Similarly, angle ϕ represents the angular position of the blue frame about y, and ψ the angular position of the red frame about Z. Axis z represents the third axis (aside from x and y) of the Cartesian system that rotates together with the disk and the blue frame. J_x, J_y and J_z are the total moments of inertia of disk and blue frame around the axis x, y and z, respectively. J_Z^r is the moment of inertia of the red frame around the axis Z, and J_x^d that of the disk around the axis x. Total external torque around the axis of rotation of the blue gimbal is denoted by M_b, and M_r is the total external torque around the axis of rotation of the red gimbal. As the static friction can be considered negligible, M_b and M_c represent the torques produced by appropriate motors.

The modeling goal is to build an LPV model scheduled by parameter $\theta = \dot{v}$ around the set point (ϕ_0, ψ_0). For this purpose the approximation of the nonlinear model (4.42) is performed. Assume that the first-order Taylor approximation of (4.42) is obtained, with $\phi = \phi_0 + \Delta\phi$ and $\psi = \psi_0 + \Delta\psi$. Taking into account $\dot{\phi}_0 = \ddot{\phi}_0 = 0$ and $\dot{\psi}_0 = \ddot{\psi}_0 = 0$, as well as $\sin\Delta\phi \approx \Delta\phi$ and $\cos\Delta\phi \approx 1$, the following linearized model is obtained:

$$J_y (\ddot{\Delta\phi}) - J_x^d \dot{v} (\dot{\Delta\psi}) \cos\phi_0 + (J_z - J_x)(\dot{\Delta\psi})^2 \sin\phi_0 \cos\phi_0 = M_b \tag{4.43}$$
$$(J_Z^r + J_z \cos^2\phi_0) \ddot{\Delta\psi} + J_x^d \dot{v} \dot{\Delta\phi} \cos\phi_0 + 2(J_x - J_z) \dot{\Delta\psi} \dot{\Delta\phi} \sin\phi_0 \cos\phi_0 = M_r.$$

The manual of the gyroscope setup [107] states that $J_x = 0.0074 kgm^2$ and $J_z = 0.0056 kgm^2$. Further, it is reasonable to assume that in the experiment $|\dot{\Delta\psi}|$ is of order of $1\dfrac{rad}{s}$. On the other hand, $J_x^d = 0.0056 kgm^2$, and the value of the angular speed $\dot{v}$ at which disk rotates in the experiment is of order $150\dfrac{rad}{s}$. With all these values in mind, and the fact that $|\sin\phi_0| \le 1$, it is reasonable to conclude that

$$\left| J_x^d \dot{v} (\dot{\Delta\phi}) \cos\phi_0 \right| \gg \left| 2(J_x - J_z)(\dot{\Delta\psi})(\dot{\Delta\phi}) \sin\phi_0 \cos\phi_0 \right|. \tag{4.44}$$

This leads to the following simplified gyroscope model around the set point (ϕ_0, ψ_0):

$$J_y \ddot{\Delta\phi} - J_x^d \dot{v} \dot{\Delta\psi} \cos\phi_0 = M_b \tag{4.45}$$
$$(J_Z^r + J_z \cos^2\phi_0) \ddot{\Delta\psi} + J_x^d \dot{v} \dot{\Delta\phi} \cos\phi_0 = M_r.$$

LPV model. The set point chosen for the experiment is $(\phi_0, \psi_0) = (0, 0)$. Consequently, $\Delta\psi$ and $\Delta\phi$ in (4.45) can be replaced by ψ and ϕ, respectively. Denoting $J_Z^0 = J_Z^r + J_z \cos^2\phi_0 = J_Z^r + J_z$, with numerical value $J_Z^0 = 0.0342\,kgm^2$, leads to the following LPV model scheduled in $\theta = \dot{\upsilon}$:

$$J_y\ddot{\phi} - J_x^d\theta\dot{\psi} = M_b \tag{4.46}$$
$$J_Z^0\ddot{\psi} + J_x^d\theta\dot{\phi} = M_r \,,$$

where $J_y = 0.0026\,kgm^2$.

Next, the torques M_b and M_c can be approximated by $M_b = K_b u_b$ and $M_r = K_r u_r$, ignoring dynamics of the power amplifier and motors. Here, u_b and u_r are the control inputs in volts, sent through the DAQ card to the power amplifier. Based on the manual values, it can be concluded that $K_b = K_r = 0.03985\dfrac{Nm}{V}$.

Finally, the following LPV model in form (4.1) is obtained:

$$\dot{\mathbf{x}}_g(t) = \begin{bmatrix} 0 & 1 & 0 & 0 \\ 0 & 0 & 0 & \dfrac{J_x^d}{J_y}\theta \\ 0 & 0 & 0 & 1 \\ 0 & -\dfrac{J_x^d}{J_Z^0}\theta & 0 & 0 \end{bmatrix}\mathbf{x}_g(t) + \begin{bmatrix} 0 & 0 \\ \dfrac{K_b}{J_y} & 0 \\ 0 & 0 \\ 0 & \dfrac{K_r}{J_Z^0} \end{bmatrix}\mathbf{u}(t) \tag{4.47}$$

$$\mathbf{y}(t) = \begin{bmatrix} 1 & 0 & 0 & 0 \\ 0 & 0 & 1 & 0 \end{bmatrix}\mathbf{x}_g(t),$$

with $\mathbf{x}_g(t) = [\phi(t), \dot{\phi}(t), \psi(t), \dot{\psi}(t)]^T$, $u(t) = [u_b(t), u_r(t)]^T$ and $\theta = \dot{\upsilon}$.

Control System Design

Initial LTI controller design. The goal of the controller design is to ensure good tracking of the angular positions of the blue and red frames to given step references. As the first step, a second-order LTI controller is designed for the nominal value of the scheduling parameter $\theta = 150\dfrac{rad}{s}$. Function `hinfstruct` of the Matlab® Robust Control Toolbox is used for the fixed-order LTI controller design. The plant model (4.47) for the fixed value of scheduling parameter $\theta = 150\dfrac{rad}{s}$ is adapted into the classical LFT form for the use with `hinfstruct`. Position references $r_b(t)$ and $r_r(t)$ are chosen as external inputs, control signals $u_b(t)$ and $u_r(t)$ as internal inputs, and position error signals $e_b(t) = r_b(t) - x_{g_1}$ and $e_r(t) = r_r(t) - x_{g_3}$ as measured outputs.

The first goal of a nominal LTI controller design is to obtain good tracking performance. For this reason the error signals $e_b(t)$ and $e_r(t)$ are chosen as the performance outputs. To obtain

good tracking for step reference, these two performance outputs are weighted by performance filter

$$W_1 = \begin{bmatrix} \dfrac{1}{s+10^{-5}} & 0 \\ 0 & \dfrac{1}{s+10^{-5}} \end{bmatrix}.$$

On the other hand, to ensure that the given controller can be applied on the real system, magnitude of the control inputs has to be kept below the saturation levels. To ensure this, two performance outputs corresponding to control inputs $u_b(t)$ and $u_r(t)$ are weighted by

$$W_3 = \begin{bmatrix} 0.15 & 0 \\ 0 & 0.15 \end{bmatrix}.$$

Such a specification leads to the following optimal second-order LTI controller for $\theta = 150\dfrac{rad}{s}$:

$$\left[\begin{array}{c|c} A_c & B_c \\ \hline C_c & D_c \end{array} \right] = \left[\begin{array}{cc|cc} -0.4029 & -94.43 & 37.3 & 39.1 \\ 65.54 & -133.8 & 49.65 & 19.38 \\ \hline -5.392 & -24.21 & 9.683 & 1.15 \\ -23.18 & 17.85 & 5.834 & 5.138 \end{array} \right]. \tag{4.48}$$

LPV controller design. For the given experiment, the bounds on the scheduling parameter and its derivative are chosen as $\Theta = [125\dfrac{rad}{s}, 175\dfrac{rad}{s}]$ and $\Delta = [-10\dfrac{rad}{s^2}, 10\dfrac{rad}{s^2}]$. The Algorithm 3 is used for the fixed-order LPV controller design. It is initialised using the LTI controller presented in the previous subsection. In one algorithm iteration the following LPV controller $A_c(\theta), B_c(\theta), C_c(\theta), D_c(\theta))$ is obtained:

$$A_c(\theta) = \begin{bmatrix} -15.9183 + 0.1550\theta & -61.9083 - 0.3490\theta \\ 40.8114 + 0.2349\theta & -85.0970 - 0.4977\theta \end{bmatrix}$$

$$B_c(\theta) = \begin{bmatrix} 26.3020 + 0.1483\theta & 39.8019 - 0.0009\theta \\ 35.6540 + 0.1785\theta & 14.8075 + 0.0301\theta \end{bmatrix}$$

$$C_c(\theta) = \begin{bmatrix} -5.8025 + 0.0136\theta & -15.9180 - 0.1083\theta \\ -19.1979 - 0.0365\theta & 6.1528 + 0.0927\theta \end{bmatrix}$$

$$D_c(\theta) = \begin{bmatrix} 8.6381 + 0.0305\theta & 4.4201 - 0.0249\theta \\ 8.8580 - 0.0249\theta & 9.7777 - 0.0243\theta \end{bmatrix}$$

As the given LPV controller has to be applied on the system using a digital computer, a discretization has to be performed. The following approximations, based on the first-order Taylor series, are used (some practical aspects of LPV controller discretization are considered

in [109]):

$$A_c^d(\theta) = e^{A_c(\theta)} \approx I + T_s A_c(\theta) = (I + T_s A_{k_0}) + \theta T_s A_{k_1}$$

$$B_c^d(\theta) = A_c^{-1}(\theta)(A_c^d(\theta) - I)B_c(\theta) \approx T_s B_c(\theta).$$

Sampling time is chosen as $T_s = 1ms$. This leads to a discretised LPV controller with preserved linear dependence on the scheduling parameter θ.

Experimental results

The goal of experiment is to illustrate that designed LPV controller preserves good performance in the presence of scheduling parameter variations. To test this assumption, the following experiment is performed. Value of the angular velocity of the disk $\dot{v}$, i.e. scheduling parameter θ, is made to track sinusoidal reference between $125\frac{rad}{s}$ and $175\frac{rad}{s}$. Simple first-order transfer function fitting provides the model between the voltage sent through the DAQ card and angular speed of disk:

$$G_{sl}(s) = \frac{6.052}{s + 0.0025}.$$

Movement of blue and red frames does not have a strong influence on the rotational speed of the disk. Hence, a simple proportional controller $K_{sl} = 0.3305$ is used to ensure this tracking, successfully as it can be observed on the first graph of Figure 4.4.

References for positions of the blue and red frame are given as rectangular functions with period of $10s$. Figure 4.4 illustrates comparison between the obtained response and the reference for the blue and the red frame. Tracking performance is excellent for both frames.

4.7   Conclusions

This chapter presents a method for designing the continuous-time fixed-order LPV controllers with state-space representations affine in the scheduling parameter vector. A set of LMI constraints guaranteeing stability of an LPV system in the presence of bounded variations of the scheduling parameters is proposed. An upper bound on the exponential stability decay-rate is treated as a performance measure, as well as induced $\mathcal{L}_2$-norm and $\mathcal{H}_2$ performance. The efficiency of the proposed method is illustrated by means of a simulation example from the literature, as well as the application to the 2DOF gyroscope experimental setup. For the application of the designed MIMO fixed-order LPV controller to the gyroscope setup, discretization has to be performed with relatively high sampling frequency, to ensure that the stability and performance are preserved. To relax this problem, a method for the direct design of discrete-time fixed-order LPV controllers is proposed in the following chapter.
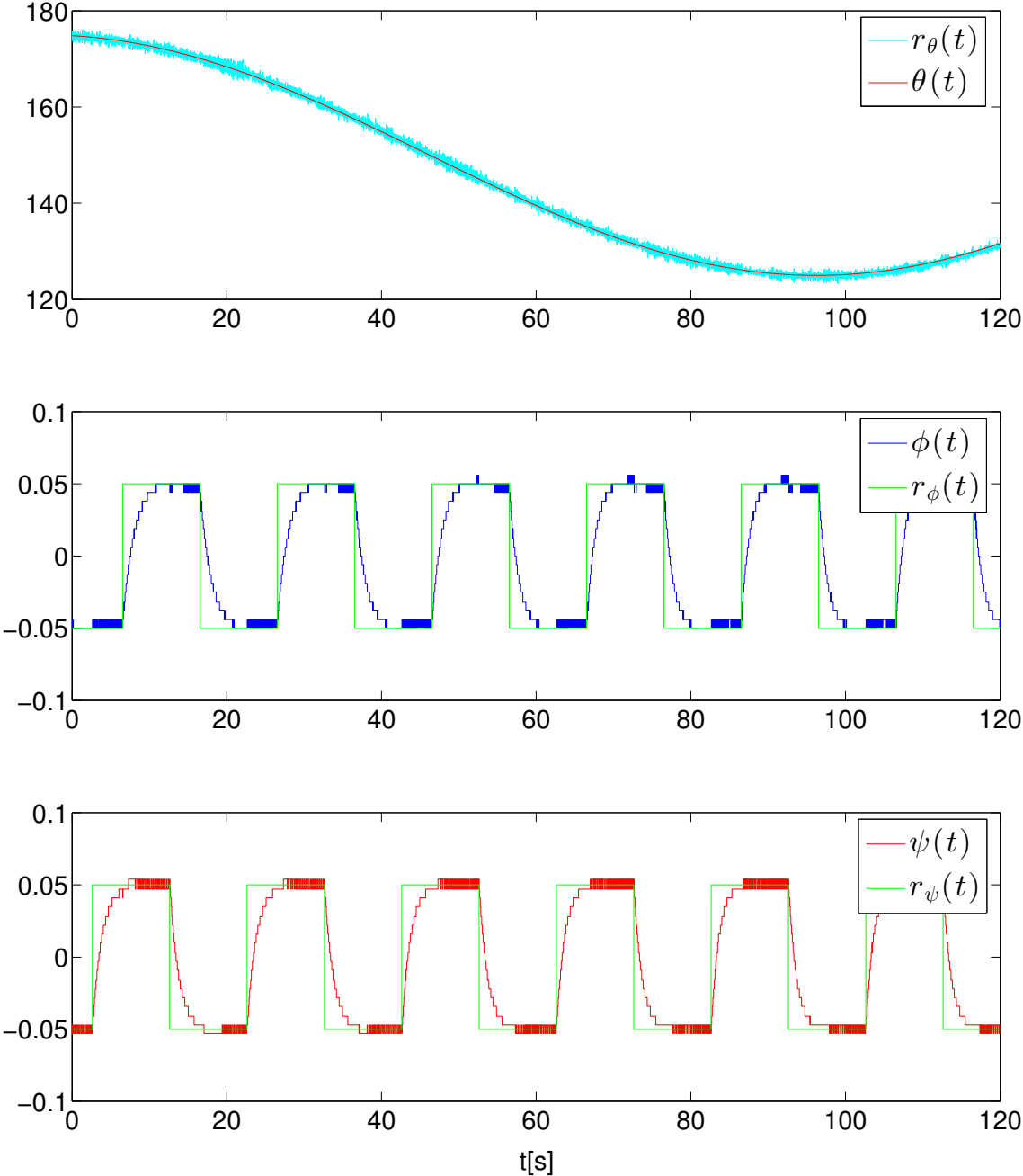
Figure 4.4 – Disk speed, blue frame and red frame position
evolution during the experiment.

5 Fixed-structure LPV Controller Design for Discrete-time LPV Systems

5.1 Introduction

The LPV controller design method presented in the previous chapter is applicable to continuous-time state-space LPV models with affine dependence on the scheduling parameter vector. However, in practice a control law is usually implemented on a digital computer. This means that a discretization of a continuous-time LPV controller has to be performed. To avoid potential problems caused by discretization error, the sampling frequency has to be high. Another issue appearing in practice is that for many systems it may be too difficult to obtain the model based on physical principles. In this case a model is obtained using identification methods, which usually leads to a discrete-time LPV model. For these reasons, if the discrete-time LPV model of the system is available, one may choose to design a discrete-time LPV controller.

In this chapter, an LPV controller design method for discrete-time LPV state-space plants affine in the scheduling parameters is proposed. As the controller parameters appear as decision variables in the convex optimization program, specific controller structure desired by the engineer can be preserved. PDLFs are used to exploit known bounds on scheduling parameter vector variations. The scheduling parameter vector uncertainty caused by the sensor measurement error is accounted for in the design. An algorithm based on the iterative convex optimization procedure can be used to optimize the $\mathcal{H}_2$ or induced l_2-norm performance of the closed-loop system. The effectiveness of the proposed method is illustrated using simulation examples, including some numerical comparison with an approach based on the similar premises.

5.2 Preliminaries

5.2.1 LPV plant and controller

The class of LPV discrete-time systems considered in this chapter can be represented by the following model:

$$
\begin{aligned}
\mathbf{x}_g(k+1) &= A_g(\boldsymbol{\theta}(k))\mathbf{x}_g(k) + B_u(\boldsymbol{\theta}(k))\mathbf{u}(k) + B_w(\boldsymbol{\theta}(k))\mathbf{w}(k)\\
\mathbf{z}(k) &= C_z(\boldsymbol{\theta}(k))\mathbf{x}_g(k) + D_{zu}(\boldsymbol{\theta}(k))\mathbf{u}(k) + D_{zw}(\boldsymbol{\theta}(k))\mathbf{w}(k)\\
\mathbf{y}(k) &= C_y\mathbf{x}_g(k) + D_{yw}\mathbf{w}(k).
\end{aligned}
\tag{5.1}
$$

Here $\mathbf{x}_g(k) \in \mathbb{R}^n$ represents the state vector, $\mathbf{u}(k) \in \mathbb{R}^{n_u}$ is the control input vector, $\mathbf{z}(k) \in \mathbb{R}^{n_z}$ is the vector of controlled outputs and $\mathbf{y}(k) \in \mathbb{R}^{n_y}$ is the vector of measured outputs. The time-varying scheduling parameter vector $\boldsymbol{\theta}(k) = [\theta_1(k), \ldots, \theta_{n_\theta}(k)]^T$ is assumed to belong to a hyperrectangle $\Theta \in \mathbb{R}^{n_\theta}$, or equivalently

$$
\theta_i(k) \in [-\overline{\theta}_i, \overline{\theta}_i],\ i = 1, \ldots, n_\theta.
\tag{5.2}
$$

Symmetric bounds around $\theta_i = 0$ are assumed without loss of generality. Scheduling parameters θ_i are assumed to be independent.

Strict properness of the plant model is a non-restrictive assumption, since in discrete-time systems there is always a delay of at least one sampling period. Similar to the Chapter 4, matrices C_y and D_{yw} are assumed to be independent of the scheduling parameter vector. However, similar results could be obtained for the case of C_y and D_{yw} depending on θ, and B_u and D_{zu} being independent.

Affine dependence on the scheduling parameter vector is assumed for all $\boldsymbol{\theta}$-dependent matrices. This can be represented, for example for A_g, as

$$
A_g(\boldsymbol{\theta}(k)) = A_{g_0} + \sum_{i=1}^{n_\theta} \theta_i(k) A_{g_i}.
\tag{5.3}
$$

The following fixed-order LPV dynamic output feedback controller structure is considered:

$$
\begin{aligned}
\mathbf{x}_c(k+1) &= A_c(\boldsymbol{\theta}(k))\mathbf{x}_c(k) + B_c(\boldsymbol{\theta}(k))\mathbf{y}(k)\\
\mathbf{u}(k) &= C_c\mathbf{x}_c(k) + D_c\mathbf{y}(k),
\end{aligned}
\tag{5.4}
$$

where $\mathbf{x}_c(k) \in \mathbb{R}^{n_c}$ represents the controller state vector. The choice of controller order n_c is fully left to user.

Matrices $A_c(\boldsymbol{\theta}(k))$ and $B_c(\boldsymbol{\theta}(k))$ are supposed to have an affine dependency on the scheduling parameter vector. This implies that the closed-loop matrices are as well affine in the scheduling

parameters. Closed-loop system equations can be written as

$$\mathbf{x}(k+1) = A_{cl}(\boldsymbol{\theta}(k))\mathbf{x}(k) + B_{cl}(\boldsymbol{\theta}(k))\mathbf{w}(k)$$
$$\mathbf{y}(k) = C_{cl}(\boldsymbol{\theta}(k))\mathbf{x}(k) + D_{cl}(\boldsymbol{\theta}(k))\mathbf{w}(k),$$

(5.5)

where $\mathbf{x}(k) = [\mathbf{x}_g(k) \, \mathbf{x}_c(k)]^T$ and

$$A_{cl}(\boldsymbol{\theta}) = \begin{bmatrix} A_g(\boldsymbol{\theta}(k)) + B_u(\boldsymbol{\theta}(k))D_c C_y & B_u(\boldsymbol{\theta}(k))C_c \\ B_c(\boldsymbol{\theta}(k))C_y & A_c(\boldsymbol{\theta}(k)) \end{bmatrix}$$

$$B_{cl}(\boldsymbol{\theta}(k)) = \begin{bmatrix} B_w(\boldsymbol{\theta}(k)) + B_u(\boldsymbol{\theta}(k))D_c D_{yw} \\ B_c(\boldsymbol{\theta}(k))D_{yw} \end{bmatrix}$$

$$C_{cl}(\boldsymbol{\theta}(k)) = \begin{bmatrix} C_z(\boldsymbol{\theta}(k)) + D_{zu}(\boldsymbol{\theta}(k))D_c C_y & D_{zu}(\boldsymbol{\theta}(k))C_c \end{bmatrix}$$

$$D_{cl}(\boldsymbol{\theta}(k)) = \begin{bmatrix} D_{zw}(\boldsymbol{\theta}(k)) + D_{zu}(\boldsymbol{\theta}(k))D_c D_{yw} \end{bmatrix}$$

(5.6)

Remark 5.1 *The closed-loop matrices in (5.6) are affine in $\boldsymbol{\theta}(k)$ as some plant matrices are limited to be independent of $\boldsymbol{\theta}(k)$. If this was not the case, the problem could be treated using the homogenous polynomials relaxations (e.g. as in [65]). However, for the simplicity of presentation this assumption is used throughout this chapter.*

5.2.2 Discrete-time LPV system stability conditions

Assessing the stability of a discrete-time LPV system through the use of a Lyapunov function quadratic in the state is well treated in the literature (e.g. [55]). In the discrete-time case, keeping the Lyapunov matrix P independent of $\boldsymbol{\theta}(k)$ is too restrictive even if the scheduling parameters can change from one extremal value to another over the course of one sampling period [57]. Usually in practical applications the maximum possible variation of a scheduling parameter is bounded as in

$$\theta_i^+ - \theta_i \in [-\overline{\delta}_i, \overline{\delta}_i], \, 0 < \overline{\delta}_i < 2\overline{\theta}_i, \, i = 1, \ldots, n_\theta,$$

(5.7)

where $\boldsymbol{\theta}^+ = \boldsymbol{\theta}(k+1)$. To exploit the bounds on the scheduling parameter variation, Lyapunov matrix affine in the scheduling parameter vector is considered:

$$P(\boldsymbol{\theta}) = P_0 + \sum_{i=1}^{n_\theta} \theta_i P_i > 0, \, \forall \boldsymbol{\theta} \in \Theta.$$

(5.8)

Using (5.8) well-known stability condition for a discrete-time LPV system can be written as

$$P(\boldsymbol{\theta}) - A_{cl}^T(\boldsymbol{\theta})P(\boldsymbol{\theta}^+)A_{cl}(\boldsymbol{\theta}) > 0.$$

(5.9)

This condition has to be satisfied for all admissible values of $(\boldsymbol{\theta}, \boldsymbol{\theta}^+)$. The limits on scheduling parameters (5.2) and their variations (5.7) imply that (θ_i, θ_i^+) belongs to a set presented by
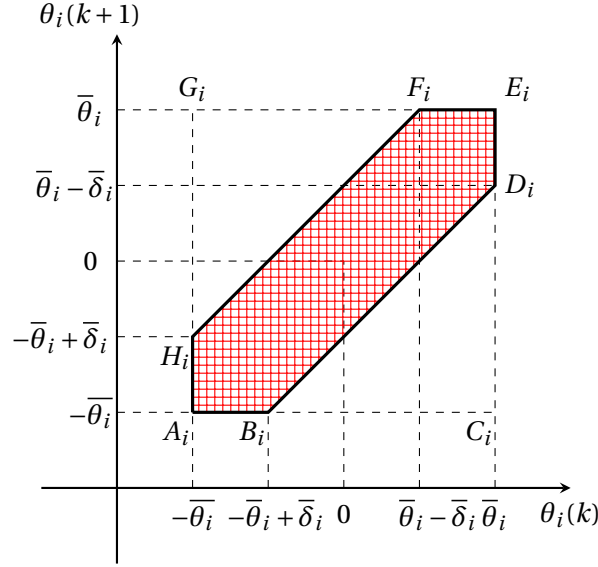
Figure 5.1 – Admissible (θ_i, θ_i^+) space (filled).

filled area on Fig. 5.1. The set of vertices of hexagon $A_i B_i D_i E_i F_i H_i$ will be denoted by Ω_{v_i}. This means that the pair $(\boldsymbol{\theta}, \boldsymbol{\theta}^+)$ always belongs to the polytope Ω whose vertex set Ω_v is given by $\Omega_v = \Omega_{v_1} \times \Omega_{v_2} \times \cdots \times \Omega_{v_{n_\theta}}$. The logic behind Fig. 5.1 is rather intuitive. For example, point H_i is defined by the fact that if $\theta_i = -\overline{\theta}_i$, then $\theta_i^+ \leq -\overline{\theta}_i + \overline{\delta}_i$, since $\overline{\delta}_i$ is maximum possible increase of θ_i over one sample. Points B_i, D_i and F_i are defined in a similar manner.

Remark 5.2 *There are two limit cases that are covered by this setup. First is the fixed scheduling parameter case, which is defined by $\overline{\delta}_i = 0$. In this case the hexagon $A_i B_i D_i E_i F_i H_i$ collapses into a line $A_i E_i$. In the case of maximum possible variations, defined by $\overline{\delta}_i = 2\overline{\theta}_i$, the filled hexagon degenerates into a square $A_i C_i E_i G_i$. However, the primary focus in this chapter is on the non-degenerate case.*

Remark 5.3 *The case of non-symmetric variation bounds could be treated straightforwardly. Symmetric bounds are assumed for the simplicity of presentation.*

Equivalent representation of (5.9) in the literature is [57]

$$
\begin{bmatrix}
P(\boldsymbol{\theta}) & A_{cl}^T(\boldsymbol{\theta}) P(\boldsymbol{\theta}^+) \\
P(\boldsymbol{\theta}^+) A_{cl}(\boldsymbol{\theta}) & P(\boldsymbol{\theta}^+)
\end{bmatrix} > 0.
\tag{5.10}
$$

As controller variables appearing in A_{cl} multiply unknown Lyapunov matrix P in (5.10), the controller synthesis problem becomes a Bilinear Matrix Inequality (BMI) optimization program. As it is a non-convex optimization problem, obtaining even (good) local solution is far from trivial. Another issue is that multiplication of $\boldsymbol{\theta}$ and $\boldsymbol{\theta}^+$ produces the infinite number

of constraints. This can be substituted by a finite number of constraints by application of some relaxation technique [110]. The idea applied in this chapter is to substitute the given infinite set of non-convex constraints on design variables by a finite number of linear matrix inequalities in the controller and Lyapunov function parameters.

5.3 Stabilizing Fixed-structure Discrete-time LPV Controller Synthesis

Over the last 15 years, stability of uncertain and LPV systems is treated using different "slack matrix variable" approaches [55, 56, 57]. Similar conditions are developed in [111] and applied to robust fixed-order controller design for uncertain polytopic systems. These results will be extended to LPV systems.

The following lemma based on the theory from [111] represents a basis for this LPV fixed-structure controller synthesis approach.

Lemma 5.1 *An SPR transfer function $H(z) = C(zI - A)^{-1}B + I$ and $H^{-1}(z) = (-C)(zI - A + BC)^{-1}B + I$ satisfy discrete-time KYP lemma with a common Lyapunov matrix P.*

Proof. KYP lemma inequality for the transfer function $H(z)$ is given as

$$\begin{bmatrix} A^T P A - P & A^T P B - C^T \\ B^T P A - C & B^T P B - 2I \end{bmatrix} < 0. \tag{5.11}$$

Next, observe the following matrix:

$$L_{\text{KYP}} = \begin{bmatrix} I & 0 \\ -C & I \end{bmatrix}. \tag{5.12}$$

This matrix is non-singular. Hence the pre-multiplication of (5.11) by L_{KYP}^T and post-multiplication by L_{KYP} does not affect the positive definiteness of inequality. But, this newly obtained inequality is

$$\begin{bmatrix} (A - BC)^T P (A - BC) - P & (A - BC)^T P B + C^T \\ B^T P (A - BC) + C & B^T P B - 2I \end{bmatrix} < 0, \tag{5.13}$$

which is exactly KYP lemma inequality for the transfer function $H^{-1}(z)$. $\qquad\square$

Lemma 5.2 *Matrix inequalities*

$$\begin{bmatrix} P - M^T P M & M^T P - M^T + T^T A_{cl}^T T^{-T} \\ P M - M + T^{-1} A_{cl} T & 2I - P \end{bmatrix} > 0 \tag{5.14}$$

and

$$\begin{bmatrix} P_T - A_{cl}^T P_T A_{cl} & A_{cl}^T P_T - A_{cl}^T X + M_T^T \\ P_T A_{cl} - X A_{cl} + M_T & 2X - P \end{bmatrix} > 0, \tag{5.15}$$

with

$$P_T = T^{-T} P T^{-1}, \; M_T = T^{-T} M T^{-1}, \; X = T^{-T} T^{-1},$$

are equivalent.

Proof. This lemma is a consequence of Lemma 5.1. Inequality (5.14) represents the KYP lemma inequality (with the reversed sign) for

$$H(z) = \left[\begin{array}{c|c} M & I \\ \hline M - T^{-1} A_{cl} T & I \end{array} \right] \tag{5.16}$$

Inequality (5.15) represents the KYP lemma inequality for

$$H^{-1}(z) = \left[\begin{array}{c|c} T^{-1} A_{cl} T & I \\ \hline T^{-1} A_{cl} T - M & I \end{array} \right] \tag{5.17}$$

which is pre- and post-multiplied by block-diagonal matrix blkdiag(T^{-T}, T^{-T}) and its transpose. $\qquad \square$

Alternatively, the equivalence of (5.14) and (5.15) can be proven using the matrix

$$L = \begin{bmatrix} T^{-1} & 0 \\ M T^{-1} - T^{-1} A_{cl} & T^{-1} \end{bmatrix}. \tag{5.18}$$

Namely, (5.15) is obtained as (5.14) pre- and post-multiplied by L^T and L. Since pre- and post-multiplication of matrix by the invertible matrix and its transpose do not change its positive definiteness, the matrix inequalities (5.14) and (5.15) are equivalent.

Remark 5.4 *It can be noticed that Schur stability of both matrices A and M is implied through the positive definiteness of the upper left blocks of given matrix inequalities.*

5.3.1 Fixed-structure LPV Controller Design Conditions

Using Lemma 5.2, a sufficient condition for the fixed-structure LPV controller synthesis is proposed.

Theorem 5.1 *Assume that are given a discrete-time LPV plant affine in scheduling parameter vector $\boldsymbol{\theta}$, bounds on the scheduling parameter vector and its variation as in Preliminaries. Furthermore, assume an LPV controller structure (5.4). Given matrices M and T, there exists*

an LPV controller stabilizing the given LPV plant for all admissible scheduling parameter trajectories if

$$\begin{bmatrix} P(\boldsymbol{\theta}) - M^T P(\boldsymbol{\theta}^+) M & (*) \\ P(\boldsymbol{\theta}^+) M - M + T^{-1} A_{cl}(\boldsymbol{\theta}) T & 2I - P(\boldsymbol{\theta}^+) \end{bmatrix} > 0, \tag{5.19}$$

$$P(\boldsymbol{\theta}) > 0 \quad , \quad \forall (\boldsymbol{\theta}, \boldsymbol{\theta}^+) \in \Omega_v,$$

with $(*)$ *representing the terms completing the symmetric matrix.*

Proof. First it can be observed that the left-hand side of (5.19) is affine in pair $(\boldsymbol{\theta}, \boldsymbol{\theta}^+)$. This means that its validity for $\forall (\boldsymbol{\theta}, \boldsymbol{\theta}^+) \in \Omega$ can be proven using an appropriate convex combination of vertex inequalities, as in Lemma 4.3.

Next, it has to be proven that validity of (5.19) implies stability condition for the closed-loop system for $\forall (\boldsymbol{\theta}, \boldsymbol{\theta}^+) \in \Omega$. Similarly to the alternative proof of Lemma 5.2, the following non-singular matrix can be considered:

$$L(\boldsymbol{\theta}) = \begin{bmatrix} T^{-1} & 0 \\ MT^{-1} - T^{-1} A_{cl}(\boldsymbol{\theta}) & T^{-1} \end{bmatrix}. \tag{5.20}$$

Pre- and post-multiplication of (5.19) by $L^T(\boldsymbol{\theta})$ and $L(\boldsymbol{\theta})$ imply

$$\begin{bmatrix} P_T(\boldsymbol{\theta}) - A_{cl}^T(\boldsymbol{\theta}) P_T(\boldsymbol{\theta}^+) A_{cl}(\boldsymbol{\theta}) & (*) \\ P_T(\boldsymbol{\theta}^+) A_{cl}(\boldsymbol{\theta}) - X A_{cl}(\boldsymbol{\theta}) + M_T & 2X - P_T(\boldsymbol{\theta}^+) \end{bmatrix} > 0 \tag{5.21}$$

for $\forall (\boldsymbol{\theta}, \boldsymbol{\theta}^+) \in \Omega$, with the same shorthands as in Lemma 5.2. The top left block of 5.21 represents the stability condition (5.9) for the closed-loop LPV system. Since its positivity for $\forall (\boldsymbol{\theta}, \boldsymbol{\theta}^+) \in \Omega$ is guaranteed by the Schur complement lemma, stability of the closed-loop system is guaranteed for all allowable scheduling parameter trajectories. $\qquad\square$

Remark 5.5 *The total number of constraints in the non-degenerate case corresponds to the cardinality of the set Ω_v, which equals 6^{n_θ}. Considering that in realistic applications there are rarely more than 3 scheduling parameters [59], this number of LMIs should be numerically tractable in acceptable execution time.*

5.3.2 Fixed-structure LPV Controller Synthesis Algorithm

All the algorithms developed for the continuous-time case presented in Chapter 4 can be applied here as well. Some of the LTI controller design methods for discrete-time systems, useful for the initialization of the algorithm, are `systune` of Matlab® and `FDRC` [101]. Since an LTI controller is needed just to initialize the algorithm, one of these or similar methods should suffice.

For the completeness, matrix inequalities that are discrete-time counterparts of those used in Algorithm 2 are given as

$$
\begin{bmatrix}
\sigma^2 P(\boldsymbol{\theta}) - M^T P(\boldsymbol{\theta}^+) M & (*) \\
P(\boldsymbol{\theta}^+) M - M + T^{-1} A_{cl}(\boldsymbol{\theta}) T & 2I - P(\boldsymbol{\theta}^+)
\end{bmatrix} > 0,
\tag{5.22}
$$

$$
\begin{bmatrix}
\sigma^2 P_T(\boldsymbol{\theta}) - A_{cl}^T(\boldsymbol{\theta}) P_T(\boldsymbol{\theta}^+) A_{cl}(\boldsymbol{\theta}) & (*) \\
P_T(\boldsymbol{\theta}^+) A_{cl}(\boldsymbol{\theta}) - X A_{cl}(\boldsymbol{\theta}) + M_T & 2X - P_T(\boldsymbol{\theta}^+)
\end{bmatrix} > 0.
\tag{5.23}
$$

Minimizing σ corresponds to the exponential decay rate minimization, and $\sigma \leq 1$ guarantees stability of the closed-loop system.

The final value of σ depends on the choice of initial controllers. In the case that the final value is not satisfactory, or that its value is above 1, another set of initial controllers should be used. Similar re-initialization is proposed in both `systune` or `HIFOO` tools for LTI controller design.

5.3.3 Treatment of Scheduling Parameter Uncertainty

In reality, the exact value of the scheduling parameter $\boldsymbol{\theta}$ is never available. Even if the scheduling parameter is measured directly (i.e. not estimated), what will be available in the real-time is the value affected by the measurement error of measurement device. Assume that the maximum absolute error of the measurement device for the ith component of the scheduling parameter vector is $\overline{\Delta}_{e_i} > 0$. If measured value of the scheduling parameter is denoted by $\hat{\boldsymbol{\theta}}$ and the exact value by $\boldsymbol{\theta}$, this means that $\hat{\theta}_i - \theta_i \in [-\overline{\Delta}_{e_i}, \overline{\Delta}_{e_i}]$, $i = 1, \ldots, n_\theta$.

Current values of the controller matrices are calculated online based on the available value of the scheduling parameter, so what will be used to control the given system is a controller $(A_c(\hat{\boldsymbol{\theta}}), B_c(\hat{\boldsymbol{\theta}}), C_c, D_c)$. This means that the closed-loop system matrices are affected by both $\boldsymbol{\theta}$ and $\hat{\boldsymbol{\theta}}$ in an affine fashion as following:

$$
\begin{aligned}
A_{cl}(\boldsymbol{\theta}, \hat{\boldsymbol{\theta}}) &= \begin{bmatrix}
A_g(\boldsymbol{\theta}) + B_u(\boldsymbol{\theta}) D_c C_y & B_u(\boldsymbol{\theta}) C_c \\
B_c(\hat{\boldsymbol{\theta}}) C_y & A_c(\hat{\boldsymbol{\theta}})
\end{bmatrix} \\
B_{cl}(\boldsymbol{\theta}, \hat{\boldsymbol{\theta}}) &= \begin{bmatrix}
B_w(\boldsymbol{\theta}) + B_u(\boldsymbol{\theta}) D_c D_{yw} \\
B_c(\hat{\boldsymbol{\theta}}) D_{yw}
\end{bmatrix} \\
C_{cl}(\boldsymbol{\theta}) &= \begin{bmatrix}
C_z(\boldsymbol{\theta}) + D_{zu}(\boldsymbol{\theta}) D_c C_y & D_{zu}(\boldsymbol{\theta}) C_c
\end{bmatrix} \\
D_{cl}(\boldsymbol{\theta}) &= \begin{bmatrix}
D_{zw}(\boldsymbol{\theta}) + D_{zu}(\boldsymbol{\theta}) D_c D_{yw}
\end{bmatrix}.
\end{aligned}
\tag{5.24}
$$

Assume again Lyapunov function quadratic in the state as $V(k) = \boldsymbol{x}(k)^T P(\boldsymbol{\theta}(k)) \boldsymbol{x}(k)$. Taking into account dynamics affected by the uncertainty as in (5.24), Lyapunov function difference

over one sampling period is

$$
\begin{aligned}
V(k+1) - V(k) &= \boldsymbol{x}^T(k+1)P(\boldsymbol{\theta}(k+1))\boldsymbol{x}(k+1) - \boldsymbol{x}^T(k)P(\boldsymbol{\theta}(k))\boldsymbol{x}(k) = \\
&= \boldsymbol{x}^T(k)A_{cl}^T(\boldsymbol{\theta}(k),\hat{\boldsymbol{\theta}}(k))P(\boldsymbol{\theta}(k+1))A_{cl}^T(\boldsymbol{\theta}(k),\hat{\boldsymbol{\theta}}(k))\boldsymbol{x}(k) - \boldsymbol{x}(k)^T P(\boldsymbol{\theta}(k))\boldsymbol{x}(k) = \\
&= \boldsymbol{x}^T(k)[A_{cl}^T(\boldsymbol{\theta}(k),\hat{\boldsymbol{\theta}}(k))P(\boldsymbol{\theta}(k+1))A_{cl}(\boldsymbol{\theta}(k),\hat{\boldsymbol{\theta}}(k)) - P(\boldsymbol{\theta}(k))]\boldsymbol{x}(k).
\end{aligned}
\tag{5.25}
$$

Consequently, the following condition has to be satisfied to guarantee the closed-loop stability:

$$
P(\boldsymbol{\theta}(k)) - A_{cl}^T(\boldsymbol{\theta}(k),\hat{\boldsymbol{\theta}}(k))P(\boldsymbol{\theta}(k+1))A_{cl}(\boldsymbol{\theta}(k),\hat{\boldsymbol{\theta}}(k)) > 0, \ \forall(\boldsymbol{\theta}(k),\hat{\boldsymbol{\theta}}(k),\boldsymbol{\theta}(k+1)). \tag{5.26}
$$

Assume that for each index i the vertex set of an allowable space of $(\theta_i, \theta_i^+, \hat{\theta}_i)$ is denoted by $\Omega_{v_i}^u$. In Fig. 5.2 overbounding set of the allowable $(\theta_i, \theta_i^+, \hat{\theta}_i - \theta_i)$ space is presented, as it allows $\hat{\theta}_i$ to reach values outside of $[-\overline{\theta_i}, \overline{\theta_i}]$. So, it is certain that the triplet $(\boldsymbol{\theta}, \boldsymbol{\theta}^+, \hat{\boldsymbol{\theta}})$ always belongs to the polytope Ω^u whose vertex set Ω_v^u is given by $\Omega_v^u = \Omega_{v_1}^u \times \Omega_{v_2}^u \times \cdots \times \Omega_{v_{n_\theta}}^u$. But, as $A_{cl}(\boldsymbol{\theta}(k),\hat{\boldsymbol{\theta}}(k))$ is affine in the couple $(\boldsymbol{\theta},\hat{\boldsymbol{\theta}})$, (5.22) and (5.23) can be replaced by

$$
\begin{bmatrix}
\sigma^2 P(\boldsymbol{\theta}) - M^T P(\boldsymbol{\theta}^+)M & (*) \\
P(\boldsymbol{\theta}^+)M - M + T^{-1}A_{cl}(\boldsymbol{\theta},\hat{\boldsymbol{\theta}}) & 2I - P(\boldsymbol{\theta}^+)
\end{bmatrix} > 0, \tag{5.27}
$$

$$
P(\boldsymbol{\theta}) > 0 \quad , \quad \forall(\boldsymbol{\theta},\boldsymbol{\theta}^+,\hat{\boldsymbol{\theta}}) \in \Omega_v^u,
$$

and

$$
\begin{bmatrix}
\sigma^2 P_T(\boldsymbol{\theta}) - A_{cl}^T(\boldsymbol{\theta},\hat{\boldsymbol{\theta}})P_T(\boldsymbol{\theta}^+)A_{cl}^T(\boldsymbol{\theta},\hat{\boldsymbol{\theta}}) & (*) \\
P_T(\boldsymbol{\theta}^+)A_{cl}(\boldsymbol{\theta},\hat{\boldsymbol{\theta}}) - XA_{cl}(\boldsymbol{\theta},\hat{\boldsymbol{\theta}}) + M_T & 2X - P_T(\boldsymbol{\theta}^+)
\end{bmatrix} > 0, \tag{5.28}
$$

$$
P(\boldsymbol{\theta}) > 0 \quad , \quad \forall(\boldsymbol{\theta},\boldsymbol{\theta}^+,\hat{\boldsymbol{\theta}}) \in \Omega_v^u.
$$

So, in the presence of non-negligible uncertainty in the scheduling parameter vector, stabilizing discrete-time LPV controller can be designed using similar algorithm as in Subsection 5.3.2, with Ω_v^u replacing Ω_v, $(\boldsymbol{\theta},\boldsymbol{\theta}^+,\hat{\boldsymbol{\theta}})$ replacing $(\boldsymbol{\theta},\boldsymbol{\theta}^+)$ and (5.27) and (5.28) replacing (5.22) and (5.23), respectively.

5.4 Induced l_2-Norm and $\mathcal{H}_2$ Performance Specifications

5.4.1 Induced l_2-Norm Performance Controller Design

Induced l_2-norm performance of an LTI system can be characterized through the well-known Bounded Real Lemma. Its extension to the LPV system case can be found in the literature (similar to e.g. [74]):
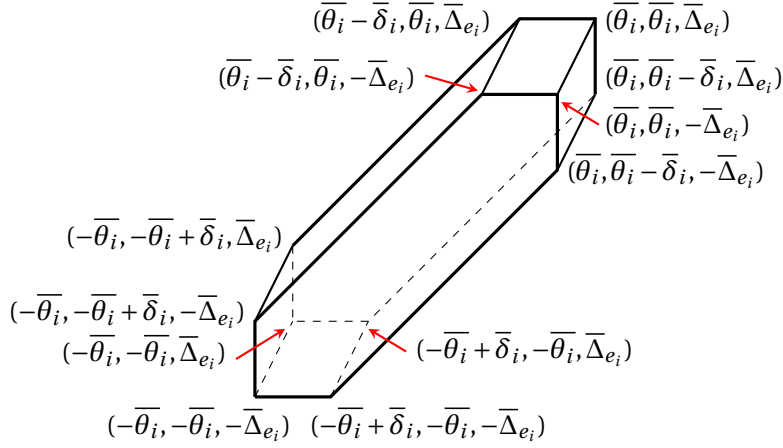
Figure 5.2 – Admissible $(\theta_i, \theta_i^+, \hat{\theta}_i - \theta_i)$ space is a polytope with 12 vertices.

Lemma 5.3 γ *is an upper bound on the induced* l_2*-norm of the LPV system (5.5) if*

$$P - A_{cl}^T P^+ A_{cl} - \gamma^{-1} C_{cl}^T C_{cl} \tag{5.29}$$
$$- (B_{cl}^T P^+ A_{cl} + \gamma^{-1} D_{cl}^T C_{cl})^T \left(I - \gamma^{-1} D_{cl}^T D_{cl} - B_{cl}^T P^+ B_{cl} \right)^{-1} (B_{cl}^T P^+ A_{cl} + \gamma^{-1} D_{cl}^T C_{cl}) > 0$$

is satisfied for $\forall (\boldsymbol{\theta}, \boldsymbol{\theta}^+) \in \Omega$*. The dependence of all matrices on* $\boldsymbol{\theta}$ *is omitted, and* $P^+ = P(\boldsymbol{\theta}^+)$*.*

The goal is to propose a method for fixed-structure discrete-time LPV controller design, guaranteeing good induced l_2-norm performance for a given LPV system. Similarly to the stabilizing LPV controller design problem, constraints (5.29) define a non-convex set in the space of design variables. The following theorem proposes an inner convex approximation of the non-convex solution set.

Theorem 5.2 *Assume that are given a discrete-time LPV plant affine in the scheduling parameter vector* $\boldsymbol{\theta}$ *, bounds on the scheduling parameter vector and its variation as in Preliminaries. Furthermore, suppose that the LPV controller structure is given by (5.4). Given decoupling matrix M and state transformation matrix T , there exists an LPV controller stabilizing the given LPV plant and ensuring the induced* l_2*-norm performance to be at most* γ *for all admissible scheduling parameter trajectories if*

$$\begin{bmatrix} P(\boldsymbol{\theta}) - M^T P(\boldsymbol{\theta}^+) M & (*) & (*) & (*) \\ P(\boldsymbol{\theta}^+) M - M + T^{-1} A_{cl}(\boldsymbol{\theta}) T & 2I - P(\boldsymbol{\theta}^+) & (*) & (*) \\ 0 & B_{cl}^T(\boldsymbol{\theta}) T^{-T} & I & (*) \\ C_{cl}(\boldsymbol{\theta}) T & 0 & D_{cl}(\boldsymbol{\theta}) & \gamma I \end{bmatrix} > 0, \tag{5.30}$$

$$P(\boldsymbol{\theta}) > 0 \quad , \quad \forall (\boldsymbol{\theta}, \boldsymbol{\theta}^+) \in \Omega_v.$$

Proof. As the expression (5.30) is affine in the pair $(\boldsymbol{\theta}, \boldsymbol{\theta}^+)$, it can be concluded that its validity for $\forall (\boldsymbol{\theta}, \boldsymbol{\theta}^+) \in \Omega_v$ ensures the validity for $\forall (\boldsymbol{\theta}, \boldsymbol{\theta}^+) \in \Omega$ as well. Next, it is proven that validity of (5.30) for $\forall (\boldsymbol{\theta}, \boldsymbol{\theta}^+) \in \Omega$ implies the satisfaction of (5.29). Consider the full-rank matrix

$$
L_{\infty_1}(\boldsymbol{\theta}) = \left[\begin{array}{cccc} T^{-T} & T^{-T} M^T - A_{cl}^T(\boldsymbol{\theta}) T^{-T} & 0 & -\gamma^{-1} C_{cl}^T(\boldsymbol{\theta}) \\ 0 & B_{cl}^T(\boldsymbol{\theta}) T^{-T} & -I & \gamma^{-1} D_{cl}^T(\boldsymbol{\theta}) \end{array} \right].
\tag{5.31}
$$

Pre- and post-multiplication of (5.30) by $L_{\infty_1}(\boldsymbol{\theta})$ and $L_{\infty_1}^T(\boldsymbol{\theta})$, and then immediate application of Schur complement lemma around the bottom-right block, produces exactly (5.29) with $P_T = T^{-T} P T^{-1}$ instead of P. This guarantees the upper bound γ on the induced l_2-norm performance for all possible scheduling parameter trajectories. $\qquad\square$

To be able to choose M and T, a matrix inequality equivalent to (5.30) in which matrices M, T and P are decoupled is proposed.

Lemma 5.4 *The matrix inequality*

$$
\left[\begin{array}{cccc} P_T(\boldsymbol{\theta}) - A_{cl}^T(\boldsymbol{\theta}) P_T(\boldsymbol{\theta}^+) A_{cl}(\boldsymbol{\theta}) & (*) & (*) & (*) \\ P_T(\boldsymbol{\theta}^+) A_{cl}(\boldsymbol{\theta}) - X A_{cl}(\boldsymbol{\theta}) + M_T & 2X - P_T(\boldsymbol{\theta}^+) & (*) & (*) \\ B_{cl}(\boldsymbol{\theta}) M_T - B_{cl}(\boldsymbol{\theta}) X A_{cl}(\boldsymbol{\theta}) & B_{cl}^T(\boldsymbol{\theta}) X & I & (*) \\ C_{cl}(\boldsymbol{\theta}) & 0 & D_{cl}(\boldsymbol{\theta}) & \gamma I \end{array} \right] > 0
\tag{5.32}
$$

is equivalent to (5.30) for $\forall (\boldsymbol{\theta}, \boldsymbol{\theta}^+) \in \Omega$.

Proof. Observe the matrix

$$
L_{\infty_2}(\boldsymbol{\theta}) = \left[\begin{array}{cccc} T^{-T} & T^{-T} M^T - A_{cl}^T(\boldsymbol{\theta}) T^{-T} & 0 & 0 \\ 0 & T^{-T} & 0 & 0 \\ 0 & 0 & I & 0 \\ 0 & 0 & 0 & I \end{array} \right].
\tag{5.33}
$$

Pre- and post-multiplication of (5.30) by $L_{\infty_2}(\boldsymbol{\theta})$ and $L_{\infty_2}^T(\boldsymbol{\theta})$ gives exactly (5.32). Since the matrix $L_{\infty_2}(\boldsymbol{\theta})$ is non-singular, these two matrix inequalities are equivalent by the same argument of Lemma 5.2. $\qquad\square$

Now similar algorithm to the one in Section 3 can be developed. Here the initialization can be performed directly using the previously designed stabilizing LPV controller. The optimal cost γ_i is monotonically non-increasing for the reason of equivalence of (5.32) and (5.30).

5.4.2 $\mathcal{H}_2$ **Performance Controller Design**

The following representation of the $\mathcal{H}_2$ performance guarantee condition can be found in the literature (similarly to e.g. [112]):

Lemma 5.5 η *is the upper bound on the $\mathcal{H}_2$ performance of the LPV system (5.5) if there exist $P(\boldsymbol{\theta})$ and $W(\boldsymbol{\theta})$ such that*

$$\begin{bmatrix} P(\boldsymbol{\theta}^+) - A_{cl}(\boldsymbol{\theta})P(\boldsymbol{\theta})A_{cl}^T(\boldsymbol{\theta}) & B_{cl}(\boldsymbol{\theta}) \\ B_{cl}^T(\boldsymbol{\theta}) & I \end{bmatrix} > 0,$$

$$\begin{bmatrix} W(\boldsymbol{\theta}) & C_{cl}(\boldsymbol{\theta})P(\boldsymbol{\theta}) & D_{cl}(\boldsymbol{\theta}) \\ P(\boldsymbol{\theta})C_{cl}^T(\boldsymbol{\theta}) & P(\boldsymbol{\theta}) & 0 \\ D_{cl}^T(\boldsymbol{\theta}) & 0 & I \end{bmatrix} > 0, \tag{5.34}$$

$$trace(W(\boldsymbol{\theta})) < \eta, \quad P(\boldsymbol{\theta}) > 0, \quad \forall(\boldsymbol{\theta}, \boldsymbol{\theta}^+) \in \Omega$$

is satisfied for $\forall(\boldsymbol{\theta}, \boldsymbol{\theta}^+) \in \Omega$.

Remark 5.6 *To avoid technical problems, it is assumed here that $C_z(\theta) = C_z$ and $D_{zu} = 0$. This leads to matrix C_{cl} not depending on $\boldsymbol{\theta}$ nor the optimization variables. If these assumptions are not met, but $B_w(\boldsymbol{\theta}) = B_w$ and $D_{yw} = 0$, the other form of (5.34) could be written in which instead of C_{cl} the matrix B_{cl} multiplies P.*

The following LPV controller design conditions based on (5.34) are proposed.

Theorem 5.3 *Suppose that the discrete-time LPV plant, which is affine in the scheduling parameter vector $\boldsymbol{\theta}$, has bounds on the scheduling parameter vector and its variation as defined in Preliminaries. Furthermore, suppose that the LPV controller structure is given by (5.4). Given decoupling matrix M and state transformation matrix T, there exists an LPV controller stabilizing given LPV plant and ensuring the $\mathcal{H}_2$-norm to be at most η for all admissible scheduling parameter trajectories if there exist such $P(\boldsymbol{\theta})$ and $W(\boldsymbol{\theta})$ that*

$$\begin{bmatrix} P(\boldsymbol{\theta}^+) - MP(\boldsymbol{\theta})M^T & (*) & (*) \\ P(\boldsymbol{\theta})M^T - M^T + T^T A_{cl}^T(\boldsymbol{\theta})T^{-T} & 2I - P(\boldsymbol{\theta}) & (*) \\ B_{cl}^T(\boldsymbol{\theta})T^{-T} & 0 & I \end{bmatrix} > 0,$$

$$\begin{bmatrix} W(\boldsymbol{\theta}) & C_{cl}TP(\boldsymbol{\theta}) & D_{cl}(\boldsymbol{\theta}) \\ P(\boldsymbol{\theta})T^T C_{cl}^T & P(\boldsymbol{\theta}) & 0 \\ D_{cl}^T(\boldsymbol{\theta}) & 0 & I \end{bmatrix} > 0, \tag{5.35}$$

$$trace(W(\boldsymbol{\theta})) < \eta, \quad P(\boldsymbol{\theta}) > 0, \quad \forall(\boldsymbol{\theta}, \boldsymbol{\theta}^+) \in \Omega_v.$$

Proof. From the affineity of (5.35) in the pair $(\boldsymbol{\theta},\boldsymbol{\theta}^+)$ and Lemma 4.3 it follows that (5.35) is valid for $\forall(\boldsymbol{\theta},\boldsymbol{\theta}^+) \in \Omega$. Next, observe the matrix

$$L_{2_1}(\boldsymbol{\theta}) = \begin{bmatrix} T & TM - A_{cl}(\boldsymbol{\theta})T & 0 \\ 0 & 0 & I \end{bmatrix}. \tag{5.36}$$

It is a full-rank matrix. From the pre- and post-multiplication of the first inequality in (5.35) by $L_{2_1}(\boldsymbol{\theta})$ and $L_{2_1}^T(\boldsymbol{\theta})$ it follows that

$$\begin{bmatrix} P_T(\boldsymbol{\theta}^+) - A_{cl}(\boldsymbol{\theta})P_T(\boldsymbol{\theta})A_{cl}^T(\boldsymbol{\theta}) & B_{cl}(\boldsymbol{\theta}) \\ B_{cl}^T(\boldsymbol{\theta}) & I \end{bmatrix} > 0, \tag{5.37}$$

with $P_T = TPT^T$, is satisfied for $\forall(\boldsymbol{\theta},\boldsymbol{\theta}^+) \in \Omega$. Similarly the matrix $L_{2_2}(\boldsymbol{\theta}) = \text{diag}(I, T, I)$ can be defined. Pre- and post-multiplication of the second inequality in (5.35) by $L_{2_2}(\boldsymbol{\theta})$ and $L_{2_2}^T(\boldsymbol{\theta})$ leads to

$$\begin{bmatrix} W(\boldsymbol{\theta}) & C_{cl}P_T(\boldsymbol{\theta}) & D_{cl}(\boldsymbol{\theta}) \\ P_T(\boldsymbol{\theta})C_{cl}^T & P_T(\boldsymbol{\theta}) & 0 \\ D_{cl}^T(\boldsymbol{\theta}) & 0 & I \end{bmatrix} > 0. \tag{5.38}$$

Finally, the third inequality of (5.35) with (5.37) and (5.38) ensures that (5.34) is satisfied $\forall(\boldsymbol{\theta},\boldsymbol{\theta}^+) \in \Omega$. $\qquad\square$

The following lemma can be used for the initial choice of M and T.

Lemma 5.6 *The system of matrix inequalities*

$$\begin{bmatrix} P_T(\boldsymbol{\theta}^+) - A_{cl}(\boldsymbol{\theta})P_T(\boldsymbol{\theta})A_{cl}^T(\boldsymbol{\theta}) & (*) & (*) \\ P_T(\boldsymbol{\theta})A_{cl}^T(\boldsymbol{\theta}) - XA_{cl}^T(\boldsymbol{\theta}) + M_T^T & 2X - P_T(\boldsymbol{\theta}) & (*) \\ B_{cl}^T(\boldsymbol{\theta}) & 0 & I \end{bmatrix} > 0,$$

$$\begin{bmatrix} W(\boldsymbol{\theta}) & C_{cl}P_T(\boldsymbol{\theta}) & D_{cl}(\boldsymbol{\theta}) \\ P_T(\boldsymbol{\theta})C_{cl}^T & P_T(\boldsymbol{\theta}) & 0 \\ D_{cl}^T(\boldsymbol{\theta}) & 0 & I \end{bmatrix} > 0, \tag{5.39}$$

trace$(W(\boldsymbol{\theta})) < \eta$,

$$P(\boldsymbol{\theta}) > 0 \quad , \quad \forall(\boldsymbol{\theta},\boldsymbol{\theta}^+) \in \Omega_v,$$

with $P_T = TPT^T$, $M_T = TMT^T$ and $X = TT^T$, is equivalent to (5.35).

Proof. By the pre-multiplication of the first inequality in (5.35) by the non-singular

$$
L_{2_3}(\boldsymbol{\theta}) = \begin{bmatrix} T & TM - A_{cl}(\boldsymbol{\theta})T & 0 \\ 0 & T & 0 \\ 0 & 0 & I \end{bmatrix} \tag{5.40}
$$

and post-multiplication by $L_{2_3}^T(\boldsymbol{\theta})$ exactly the first inequality in (5.39) is obtained. As already mentioned, the second inequality of (5.39) can be obtained from the second inequality of (5.35) using $L_{2_2}(\boldsymbol{\theta})$. Now, as both $L_{2_2}(\boldsymbol{\theta})$ and $L_{2_3}(\boldsymbol{\theta})$ are square and invertible, equivalence of (5.39) and (5.35) is ensured. $\qquad\square$

An algorithm similar to the one in Section 5.3 can be used for the iterative controller improvement. It will ensure the monotonically non-increasing behavior of η.

5.5   Simulation results

5.5.1   Randomly generated discrete-time LPV plant

To illustrate the potential of the proposed method, an LPV controller is designed for a random 4th order discrete-time LPV system. Generated plant matrices are :

$$
A(\theta) = \begin{bmatrix} 0.5216 & -0.1788 & 0.6895 & -0.4840 \\ 0.4259 + 0.5412\theta & 0.4998 & -0.8022 & 0.1666 \\ -0.6085 & 0.8867 & 0.4388 & -0.0190 \\ 0.4358 & -0.1857 & 0.1947 + 0.1725\theta & 0.6140 \end{bmatrix},
$$

$$
B_u^T = \begin{bmatrix} -2.0259 & -4.5084 & 1.9318 & 1.5011 \end{bmatrix},
$$

$$
B_w^T = \begin{bmatrix} 0.1629 & 0.1812 & 0.0254 & 0.1827 \end{bmatrix},
$$

$$
C_y = C_z = \begin{bmatrix} 4.8299 & 0.5267 & -0.9993 & -3.0121 \end{bmatrix},
$$

$$
D_{yw} = D_{zw} = 0.1897, \quad D_{yu} = D_{zu} = 0.
$$

Bounds on the scheduling parameter and its variation are assumed as $\theta \in [-1, 1]$ and $\delta \in [-1/3, 1/3]$. It is important to notice that the given system is unstable even for frozen values of θ. The LPV controller order is chosen equal to 2, and all controller matrices are assumed to be θ-dependent (this causes no problem as only A_g depends on θ).

First, random initial controllers of order 2 are designed for two vertices of the scheduling parameter interval. Motivation for this comes from the initialization procedure in the HIFOO toolbox [100]. For this purpose the function *fminunc* from the Matlab® Optimization Toolbox is used. The cost function is chosen as the spectral radius of the closed-loop state matrix. For each of 2 vertices, 50 runs of *fminunc* with different randomly chosen initial points are performed. As a result, 4 stabilizing LTI controllers are found for the first vertex, and 11 stabilizing LTI controllers for the second one. Obtained closed-loop spectral radii all belong to

the interval $[0.9, 1]$.

Next, a search for the stabilizing LPV controller of order 2 can be performed using the Algorithm 2 for the discrete-time LPV controller design. In total, 44 experiments are performed for each possible combination of 4 initial controllers for the first vertex and 11 for the second one. As a convex optimization solver, SDPT3 [94] is used. For any initial controller combination, algorithm stalls after 15 to 25 iterations. In only one out of 44 cases the final controller is not stabilizing (spectral radius of 1.0478). In 35 out of 44 cases the final spectral radius is in $[0.74, 0.75]$, a great improvement from initial radius valid just for vertices. It is interesting to notice that in the first few iterations of the algorithm, obtained LPV controllers do not stabilize the system, spectral radius begin larger than 1. The execution time depends on the initial controller and is in the interval $[150, 250]$s, but there may be a way to reduce this for one order of magnitude by avoiding bisection over σ.

Finally, obtained stabilizing LPV controllers can be used as starting points for the induced l_2-norm performance controller design. The execution time here is much smaller (around 20 seconds) since no bisection algorithm is involved. For more than half of the controllers, the final γ is between 63 and 64. The optimal γ is 63.7044, and the optimal controller:

$$
\begin{aligned}
A_k(\theta) &= \begin{bmatrix} -1.8304 & -1.2880 \\ -3.1562 & -0.9414 \end{bmatrix} + \theta \begin{bmatrix} 0.2477 & 0.2138 \\ 0.3821 & -0.0529 \end{bmatrix} \\
B_k(\theta) &= \begin{bmatrix} 0.4548 \\ 0.6232 \end{bmatrix} + \theta \begin{bmatrix} -0.1210 \\ -0.1126 \end{bmatrix} \\
C_k^T(\theta) &= \begin{bmatrix} -0.3958 \\ -0.2988 \end{bmatrix} + \theta \begin{bmatrix} 0.1101 \\ 0.0003 \end{bmatrix} \\
D_k(\theta) &= 0.0762 - 0.0380\theta.
\end{aligned}
$$

Finally, starting from the same stabilizing LPV controllers $\mathcal{H}_2$ performance of the system can be optimized. Here the total number of optimization iterations varies with change of initial stabilizing controller, and so does the calculation time. The obtained performance level depends as well on the initial controller, with much larger variance than in the case of induced l_2-norm performance. Optimal value of η is 26.2512, obtained for the following controller:

$$
\begin{aligned}
A_k(\theta) &= \begin{bmatrix} 1.2773 & -0.1865 \\ 3.8910 & -1.9121 \end{bmatrix} + \theta \begin{bmatrix} -0.4542 & 0.2430 \\ -0.6284 & 0.3571 \end{bmatrix} \\
B_k(\theta) &= \begin{bmatrix} 0.1760 \\ 0.0887 \end{bmatrix} + \theta \begin{bmatrix} 0.0241 \\ 0.0742 \end{bmatrix} \\
C_k(\theta) &= \begin{bmatrix} -0.7786 & 0.5359 \end{bmatrix} + \theta \begin{bmatrix} 0.0094 & -0.0188 \end{bmatrix} \\
D_k(\theta) &= 0.0106 - 0.0246\theta.
\end{aligned}
$$

5.5.2 Numerical comparison

To illustrate the potential of the proposed method and compare it with the method developed in [73], simulation example from [73] is used. Plant matrices are given as following:

$$A(\theta) = \begin{bmatrix} 0.7370 & 0.0777 & 0.0810 & 0.0732 \\ 0.2272 & 0.9030 & 0.0282 & 0.1804 \\ -0.0490 & 0.0092 & 0.7111 & -0.2322 \\ -0.1726 & -0.0931 & 0.1442 & 0.7744 \end{bmatrix} + \theta \begin{bmatrix} 0.0819 & 0.0086 & 0.0090 & 0.0081 \\ 0.0252 & 0.1003 & 0.0031 & 0.0200 \\ -0.0055 & 0.0010 & 0.0790 & -0.0258 \\ -0.0192 & -0.0103 & 0.0160 & 0.0860 \end{bmatrix},$$

$$B_w = \begin{bmatrix} 0.0953 & 0 & 0 \\ 0.0145 & 0 & 0 \\ 0.0862 & 0 & 0 \\ -0.0011 & 0 & 0 \end{bmatrix}, \ B_u = \begin{bmatrix} 0.0045 & 0.0044 \\ 0.1001 & 0.0100 \\ 0.0003 & -0.0136 \\ -0.0051 & 0.0936 \end{bmatrix},$$

$$C_z = \begin{bmatrix} 1 & 0 & -1 & 0 \\ 0 & 0 & 0 & 0 \\ 0 & 0 & 0 & 0 \end{bmatrix}, \ C_y = \begin{bmatrix} 1 & 0 & 0 & 0 \\ 0 & 0 & 1 & 0 \end{bmatrix},$$

$$D_{zu} = \begin{bmatrix} 0 & 0 \\ 1 & 0 \\ 0 & 1 \end{bmatrix}, \ D_{yw} = \begin{bmatrix} 0 & 1 & 0 \\ 0 & 0 & 1 \end{bmatrix}, \ D_{zw} = \begin{bmatrix} 0 & 0 & 0 \\ 0 & 0 & 0 \\ 0 & 0 & 0 \end{bmatrix}.$$

Bounds on the scheduling parameter are given as $\theta \in [-1, 1]$. Analysis of the system for fixed values of the scheduling parameter shows that the number of unstable poles changes over the interval, as all the poles lie inside the unit circle for $\theta = -1$, but one pole is outside of it for $\theta = 1$.

In [73], variation of the scheduling parameter is assumed to belong to the interval $[-0.01, 0.01]$. Here, larger bounds $\delta \in [-1, 1]$ are assumed, which means that the scheduling parameter can move over the half of its bounding interval over one sampling period. Control goal defined in [73] is to design a fourth order decentralized controller. It is shown that the goal can be achieved after 46 iterations and that the final 4th order decentralized controller is obtained with optimal γ equal to 4.78.

In this chapter, much simpler decentralized static output-feedback controller is designed instead of the 4th order decentralized controller. Initial decentralized static output-feedback controllers K_1^0 and K_2^0 for $\theta = -1$ and $\theta = 1$ are designed using `hinfstruct`. Obtained controllers are

$$K_1^0 = \begin{bmatrix} 0.0101 & 0 \\ 0 & 0.03838 \end{bmatrix}, \ K_2^0 = \begin{bmatrix} 1.26 & 0 \\ 0 & 0.4108 \end{bmatrix},$$

with corresponding $\mathscr{H}_\infty$ performances of 0.0977 and 1.8392. Note that these values correspond to the square root of the induced-l_2 norm performance indicator γ used in [73] and here, so the

comparable value from [73] is $\sqrt{4.78} = 2.1863$. Starting from the presented initial controllers, in only two iterations presented algorithm converges to a decentralized static output-feedback LPV controller

$$K(\theta) = \begin{bmatrix} 0.7056 & 0 \\ 0 & 0.3549 \end{bmatrix} + \theta \begin{bmatrix} 0.5549 & 0 \\ 0 & 0.0559 \end{bmatrix}.$$

The controller is designed using SDPT3 ([94]) as a convex optimization solver, and obtained performance indicator is $\sqrt{\gamma} = 1.8449$.

This means that a better level of performance is reached with simpler controller than the one obtained in [73], as well for larger possible variations of the scheduling parameter. Also, obtained level of performance is just marginally worse than the one obtained with the LTI decentralized static output-feedback for the second vertex (1.8392). To further illustrate obtained level of performance and usefulness of fixed-structure controller design, for 51 values of θ from $[-1, 1]$ optimal full-order output-feedback LTI controllers are designed using `hinfsyn` of Matlab®. The worst-case $\mathscr{H}_\infty$ norm obtained for these controllers is 1.6214. Given relatively low loss of performance for the gain of much simpler controller structure (full-order output-feedback vs. decentralized static output-feedback), it may be concluded that given method provides a good alternative control solution.

5.6   Conclusion

In this chapter a method for designing fixed-structure dynamic output-feedback LPV controllers for discrete-time LPV systems with bounded scheduling parameter variations is presented. Proposed controller design scheme can iteratively improve induced l_2-norm and $\mathscr{H}_2$ performance of the controlled system. Provided simulation result illustrate that good performance can be achieved in a relatively low number of iterations, even for an LPV controller with very limited order and structure.

6 Conclusions

6.1 Summary

In this thesis, some methods for fixed-order gain-scheduled and LPV controller design are proposed. Methods are developed for different classes of models available in practice, ranging from the frequency-domain models dependent on the scheduling parameter, to state-space continuous- and discrete-time LPV models with affine dependence on the scheduling parameter. Different performance measures, such as $\mathscr{H}_\infty$, $\mathscr{H}_2$ and exponential decay rate, are optimized with the different methods. LPV methods using the state-space models take into account the realistic assumption on bounded scheduling parameter variations, as this can be beneficial for obtaining good performance.

Chapter 2 presents a method for the fixed-order gain-scheduled controller design using frequency-domain models dependent on the scheduling parameter vector. Using a linearly parameterized gain-scheduled controller structure and a desired open-loop transfer function, the $\mathscr{H}_\infty$ performance of the weighted closed-loop transfer functions is presented in the Nyquist diagram as a set of convex constraints. Hence, use of convex optimization tools directly leads to the gain-scheduled controller guaranteeing stability and performance for all values of the scheduling parameters considered in the design. Controllers designed using this method are successfully applied to the benchmark in adaptive regulation for the active suspension testbed.

Chapter 3 describes a method for the design of fixed-order LPV controllers for LTI plants with guaranteed level of $\mathscr{H}_\infty$ performance and stability for all values of the scheduling parameters belonging to a polytopic set. The LPV controller parameterization considered in this approach leads to design variables in both the numerator and denominator of the controller. Robust stability conditions for all fixed values of the scheduling parameter vector are derived as a set of LMIs. Additionally, the $\mathscr{H}_\infty$ performance conditions for all fixed values of the scheduling parameter vector are given in terms of LMIs. Special attention is given to the problem of the rejection of a sinusoidal disturbance with a time-varying frequency, which is used as a motivating application.

A new fixed-order output-feedback LPV controller design method for continuous-time state-space LPV plant models with affine dependence on the scheduling parameter vector is presented in Chapter 4. Bounds on the scheduling parameters and their variation rates are exploited through the use of affine PDLFs. The decay rate related to the exponential stability of the closed-loop system is considered as a performance measure. Next, LMI constraints guaranteeing $\mathscr{H}_\infty$ and $\mathscr{H}_2$ performance for the closed-loop control system are derived. A controller design algorithm based on these constraints is discussed. Application of the proposed method to the 2DOF gyroscope experimental setup is described in detail.

In Chapter 5 a class of discrete-time LPV state-space plants, affine in the scheduling parameter vector, is considered. The user imposed controller structure is preserved since controller parameters appear directly as decision variables in the convex optimization program. The realistic case of limited scheduling parameter variations is treated through the use of PDLF affine in the scheduling parameter vector. Uncertainty in the scheduling parameter vector due to sensor measurement error can be considered in the design. The upper bound on the $\mathscr{H}_2$ and induced l_2-norm performance of a control system is enhanced through the use of an iterative convex optimization procedure. An illustrative simulation example and a comparison to a similar method are given.

These methods are tested on different simulation and experimental examples. One of the applications in focus is multi-sinusoidal disturbance rejection. Gain-scheduled controllers are designed for the international benchmark on adaptive regulation. The obtained controllers are successfully applied to the real testbed, and are so far the only fixed-order control strategy that has been applied to the benchmark problem. A continuous-time LPV controller is designed for the MIMO position control of the 2DOF gyroscope experimental setup with time-varying speed of the rotor disk. Good tracking of the step reference is obtained in the real-time experiment using this controller.

6.2   Conclusions and Perspectives

Similar to most of the design methods in control, all LPV controller design methods presented here have some advantages and disadvantages. The following few paragraphs give some conclusions with regard to the proposed methods together with propositions for possible improvements and extensions:

- The frequency-domain gain-scheduled controller design method can be quite useful in practice, as can be seen from the benchmark application. One of its main advantages, apart from the fact that no parametric model is needed, is the use of linear programming as an underlying optimization tool. Linear programming as a numerical procedure is relatively reliable, allowing for a large number of constraints to be considered without introducing numerical issues. However, linear constraints also represent the weak point of the gain-scheduled approach. As the sampling of constraints is performed in both

the frequency domain and the scheduling parameter space, the number of constraints grows polynomially with the number of scheduling parameters, even if usually the number of scheduling parameters is not higher than 3 in practice [59].

Sampling the constraints using the scenario approach is proposed in Chapter 2. A large number of constraints has to be considered to achieve a very low probability of design failure and a low probability of constraint violation. However, the scenario approach does not at all take into account the manner in which constraints depend on the frequency and scheduling parameters. This information could potentially be used to ensure finer sampling of the more important constraints, hence reducing the calculation complexity. The other interesting issue is the choice of the desired open-loop transfer function L_d. Simple choices work well in the case of LTI controller design [113]. However, for the case of gain-scheduled controllers this choice may have a significantly greater influence on the final outcome of the design, as can be seen in the application of the method to the benchmark problem.

- Tuning of the proposed LPV controller design method is relatively simple in the transfer function setting, as only the poles of the plant and controller transfer functions have to be chosen. While this task is not trivial in the general case, for a system of a reasonable size a few trials usually lead to a good result. For a system of larger complexity this issue may be more limiting, as the execution time would grow for each trial and the number of trials may grow as well. Finally, the fact that the method in its current state treats only LTI plant with LPV controllers limits the scope of its applicability.

  An extension of this method to the class of LPV systems with polynomial dependence on the scheduling parameter vector should be considered. This would also enable the use of LPV controllers with the same type of dependence, and possibly the use of polynomial parameter dependent Lyapunov functions. Another important issue is the internal stability of a closed-loop system comprised of an LPV plant and a controller given in transfer function form. This is not a trivial issue, and is often ignored in the literature. Some results are available for observer-based controllers based on the Youla-Kučera parameterization [114]. Extension of these results to the to the design of fixed-order LPV controllers with a transfer-function representation could potentially enable the inclusion of the scheduling parameter variation rate bounds in the design as well.

- The methods described in Chapters 4 and 5 use PDLF affine in scheduling parameters for determining stability and performance. The use of affine PDLF is sufficient for many LPV systems affine in scheduling parameters. However, in [115] it is shown that this is not always the case with regard to stability analysis. The results obtained from some simulation examples suggests that this problem can only worsen when performance is examined.

  Lyapunov functions and LPV plants and controllers that are polynomially dependent on scheduling parameters could be considered in order to enlarge the applicability of the methods presented in Chapters 4 and 5. To handle matrix inequalities polynomially

dependent on scheduling parameters, different relaxation techniques (such as sum-of-squares based relaxations [110]) can be applied. These techniques inevitably lead to computationally demanding optimization problems, as there are no sharp bounds on the complexity of the relaxation needed for a given problem. There is an inherent tradeoff between the computation time and the quality of the obtained solution. It should also be kept in mind that the exact performance improvement coming from the increased computational complexity in the case of controller synthesis may be very plant dependent.

- Some numerical issues are observed when the iterative convex optimization is performed for the methods in Chapters 4 and 5. One issue arises when enforcing the strict positive definiteness when the alternation is performed between two sets of LMIs, as e.g. in Algorithm 2. These two sets of LMIs can have eigenvalues of different orders of magnitude. However, as these orders of magnitude are not known in advance, the strict feasibility of both LMI sets is enforced by making them "more negative definite" than some $-\epsilon I$, where ϵ is small positive constant close to zero. This can lead to losing feasibility between two steps of the same iteration of the algorithm, because the eigenvalues of one set of constraints may be smaller than $-\epsilon$, while the eigenvalues of the other set may be larger. One way to avoid this is to use the same set of LMIs for both steps as proposed for the induced $\mathscr{L}_2$-norm performance, only fixing the values of the different variable subsets in two phases. Another intriguing issue is related to finding an appropriate value of γ for the induced $\mathscr{L}_2$-norm performance. For some plants and controllers standard convex optimization solvers run into numerical problems when the value of γ is minimized. However, if bisection over γ is performed instead, i.e., if a feasibility problem is solved for some fixed values of γ, then this kind of problem does not appear. This modification is usually undesirable, as the constraints are already convex in γ and bisection increases the execution time by an order of the magnitude.

  Numerical issues only get worse for large-scale problems, when the order of the system and/or number of scheduling parameters grow significantly. Current state-of-the-art solvers may easily fail to provide any solution to the underlying problem. There are some signs that things may be changing, as there is a growing community working on new algorithms for solving large scale convex optimization problems ([116] and papers that extend this work).

- Another important issue is which class of optimization tools may lead to better fixed-structure LPV controller design methods. For LTI systems a state-of-the-art $\mathscr{H}_\infty$ fixed-order LTI controller design tool is `hinfstruct`. It is based on the use of non-smooth non-convex optimization theory. Based on the author's experience, it is very fast and numerically reliable. An important feature of `hinfstruct` is that it allows for direct optimization over the controller parameters as optimization variables, hence giving the user full control of the order and the structure of the controller. Allowing the algorithm to start optimization from a few different initial points seems to lead to performance values very close to the globally optimal one, even though there is no guarantee for this. These

issues worsen with increased plant order. Still, for the magnitude of orders for which the LMI based controller design tools can perform well, `hinfstruct` is a competitive tool. However, the majority of the computational savings of `hinfstruct` come from the choice of constraints and the absence of auxiliary variables. This is important as introducing the Lyapunov matrix heavily increases the number of optimization variables. If it would be possible to characterize the existence of the Lyapunov function in the frequency domain, it would allow for the application of non-smooth non-convex optimization to fixed-order LPV controller design. Even though this is certainly not a simple problem, some preliminary work on the topic can be found in the literature [117].

The other option is to continue using the Lyapunov function directly, as it enables the extension of the stability or performance guarantees to the whole set of systems in the case of robust or LPV controller design. One possible path to continue using these is a development of more numerically stable convex optimization routines. This would as well demand a further study of the convergence of the iterative convex optimization schemes. For example, for the optimization scheme applied in Chapters 4 and 5 the only thing that can be guaranteed is that the cost is monotonically non-increasing. However, there is no guarantee that the point to which the scheme converges represents the local minimum [118]. In the case that this guarantee cannot be obtained, it would at least be useful to develop optimization algorithms capable of reaching the local minimum starting from the feasible point (e.g. [119]).

A very different path for obtaining new fixed-structure controller design tools is the development of custom BMI solvers for these kinds of problems. Namely, the current state-of-the-art general-purpose BMI solvers [120] often fail to provide a reasonable solution for the class of problems of interest. It is certainly very tempting to try to develop another general purpose BMI solver as many different problems in control (and not just in control) can be stated in terms of BMIs. However, a lot of research on it has already been performed and it is hard to predict if some reasonable solution will emerge any time soon. As such, it may be more reasonable to expect that some tool exploiting the structural properties of a class of BMI problems will emerge. In order for this to happen, a deeper understanding of some of the properties of the underlying problems could help. One such property that is often observed, but not well studied in the literature, is existence of many local sub-optimums for the $\mathscr{H}_\infty$ (or induced $\mathscr{L}_2$-norm) performance that have a performance close to the global optimum. This can be observed in the first example of Chapter 5. This may be one of the implicit properties that makes `hinfstruct` fast. Evidently, if these kinds of properties could be better understood, it would aid in the initialization of the optimization problem and possibly lead to convergence guarantees for the optimization scheme.

A Appendix: Short Description of 2DOF Gyroscope Virtual Instrument

A.1 2DOF Gyroscope Experimental Setup Description

The gyroscope setup used for performing control experiments described in Chapter 4 is presented in Figure A.1. A custom LabView virtual instrument is made to perform communication with sensors and actuators, to calculate the control action, to enable the user to define the experimental conditions and to store and visualize the data. All of these tasks should be done in real-time at sufficiently high sampling rates.

In the experiment described in Chapter 4 the grey frame is fixed, so the appropriate sensor and actuator are not treated in the virtual instrument. The angular positions of the disk, the blue and the red frame are measured using quadrature encoders. Three DC motors are used to actuate the disk, the blue and the red frame about their axis of rotation. Data acquisition is performed using the National Instruments DAQ card and a Mac Pro computer. A power amplifier converts the voltage outputs of the DAQ card to current signals applied to the DC motors. In the following sections the functioning of the virtual instrument and elements of its interface are described in detail.

A.2 Functioning of the Virtual Instrument

As previously explained, the role of the described virtual instrument is to perform the bidirectional communication with the hardware and user, to perform the control-related calculations and to store the important data to a hard drive. Some details of the the functionality implementation are given as follows:

- Initialization of all Input/Output (I/O) tasks, Graphical User Interface (GUI) controls and indicators, internal variables and buffers is performed so that the smooth start of the experimental system and virtual instrument is ensured. The LPV controller is loaded from the text file in the initialization phase. The first line of the file should carry the information on the controller order, number of plant outputs, number of plant inputs

Figure A.1 – Quanser gyroscope experimental platform [107].

and number of scheduling parameters. Hence an LTI controller may be applied as well, and the same module for controller loading may be reused on another setup.

- Communication with sensors and actuators is done at a different sampling rate than the communication with the user through GUI. This is performed through the use of two loops. The faster one, used for the communication with the hardware, runs at a sampling frequency of 1kHz. High sampling frequency is used to ensure that the simple discretization of the designed continuous-time LPV controller preserves the good performance obtained in the simulation. The reliable operation of the fast loop has to be ensured in order to have equidistant sampling and control signal calculation.

  The other task performed in the fast loop is the control input calculation. The necessary data are LPV controller matrices, loaded in the initialization phase, new values of reference and output signals, and the controller state buffer. It is a fast operation as only several matrix multiplications and additions are performed.

- Communication with a user is not so time-critical, so a sampling frequency of 10Hz is used. Another reason for much lower sampling frequency is the time necessary to update the state of the GUI. This is very time-consuming operation, comprising of checking the states of user controls, refreshing the values of indicators and refreshing the graphs. The update of graphs is the most time-consuming operation, but according

to the system dynamics 10Hz should be sufficient. More importantly, this is a speed at which the slower loop does not jeopardize the functioning of the fast loop.

Another time-consuming task performed in the slow loop is writing the data into the file on the hard drive. This is a very sensitive operation. In the first version of the virtual instrument all the measurement and actuator signals were buffered into an array whose size was increasing at each iteration of the slow loop. Writing into the file was performed only at the very end of virtual instrument operation. The problem with this approach is that LabView occasionally allocates a bigger chunk of the memory to be able to accept the buffer of the increased size. But this operation has a higher priority than the fast loop. Hence, at these moments the fast loop operation was interrupted, so some data was lost and actuators were not properly controlled. All of this resulted in an unexpected behavior of the control system.

In the described version of the virtual instrument saving the data is performed in a different manner. On every run of the fast loop the new data is added to the queue, while in every slow loop run the content of the queue is written into the file on hard drive. As this transfer is done asynchronously and in a time well bellow the sampling time of the slow loop, the operation of the fast loop is never jeopardized and data is properly saved.

A.3 Virtual Instrument Interface Description

The elements of the GUI of the designed virtual instrument can be classified in 6 different groups:

1. General command and indicator group

2. Graph group

3. Disk actuator group

4. Blue and red frame actuator group

5. "Synchronize references" button

6. Grey frame group

As the grey frame of the gyroscope is fixed in the proposed experiment, appropriate functionalities for the grey frame are not implemented. The graph group contains 6 different graphs displaying disk position, disk speed, blue, red and grey frame positions, and all 4 control inputs on the last graph. The role of the "synchronize references" button is explained together with blue and red frame actuator group, as it is naturally linked to them.
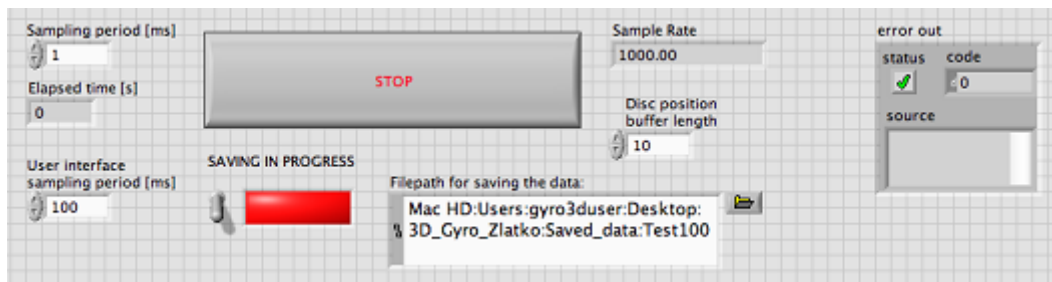
Figure A.2 – General command and indicator group

A.3.1   General command and indicator group

The following elements of the interface belong to this group (see Fig. A.2):

- "Sampling period [ms]" control - defines the sampling period (in milliseconds) of the fast loop

- "Elapsed time [s]" indicator - displays the time elapsed since the start of the operation (in seconds)

- "User interface sampling period" control - defines the sampling period (in milliseconds) of the slow loop

- "Stop" button - shuts down the operation of the virtual instrument

- "Saving in progress" switch - if the switch is on (and indicator field is green) I/O data is saved to the file indicated in the field "Filepath for saving the data"

- "Sample Rate" indicator - displays the sample rate of the fast loop

- "Disc position buffer length" control - the length of the buffer used for filtering the disk encoder measurements in order to estimate more precisely the rotational speed of the disk

- "error out" indicator - used to signalize if there is some error in the functioning of the virtual instrument related to the proper communication with the hardware

A.3.2   Disk actuator group

The following elements of the interface are related to disk (see group denoted by 1 in Fig. A.3):

- "Disc motor enable" control - used to enable the disk actuator operation

- "Closed loop disc" control - used to enable operation of the disk in closed loop and to define if the signal defined below is used as an excitation (in the open-loop operation) or as a reference (in the closed-loop)

Figure A.3 – Several interface groups: 1) disk actuator group, 2) blue and red frame actuator group, 3) "synchronize references"

- "Reference type" list box - choice of reference type for the disk speed (manual value/sinusoidal/squares/step/PRBS)

- "Controller type" list box - proportional controller is the only choice at the moment

- "Kp disc" control - the value of the proportional gain

- "Manual reference" slider - used to define value of the manual reference for the disk speed

- "Offset" control - used to set the offset value of the reference signal

- "Amplitude" control - used to set the amplitude of the reference signal

- "Frequency" control - used to set the frequency of the reference signal (for sinusoidal and squares reference types)

- "Shift register length" control - the length of shift register for generating the PRBS signal

- "Reference factor" - used to multiply the value of the manual reference (as slider provides values only between -10 and 10)

A.3.3   Blue and red frame actuators group

Most elements of the blue and red frame actuators group (group 2 in Figure A.3) behave analogous to those described in the disk actuator group. One additional control is "Phase shift [s]" that is used for setting the value of the phase shift of the reference signal. The "MIMO controller parameters" dialog is used for loading the LPV controller for the blue and red frame position control. "MIMO controller enable [master]" is the master switch for closing the loop with the LPV controller. The "Red gimbal position offset" control can be used to influence the position of the red frame in a feedforward manner. Finally, the previously mentioned "synchronize references" button (group 3 in Figure A.3) is used to start the experiment described in Chapter 4. It as well ensures that the references for disk speed and blue and red frame positions maintain the phase difference defined by the user in the "Phase Shift" controls.

Bibliography

[1] J. C. Maxwell, "On governors," *Proceedings of the Royal Society of London*, vol. 16, pp. 270–283, 1867.

[2] A. M. Lyapunov, "The general problem of the stability of motion (in russian)," Ph.D. dissertation, Univ. Kharkov, 1892.

[3] H. Nyquist, "Regeneration theory," *Bell System Technical Journal*, no. 11, pp. 126–147, 1932.

[4] H. W. Bode, *Network Analysis and Feedback Amplifier Design.* New York, Van Nostrand, 1945.

[5] K. J. Åström and P. R. Kumar, "Control: A perspective." *Automatica*, vol. 50, no. 1, pp. 3–43, 2014.

[6] B. A. Francis and W. M. Wonham, "The internal model principle of control theory," *Automatica*, vol. 12, no. 5, pp. 457–465, 1976.

[7] K. K. Chew and M. Tomizuka, "Digital control of repetitive errors in disk drive systems," in *American Control Conference*, Pittsburgh, PA, USA, 1989, pp. 540–548.

[8] A. Sacks, M. Bodson, and P. Khosla, "Experimental results of adaptive periodic disturbance cancelation in a high performance magnetic disk drive," *ASME Journal of Dynamic Systems Measurement and Control*, vol. 118, no. 3, pp. 416–424, 1996.

[9] S. M. Kuo and D. R. Morgan, *Active noise control systems: Algorithms and DSP implementations.* New York, NY, USA: John Wiley & Sons, Inc., 1995.

[10] P. Arcara, S. Bittanti, and M. Lovera, "Periodic control of helicopter rotors for attenuation of vibrations in forward flight," *IEEE Transactions on Control Systems Technology*, vol. 8, no. 6, pp. 883–894, 2000.

[11] M. Bodson, A. Sacks, and P. Khosla, "Harmonic generation in adaptive feedforward cancelation schemes," *IEEE Transactions on Automatic Control*, vol. 33, no. 12, pp. 2213–2221, December 1994.

Bibliography

[12] M. Bodson, "Rejection of periodic disturbances of unknown and time-varying frequency," *International Journal of Adaptive Control and Signal Processing*, vol. 19, pp. 67–88, 2005.

[13] I. D. Landau, A. Constantinescu, and D.Rey, "Adaptive narrow band disturbance rejection applied to an active suspension - an internal model principle approach," *Automatica*, vol. 41, no. 4, pp. 563–574, 2005.

[14] I. D. Landau, A. Castellanos Silva, T.-B. Airimiţoaie, G. Buche *et al.*, "Benchmark on adaptive regulation - rejection of unknown/time-varying multiple narrow band disturbances," *European Journal of Control*, vol. 19, no. 4, pp. 237–252, 2013.

[15] A. Karimi and Z. Emedi, "H_∞ gain-scheduled controller design for rejection of time-varying narrow-band disturbances applied to a benchmark problem," *European Journal of Control*, vol. 19, no. 4, pp. 279–288, 2013.

[16] T.-B. Airimiţoaie, A. Castellanos Silva, and I. D. Landau, "Indirect adaptive regulation strategy for the attenuation of time varying narrow-band disturbances applied to a benchmark problem," *European Journal of Control*, vol. 19, no. 4, pp. 313–325, 2013.

[17] A. Castellanos Silva, I. D. Landau, and T.-B. Airimiţoaie, "Direct adaptive rejection of unknown time-varying narrow band disturbances applied to a benchmark problem," *European Journal of Control*, vol. 19, no. 4, pp. 326–336, 2013.

[18] X. Chen and M. Tomizuka, "Selective model inversion and adaptive disturbance observer for time-varying vibration rejection on an active-suspension benchmark," *European Journal of Control*, vol. 19, no. 4, pp. 300–312, 2013.

[19] R. A. de Callafon and H. Fang, "Adaptive regulation via weighted robust estimation and automatic controller tuning," *European Journal of Control*, vol. 19, no. 4, pp. 266–278, 2013.

[20] Z. Wu and F. Ben Amara, "Youla parameterized adaptive regulation against sinusoidal exogenous inputs applied to a benchmark problem," *European Journal of Control*, vol. 19, no. 4, pp. 289–299, 2013.

[21] S. Aranovskiy and L. B. Freidovich, "Adaptive compensation of disturbances formed as sums of sinusoidal signals with application to an active vibration control benchmark," *European Journal of Control*, vol. 19, no. 4, pp. 253–265, 2013.

[22] H. Du, L. Zhang, Z. Lu, and X. Shi, "LPV technique for the rejection of sinusoidal disturbance with time-varying frequency," *IEE Proceedings - Control Theory and Applications*, vol. 150, no. 2, pp. 132–138, 2003.

[23] P. Gahinet and P. Apkarian, "A linear matrix inequality approach to H_∞ control," *International Journal of Robust and Nonlinear Control*, vol. 4, pp. 421–448, 1994.

[24] P. Apkarian, P. Gahinet, and G. Becker, "Self-scheduled H_∞ control of linear parameter-varying systems: a design example," *Automatica*, vol. 31, no. 9, pp. 1251–1261, 9 1995.

[25] W. Heins, P. Ballesteros, X. Shu, and C. Bohn, "LPV gain-scheduled observer-based state feedback for active control of harmonic disturbances with time-varying frequencies," *Advances on Analysis and Control of Vibrations - Theory and Applications*, 2012.

[26] P. Ballesteros, X. Shu, W. Heins, and C. Bohn, "LPV gain-scheduled output feedback for active control of harmonic disturbances with time-varying frequencies," *Advances on Analysis and Control of Vibrations - Theory and Applications*, 2012.

[27] B. Paijmans, W. Symens, H. van Brussel, and J. Swevers, "A gain-scheduling-control technique for mechatronic systems with position-dependent dynamics," in *IEEE American Control Conference*, Minneapolis, Minnesota, USA, June 2006, pp. 2933–2938.

[28] D. Stilwell and W. J. Rugh, "Interpolation of observer state feedback controllers for gain scheduling," *IEEE Transactions on Automatic Control*, vol. 44, no. 6, pp. 1225–1229, 1999.

[29] ——, "Stability preserving interpolation methods for the synthesis of gain scheduled controllers," *Automatica*, vol. 36, no. 5, pp. 665–671, 2000.

[30] I. Kaminer, A. M. Pascoal, P. P. Khargonekar, and E. E. Coleman, "A velocity algorithm for the implementation of gain-scheduled controllers," *Automatica*, vol. 31, no. 8, pp. 1185–1191, 1995.

[31] K. J. Hunt and T. A. Johansen, "Design and analysis of gain-scheduled control using local controller networks," *International Journal of Control*, vol. 66, no. 5, pp. 619–652, 1997.

[32] J. Shamma and M. Athans, "Analysis of gain scheduled control for nonlinear plants," *IEEE Transactions on Automatic Control*, vol. 35, no. 8, pp. 898–907, 1990.

[33] ——, "Guaranteed properties of gain scheduled control for linear parameter-varying plants," *Automatica*, vol. 27, no. 3, pp. 559–564, 1991.

[34] D. J. Leith and W. E. Leithead, "Survey of gain-scheduling analysis and design," *International Journal of Control*, vol. 73, no. 11, pp. 1001–1025, July 2000.

[35] J. S. Shamma, "An overview of LPV systems," in *Control of Linear Parameter Varying Systems with Applications.* Springer, 2012, pp. 3–26.

[36] F. D. Bianchi, R. J. Mantz, and C. F. Christiansen, "Control of variable-speed wind turbines by LPV gain scheduling," *Wind Energy*, vol. 7, pp. 1–8, 2004.

[37] F. D. Adegas, C. Sloth, and J. Stoustrup, "Structured linear parameter varying control of wind turbines," in *Control of Linear Parameter Varying Systems with Applications.* Springer, 2012, pp. 303–337.

Bibliography

[38] W. Gilbert, D. Henrion, J. Bernussou, and D. Boyer, "Polynomial LPV synthesis applied to turbofan engines," *Control Engineering Practice*, vol. 18, pp. 1077–1083, 2010.

[39] G. J. Balas, "Linear, parameter-varying control and its application to a turbofan engine," *International Journal of Robust and Nonlinear Control*, vol. 12, no. 9, pp. 763–796, 2002.

[40] M. G. Wassink, M. van de Wal, C. Scherer, and O. Bosgra, "LPV control for a wafer stage: beyond the theoretical solution," *Control Engineering Practice*, vol. 13, pp. 231–245, 2005.

[41] J-M Biannic and P. Apkarian, "Missile autopilot design via a modified LPV synthesis technique," *Aerospace Science and Technology*, vol. 3, no. 3, pp. 153–160, 1999.

[42] P. C. Pellanda, P. Apkarian, and H. D. Tuan, "Missile autopilot design via a multi-channel LFT/LPV control method," *International Journal of Robust and Nonlinear Control*, vol. 12, no. 1, pp. 1–20, 2002.

[43] L. H. Crater and J. S. Shamma, "Gain-scheduled bank-to-turn autopilot design using linear parameter varying transformations," *Journal of guidance, control, and dynamics*, vol. 19, no. 5, pp. 1056–1063, 1996.

[44] F. Wu, A. Packard, and G. Balas, "LPV control design for pitch-axis missile autopilots," in *34th IEEE Conference on Decision and Control*, vol. 1.   IEEE, 1995, pp. 188–193.

[45] C. Poussot-Vassal, O. Sename, L. Dugard, P. Gaspar, Z. Szabo, and J. Bokor, "A new semi-active suspension control strategy through LPV technique," *Control Engineering Practice*, vol. 16, no. 12, pp. 1519–1534, 2008.

[46] G. Panzani, S. Formentin, and S. M. Savaresi, "Active motorcycle braking via direct data-driven load transfer scheduling," in *16th IFAC Symposium on System Identification, SYSID 2012*, Brussels, Belgium, 2012.

[47] J. Mohammadpour and e. C. Scherer, *Control of linear parameter varying systems with applications.*   Springer, 2012.

[48] O. Sename, P. Gáspár, and e. J. Bokor, *Robust control and linear parameter varying approaches.*   Springer, 2013.

[49] R. Toth, P. S. C. Heuberger, and P. M. Van den Hof, "Asymptotically optimal orthonormal basis functions for LPV system identification," *Automatica*, vol. 45, no. 6, pp. 1359 – 1370, 2009.

[50] V. Cerone, D. Piga, D. Regruto, and R. Toth, "Input-output LPV model identification with guaranteed quadratic stability," in *16th IFAC Symposium on System Identification*, Brussels, Belgium, July 2012.

[51] V. Verdult, "Nonlinear system identification: A state-space approach," Ph.D. dissertation, University of Twente, Enschede, The Netherlands, 2002.

[52] R. Tóth, *Modeling and identification of linear parameter-varying systems.* Springer, 2010, vol. 214.

[53] S. Formentin, D. Piga, R. Tóth, and S. Savaresi, "Direct data-driven control of linear parameter-varying systems," in *52nd IEEE Conference on Decision and Control*, Florence, Italy, December 2013.

[54] D. Henrion, M. Sebek, and V. Kucera, "Positive polynomials and robust stabilization with fixed-order controllers," *IEEE Transactions on Automatic Control*, vol. 48, no. 7, pp. 1178–1186, 2003.

[55] M. C. de Oliveira, J. C. Geromel, and L. Hsu, "LMI characterization of structural and robust stability: the discrete-time case," *Linear Algebra and its Applications*, vol. 296, pp. 27–38, 1999.

[56] R. C. L. F. Oliveira and P. L. D. Peres, "Stability of polytopes of matrices via affine parameter-dependent lyapunov functions: Asymptotically exact LMI conditions," *Linear Algebra and its Applications*, vol. 405, pp. 209–228, 2005.

[57] J. Daafouz and J. Bernussou, "Parameter dependent lyapunov functions for discrete time systems with time varying parametric uncertainties," *System and Control Letters*, vol. 43, pp. 355–359, 2001.

[58] J. C. Geromel, M. C. de Oliveira, and L. Hsu, "LMI characterization of structural and robust stability," *Linear Algebra and its Applications*, vol. 285, pp. 69–80, 1998.

[59] F. Wu, X. H. Yang, A. Packard, and G. Becker, "Induced l_2-norm control for LPV system with bounded parameter variation rate," in *Proceedings of the American Control Conference*, Seattle, Washington, USA, 1996.

[60] P. Apkarian and R. J. Adams, "Advanced gain-scheduling techniques for uncertain systems," *IEEE Transactions on Control Systems Technology*, vol. 6, no. 1, pp. 21–32, 1998.

[61] M. Sato, "Gain-scheduled output-feedback controllers depending solely on scheduling parameters via parameter-dependent Lyapunov functions," *Automatica*, vol. 47, pp. 2786–2790, 2011.

[62] F. Wu, "A generalized LPV system analysis and control synthesis framework," *International Journal of Control*, vol. 74, no. 7, pp. 745–759, 2001.

[63] R. C. L. F. Oliveira and P. L. D. Peres, "Time-varying discrete-time linear systems with bounded rates of variation: Stability analysis and control design," *Automatica*, vol. 45, pp. 2620–2626, 2009.

[64] F. Amato, M. Mattei, and A. Pironti, "Gain scheduled control for discrete-time systems depending on bounded rate parameters," *International Journal of Robust and Nonlinear Control*, vol. 15, pp. 473–494, 2005.

[65] J De Caigny, J. F. Camino, R. C. L. F. Oliveira, P. L. D. Peres, and J. Swevers, "Gain-scheduled dynamic output feedback control for discrete-time LPV systems," *International Journal of Robust and Nonlinear Control*, vol. 22, pp. 535–558, 2012.

[66] W.P.M. Heemels, J. Daafouz, and G. Millerioux, "Observer-based control of discrete-time LPV systems with uncertain parameters," *IEEE Transactions on Automatic Control*, vol. 55, no. 9, pp. 2130–2135, 2010.

[67] P. Apkarian and P. Gahinet, "A convex characterization of gain-scheduled H_∞ controllers," *IEEE Transactions on Automatic Control*, vol. 40, no. 5, pp. 853–864, May 1995.

[68] A. Packard, "Gain scheduling via linear fractional transformations," *Systems and Control Letters*, vol. 22, no. 2, pp. 79–92, 1994.

[69] J. C. Geromel, R. H. Korogui, and J. Bernussou, "H_2 and H_∞ robust output feedback control for continuous time polytopic systems," *IET Control Theory and Applications*, vol. 1, no. 5, pp. 1541–1549, September 2007.

[70] C. Beck, "Coprime factors reduction methods for linear parameter varying and uncertain systems," *Systems & control letters*, vol. 55, no. 3, pp. 199–213, 2006.

[71] N.R. Sandell, P. Varaiya, M. Athans, and M.G. Safonov, "Survey of decentralized control methods for large scale systems," *IEEE Transactions on Automatic Control*, vol. 23, no. 2, pp. 108–128, 1978.

[72] R. D'Andrea and G.E. Dullerud, "Distributed control design for spatially interconnected systems," *IEEE Transactions on Automatic Control*, vol. 48, no. 9, pp. 1478–1495, 2003.

[73] F.D. Adegas and J. Stoustrup, "Structured control of affine linear parameter varying systems," in *American Control Conference (ACC), 2011*. IEEE, 2011, pp. 739–744.

[74] C.E. de Souza, K.A. Barbosa, and A. Trofino, "Robust $\mathscr{H}_\infty$ filtering for discrete-time linear systems with uncertain time-varying parameters," *IEEE Transactions on Signal Processing*, vol. 54, no. 6, pp. 2110–2118, 2006.

[75] A. Karimi and G. Galdos, "Fixed-order H_∞ controller design for nonparametric models by convex optimization," *Automatica*, vol. 46, no. 8, pp. 1388–1394, 2010.

[76] I. D. Landau, T. B. Airimitoaie, A. C. Silva, and Gabriel Buche, "An active vibration control system as a benchmark on adaptive regulation," in *Submitted to European Control Conference*, Zurich, Switzerland, 2013. [Online]. Available: http://www.gipsa-lab.grenoble-inp.fr/~ioandore.landau/benchmark_adaptive_regulation

[77] P. Mäkilä, "Approximation of stable systems by laguerre filters," *Automatica*, vol. 26, no. 2, pp. 333–345, 3 1990.

[78] C. J. Doyle, B. A. Francis, and A. R. Tannenbaum, *Feedback Control Theory*. New York: Mc Millan, 1992.

[79] A. L. Yuille and A. Rangarajan, "The concave-convex procedure," *Neural Computation*, vol. 15, no. 4, pp. 915–936, 2003.

[80] T. Lipp and S. Boyd, "Variations and extensions of the convex-concave procedure," 2014.

[81] G. Calafiore and M. C. Campi, "The scenario approach to robust control design," *IEEE Transactions on Automatic Control*, vol. 51, no. 5, pp. 742–753, May 2006.

[82] G. Galdos, A. Karimi, and R. Longchamp, "Robust controller design by convex optimization based on finite frequency samples of spectral models," in *49th IEEE Conference on Decision and Control*, Atlanta, USA, 2010.

[83] I. D. Landau, R. Lozano, M. M'Saad, and A. Karimi, *Adaptive Control: Algorithms, Analysis and Applications.* London: Springer-Verlag, 2011.

[84] A. Karimi, H. Khatibi, and R. Longchamp, "Robust control of polytopic systems by convex optimization," *Automatica*, vol. 43, no. 6, pp. 1395–1402, 2007.

[85] S. P. Bhattacharyya, H. Chapellat, and L. H. Keel, *Robust Control: The Parametric Approach.* NJ, USA: Prentice Hall Information and System Sciences Series, 1995.

[86] B. D. O. Anderson, S. Dasgupta, P. P. Khargonekar, F. J. Kraus, and M. Mansour, "Robust strict positive realness: Characterization and construction," *IEEE Transactions on Circuits and Systems*, vol. 37, pp. 869–876, 1990.

[87] H. Akcay and B. Ninness, "Orthonormal basis functions for modeling continuous-time systems," *Signal Processing*, vol. 77, pp. 261–274, 1999.

[88] R. Tóth, H. S. Abbas, and H. Werner, "On the state-space realization of LPV input-output models: Practical approaches," *IEEE Transactions on Control Systems Technology*, vol. 20, no. 1, pp. 139–153, 2012.

[89] B. D. O. Anderson, "The small-gain theorem, the passivity theorem and their equivalence," *Journal of the Franklin Institute*, vol. 293, no. 2, pp. 105–115, February 1972.

[90] W. M. Haddad and D. S. Bernstein, "Robust stabilization with positive real uncertainty: Beyond the small gain theorem," in *29th IEEE Conference on Decision and Control*, Honolulu, Hawaii, 1990, pp. 2054–2059.

[91] H. Khatibi and A. Karimi, "H_∞ controller design using an alternative to Youla parameterization," *IEEE Transactions on Automatic Control*, vol. 55, no. 9, pp. 2119–2123, 2010.

[92] I. D. Landau, M. Alma, J. J. Martinez, and G. Buche, "Adaptive suppression of multiple time-varying unknown vibrations using an inertial actuator," *IEEE Transactions on Control System Technology*, vol. 19, no. 6, pp. 1327–1338, 2010.

Bibliography

[93] J. Löfberg, "YALMIP: A toolbox for modeling and optimization in MATLAB," in *CACSD Conference*, 2004. [Online]. Available: http://control.ee.ethz.ch/~joloef/yalmip.php

[94] K. C. Toh, M. J. Todd, and R. H. Tutuncu, "SDPT3: a MATLAB software package for semidefinite programming," *Optimization Methods and Software*, vol. 11, pp. 545–581, 1999.

[95] H. K. Khalil, *Nonlinear Systems*. New Jersey: Prentice Hall, 2006.

[96] Z. Emedi and A. Karimi, "Fixed-order LPV controller design for rejection of a sinusoidal disturbance with time-varying frequency," in *IEEE Multi-Conference on Systems and Control*, Dubrovnik, Croatia, 2012.

[97] A. Karimi and M. S. Sadabadi, "Fixed-order controller design for state space polytopic systems by convex optimization," in *5th IFAC Symposium on System Structure and Control*, Grenoble, France, 2013.

[98] A. Albert, "Conditions for positive and nonnegative definiteness in terms of pseudoinverses," *SIAM Journal on Applied Mathematics*, vol. 17, no. 2, pp. 434–440, 1969.

[99] P. Apkarian and D. Noll, "Nonsmooth H_∞ synthesis," *IEEE Transactions on Automatic Control*, vol. 51, no. 1, pp. 71–86, 2006.

[100] J. V. Burke, D. Henrion, and A. S. L. M. L. Overton, "HIFOO : a MATLAB package for fixed-order controller design and H_∞ optimization," in *Fifth IFAC Symposium on Robust Control Design, Toulouse*, 2006.

[101] M. Sadeghpour, V. de Oliveira, and A. Karimi, "A toolbox for robust PID controller tuning using convex optimization," in *IFAC Conference in Advances in PID Control*, Brescia, Italy, 2012.

[102] P. J. de Oliveira, R. C. L. F. Oliveira, V. J. S. Leite, V. F. Montagner, and P. L. D. Peres, "H_∞ guaranteed cost computation by means of parameter-dependent Lyapunov functions," *Automatica*, vol. 40, no. 6, pp. 1053–1061, 2004.

[103] K. Zhou and J. C. Doyle, *Essentials of robust control*. N.Y.: Prentice-Hall, 1998.

[104] P. J. de Oliveira, R. C. L. F. Oliveira, V. J. S. Leite, V. F. Montagner, and P. L. D. Peres, "H_2 guaranteed cost computation by means of parameter dependent Lyapunov functions," *International Journal of Systems Science*, vol. 35, no. 5, pp. 305–315, 2004.

[105] A. Karimi, "Frequency-domain robust controller design: A toolbox for MATLAB," Automatic Control Laboratory, EPFL, Switzerland, 2012. [Online]. Available: http://la.epfl.ch/FDRC_Toolbox

[106] A. Visioli, *Practical PID Control*. London: Springer-Verlag, 2006.

[107] Q. C. Inc., *Gyroscope Position Control*, 119 Spy Court, Markham, Ontario, L3R 5H6, Canada, Revision 1.0. [Online]. Available: http://www.quanser.com

[108] R. H. Cannon, *Dynamics of physical systems*. Courier Dover Publications, 2003.

[109] D. Robert, O. Sename, and D. Simon, "An LPV design for sampling varying controllers: Experimentation with a T-Inverted pendulum," *IEEE Transactions on Control Systems Technology*, vol. 18, no. 3, pp. 741–749, 2010.

[110] C. W. Scherer, "LMI relaxations in robust control," *European Journal of Control*, vol. 12, no. 1, pp. 3–29, 2006.

[111] M. S. Sadabadi and A. Karimi, "An LMI formulation of fixed-order $\mathcal{H}_\infty$ and $\mathcal{H}_2$ controller design for discrete-time systems with polytopic uncertainty," in *52nd IEEE Conference on Decision and Control*, Florence, Italy, December 2013.

[112] K.A. Barbosa, C.E. de Souza, and A. Trofino, "Robust $\mathcal{H}_2$ filtering for discrete-time uncertain linear systems using parameter-dependent lyapunov functions," in *Proceedings of the American Control Conference*, vol. 4. IEEE, 2002, pp. 3224–3229.

[113] G. Galdos, "Robust controller design by convex optimization using spectral models," Ph.D. dissertation, Ecole Polytechnique Fédérale de Lausanne, Switzerland, 2010.

[114] F. Blanchini, D. Casagrande, S. Miani, and U. Viaro, "Stable LPV realization of parametric transfer functions and its application to gain-scheduling control design," *IEEE Transactions on Automatic Control*, vol. 55, no. 10, pp. 2271–2281, 2010.

[115] Y. Ebihara and T. Hagiwara, "On the degree of polynomial parameter-dependent Lyapunov functions for robust stability of single parameter-dependent LTI systems: A counter-example to Barmish's conjecture," *Automatica*, vol. 42, no. 9, pp. 1599–1603, September 2006.

[116] Y. Nesterov, "Efficiency of coordinate descent methods on huge-scale optimization problems," *SIAM Journal on Optimization*, vol. 22, no. 2, pp. 341–362, 2012.

[117] M. Kunze, "Frequency-domain controller design by linear programming," Ph.D. dissertation, Ecole Polytechnique Fédérale de Lausanne, Laboratoire d'Automatique, 2009.

[118] E. Simon, "A perspective for optimization in systems and control: from LMIs to derivative-free methods," Ph.D. dissertation, Université catholique de Louvain, 2012.

[119] Q. T. Dinh, S. Gumussoy, W. Michiels, and M. Diehl, "Combining convex–concave decompositions and linearization approaches for solving BMIs, with application to static output feedback," *IEEE Transactions on Automatic Control*, vol. 57, no. 6, pp. 1377–1390, 2012.

[120] M. Kocvara and M. Stingl, "See www.penopt.com for a free developer version," *Version 2.1*, 2006.

Curriculum Vitæ

EMEDI Zlatko

E-mail: zlatko.emedji@gmail.com

Date of birth: 30th April 1985

Nationality: Serbian

Education:

- 2009-2014: **Doctoral Studies and research** at the Automatic Control Laboratory, Swiss Federal Institute of Technology Lausanne (EPFL).

- 2004-2005: **Master of Electrical Enginering and Computer Science**, Control Systems Department at Faculty of Technical Sciences, University of Novi Sad, Serbia.

- 2001-2004: Mathematical Grammar School, Belgrade, Serbia.

Publications:

Published:

- Z. Emedi and A. Karimi. Fixed-order LPV Controller Design for Rejection of a Sinusoidal Disturbance with Time-varying Frequency. *2012 IEEE Multi-Conference on Systems and Control*, Dubrovnik, Croatia, October 3 - 5, 2012.

- Z. Emedi and A. Karimi. Fixed-order LPV Controller Design for LPV Systems by Convex Optimization. *IFAC Joint Conference*, Grenoble, France, February 4-6, 2013.

- A. Karimi and Z. Emedi. $\mathscr{H}_{\infty}$ Gain-scheduled Controller Design for Rejection of Time-varying Narrow-band Disturbances Applied to a Benchmark Problem, in *European Journal of Control*, 2013.

- A. Karimi and Z. Emedi. $\mathscr{H}_\infty$ Gain-Scheduled Controller Design for Rejection of Time-Varying Disturbances with Application to an Active Suspension System. *52nd IEEE Conference on Decision and Control*, Firenze, Italy, December 10-13, 2013.

- Z. Emedi and A. Karimi. Fixed-order Discrete-time LPV Controller Design. *19th IFAC World Congress*, Cape Town, South Africa, August 25-29, 2014.

- J. Schoukens, G. Vandersteen, R. Pintelon, Z. Emedi and Y. Rolain. Study of the maximal interpolation errors of the local polynomial method for frequency response function measurements. *2012 IEEE International Instrumentation and Measurement Technology Conference*, Graz, Austria, 2012.

- J. Schoukens, G. Vandersteen, R. Pintelon, Z. Emedi and Y. Rolain. Bounding the Polynomial Approximation Errors of Frequency Response Functions, in *IEEE Transactions on Instrumentation and Measurement*, vol. 62, num. 5, p. 1346-1353, 2013.

Submitted:

- Z. Emedi and A. Karimi. Fixed-structure LPV Discrete-time Controller Design with Induced l_2-Norm and $\mathscr{H}_2$ Performance. Submitted to *International Journal of Control*.

- Z. Emedi and A. Karimi. Fixed-order Linear Parameter Varying Controller Design for a 2DOF Gyroscope. Submitted to *IEEE Transactions on Control Systems Technology*.